ANALYSIS OF DELAMINATION RELATED FRACTURE PROCESSES IN COMPOSITES

Erian A. Armanios

School of Aerospace Engineering
Georgia Institute of Technology
Atlanta, Georgia 30332-0150

Preliminary Final Report
NASA Grant NAG-1-637

INTRODUCTION

The work described herein was performed at the School of Aerospace Engineering, Georgia Institute of Technology during the period 12 February 1986 - September 1988. Professors Erian A. Armanios and Lawrence W. Rehfield were the Principal Investigators.

This research concerns the analysis and prediction of delamination damage that occur in composite structure on the on the sublaminate scale --that is the scale of individual plies or groups of plies. The objective have been to develop analytical models for mixed-mode delamination in composites. These includes:

(1) the influence of residual thermal and moisture strains
(2) local or transverse crack tip delamination originating at the tip of transverse matrix cracks
(3) delamination in tapered composite under tensile loading.

Computer codes based on the analytical models in (1) and (2) have been developed and comparisons of predictions with available experimental and analytical results in the literature have been performed. A simple analysis for item (3) has been developed and comparisons of predictions with finite element simulation is underway.

The usual approach to dealing with localized phenomena is large scale numerical simulation and analysis, mostly by general purpose finite element codes. This approach is often supplemented by a "build and test" demonstration, or series of demonstrations if repeated failures are encountered. While such approaches are often costly and inefficient, their major drawback is that fundamental principles are not discovered which provide the means to produce better results. Furthermore, the steps must be repeated all over again the next time a similar situation arises.

Overview of the Research

The research program can be separated into three elements: The influence of residual thermal and moisture stresses on the mixed-mode edge delamination of composites. The analyses of transverse crack-tip delamination and delamination analysis in tapered laminates under tensile loading. A detailed account of the analysis and applications of each element is provided in Appendices I through III. A brief description and summary of the major findings of each research element is presented in the following sections.

Influence of Hygrothermal Stresses

The sublaminate edge delamination analysis and code which had its origin in the research conducted under the earlier grant NAG-1-558 has been modified to include the effects of hygrothermal stresses.

The model is applied to mixed mode edge delamination specimens made of T300/5208 graphite/epoxy material. Residual thermal and moisture stresses significantly influenced the strain energy release rate and interlaminar stresses. Both experienced large increases when thermal conditions were added to the mechanical strains. These effects were alleviated when moisture stresses were included. Thermal effects on the interlaminar shear stress and total energy release rate were totally alleviated for the same specific moisture content. Moreover, this value of moisture content was not significantly affected by the stacking sequence for the laminates considered. This work is presented in accomplishments 3,4 and 12. A complete derivation of the analytical model, Fortran program listing and applications are provided in a accomplishment 3 and Appendix I.

Transverse Crack Tip Analysis

Transverse crack tip delaminations originate at the tip of transverse matrix cracks. This situation appears in Figure 1 where a symmetric laminate made of 90° plies in the core region and angle plies in the top and bottom portions is subjected to a tensile loading. Under tensile loading transverse

matrix cracks initiate in the core region reaching a saturation level at a crack spacing denoted by λ in the figure. Delamination often initiate at the tip of these transverse cracks. This situation is depicted in the generic model shown in Figure 1 of a symmetric delamination growing from a transverse crack tip.

Three analytical models, sublaminate shear, membrane and shear lag have been developed in order to estimate the saturated crack spacing distance. The saturation crack spacing corresponds to the distance from the crack where the broken plies regain their uniform stress/strain state i.e. where the interlaminar shear stress has decayed down to its far field (uniform) value. Based on the closed form expression for the interlaminar shear stress the crack spacing predicted by each model is presented in Table I. The experimental result in the table is based on Reifsnider's work for a $[0/90]_s$ laminate. A complete derivation of these models is provided in Appendix II.

The analysis of transverse crack tip delamination is presented in Appendix II and applied to $[\pm 25/90_n]$s laminates in the range n=0.5 to 8 made of T300/934 graphite/epoxy material. Closed form expressions for the interlaminar stresses, total strain energy release rate and energy release rate components are obtained. A computer code based on this analysis is developed and implemented into an earlier mixed-mode edge delamination code developed under the previous NASA grant NAG-1-558 and presented in accomplishment 6 and 7. This code was used to estimate the critical strain levels and the associated delamination damage mode with increasing number of 90° plies in the $[\pm 25/90_n]_s$. Since mid-plane edge delamination is a possible damage mode in this type of laminates a mid-plane delamination analysis was developed and presented in accomplishment 10. A computer code based on this analysis is developed and implemented in the mixed-mode edge delamination code. The critical strain and associated delamination damage modes predicted appear in Figure 2 and Table II. The critical stresses and associated delamination damage mode are provided in Table III.

Experimental results show that the local (crack tip) delamination phenomenon is the predominant damage mode only for n=4, 6 and 8 specimens. For n<4 edge delamination either in the mid-plane or in the 25/90 interface were observed in tests. The present analysis predicts mid-plane edge delamination for n=1/2 and 1 and mixed mode edge delamination for n=2 and 3, respectively. For n=4, 6 and 8 local delaminations are predicted to be the controlling damage mode with approximately 25 percent Mode II for the three specimens. The critical strains in Figure 2 and Table II are computed based on a fracture toughness values of 415 J/m^2, 140 J/m^2 and 120 J/m^2 for local delamination, mixed mode edge delamination and mid-plane edge delamination, respectively. A complete account of this work appears in Appendix II.

Analysis of Tapered Composites

A generic configuration of a tapered laminated composite is shown in Figure 3 where a 38 ply thick laminate is reduced to 26 ply by dropping three inner sets of plies. The basic analysis approach that is adopted utilizes two levels of modeling, a global scale and a local scale. The global scale is concerned with overall generalized forces and strains such as axial force and extension. A simple consistent deformation assumption is the foundation of this model. Global equilibrium equations are written and solved.

The generalized strains determined from the global analysis serve to provide estimates for the key primary stresses in the belt of the tapered section. Local estimates of interlaminar stresses are determined on the basis of equilibrium condition.

The total strain energy release rate is computed from the work done by the external applied loads. The work done by the external forces is based on the axial stiffness of the different elements in the tapered configurations. These elements are represented by the six sublaminates shown in Figure 4 where A_B denote the effective axial stiffness of the uncracked belt portion, A_{B1} the effective axial stiffness of the cracked belt portion. The uncracked belt portion in the tapered region makes an angle β with the loading axis while the

cracked portion makes an angle α due to delaminations along the taper and the uniform regions. These are denoted by a and b in Figure 4. The effective axial stiffness of the uncracked and cracked dropped plies are denoted by A_u and A_c respectively. The axial stiffness of the straight portion is denoted by A_s for the belt and A_f for the core plies.

The extent of delamination along the tapered and the uniform portion of the laminate has a significant influence on the axial stiffnesses A_u, A_c and A_{B1}. This is due to the discrete number of ply drops in the core region as illustrated in Figure 5 and the pop-off of the delaminated belt region.

A three-dimensional transformation is required in order to estimate the effective axial stiffness of the belt regions A_B and A_{B1}. This is due to the belt layup and the orientation of the different belt portions to the loading axis as shown in Figure 6.

The interlaminar stresses between the belt and the core plies are predicted by considering the equilibrium of the belt region. The equilibrium equations are derived using a complementary potential energy formulation of the belt on an elastic foundation. The elastic foundation is made of two contributions. The first, is a continuous shear restraint provided by the resin pocket regions at the interface between the belt and the inner core plies. The second, is a discrete number of concentrated transverse normal (R_i) and shear (T_i) forces at the ply drop locations as shown in figure 7 for i=1-4. The distributed shear stiffness is denoted by G in Figure 8 while the transverse normal and shear stiffnesses at the ply drop locations are denoted by k_i and g_i (i=1-4), respectively.

The variation of the total strain energy release rate G with delamination a growing along the tapered region appears in Figure 9. The effect of delamination b along the uniform portion on a is also shown in the figure. The discrete jumps at a/h equal 20 and 40 correspond to the ply drop. A plot of the concentrated transverse normal and shear forces and the interface between the belt and the inner core appears in Figure 10.

A detailed description of the analysis, closed form expressions for the total energy release rate and interlaminar stresses is provided in Appendix III. Additional refinements are planned within this general framework such as accounting for shear strains in the belt and increasing the number of sublaminate elements in the analysis.

ACCOMPLISHMENTS

Publications

1. Armanios, E.A. and Rehfield, L.W., "Interlaminar Analysis of Laminated Composites Using a Sublaminate Approach," Proceedings of the AIAA/ASME/ASCE/AHS 27th Structures, Structural Dynamics, and Materials (SDM) Conference, San Antonio, Texas, 19-21 May, 1986. AIAA Paper No. 86-0969CP, Part 1, pp. 442-452.

2. Rehfield, L.W., Armanios, E.A. and Weinstein, F., "Analytical Modeling of Interlaminar Fracture in Laminated Composites," Composites '86: Recent Advances in Japan and the United States, Proceedings of the Third Japan-U.S. Conference on Composite Materials, K. Kawata, S. Umekawa, and A. Kobayashi Eds., 1986 pp. 331-340.

3. Mahler, M.A., "A Study on the Thermal and Moisture Influences on the Free-edge Delamination of Laminated Composites," Special Problem in Partial Fulfillment for M. Sc., School of Aerospace Engineering, Georgia Institute of Technology, September, 1987.

4. Armanios, E.A. and Mahler, M.A., "Residual Thermal and Moisture Influences on the Free-Edge Delamination of Laminated Composites," Proceedings of the AIAA/ASME/ASCE/AHS 29th Structures, Structural Dynamics and Materials (SDM) Conference, Part 1, pp. 371-381, 1988.

5. Armanios, E.A. and Rehfield, L.W., "Interlaminar Fracture Analysis of Composite Laminates Under Bending and Combined Bending and Extension," Composite Materials: Testing and Design (Eighth Conference), ASTM STP 972, J. D. Whitcomb, Eds., American Society for Testing and Materials, Philadelphia, 1988, pp. 81-94.

Publications Pending

6. Armanios, E.A. and Rehfield, L.W., "Sublaminate Analysis of Interlaminar Fracture in Composites: Part I-Analytical Model," Journal of Composites Technology and Research, July, 1988.

7. Armanios, E.A., Rehfield, L.W., Raju, I.S. and O'Brien, T.K.," Sublaminate Analysis of Interlaminar Fracture in Composites: Part II - Applications," Journal of Composites Technology and Research, July, 1988.

8. Armanios, E.A. and Rehfield, L.W., "A Simplified Approach to Strain Energy Release Rate Computations for Interlaminar Fracture of Composites," Composites '88: Recent Advances in Japan and the United States, Proceedings of the Fourth Japan - U.S. Conference on Composite Materials.

9. Sriram, P. and Armanios, E.A., "Fracture Analysis of Local Delaminations in Laminated Composites," to appear in the proceedings of the AIAA/ASME/ASCE/AHS/ASC 30th Structures, Structural Dynamics and Materials (SDM) Conference, April, 1989.

10. Armanios, E.A., Sriram, P. and Badir, A., "Sublaminate Analysis of Mode I Edge Delamination in Laminated Composites," to appear in the proceedings of the AIAA/ASME/ASCE/AHS/ASC 30th Structures, Structural Dynamics and Materials (SDM) Conference, April, 1989.

Presentations

11. Armanios, E.A. and Mahler, M.A., "Residual Thermal and Moisture Influences on the Free-edge Delamination of Laminated Composites," presented at the 29th Structures, Structural Dynamics and Materials (SDM) Conference, Williamsburg, VA, April 18-20, 1988.

Table I Comparison of Transverse Crack Spacing

Model		Saturated Crack Spacing (mm)
Shear	2 Sublaminates	1.651
	4 sublaminates, $a \rightarrow 0$	1.105
Membrane		1.004
Shear Lag		1.160
Experimental		1.131

Table II Critical Strains and Associated Delamination Damage Modes

Critical Strains (%)

Number of 90° plies	Experimental	Local Delamination	Edge Delamination	
			Mixed Mode	Mid-Plane
1/2	0.6058	1.6747	0.6819	0.6058
1	0.5936	1.1685	0.6262	0.5677
2	0.5934	0.8058	0.5964	0.6402
3	0.5934	0.6427	0.5862	0.7582
4	0.5369	0.5444	0.5810	0.8815
6	0.3914	0.4264	0.5757	1.1133
8	0.3589	0.3555	0.5731	1.3199

Table III Critical Stresses and Associated Delamination Damage Modes

Critical Stresses (MPa)

Number of 90° plies	Experimental	Local Delamination	Edge Delamination	
			Mixed Mode	Mid-Plane
1/2	438	1313.9	535.0	475.3
1	409	784.0	420.1	380.9
2	324	426.2	315.4	338.6
3	270	285.1	260.1	336.4
4	211	210.6	224.7	341.0
6	128	134.7	181.8	351.6
8	94.4	97.1	156.6	360.5

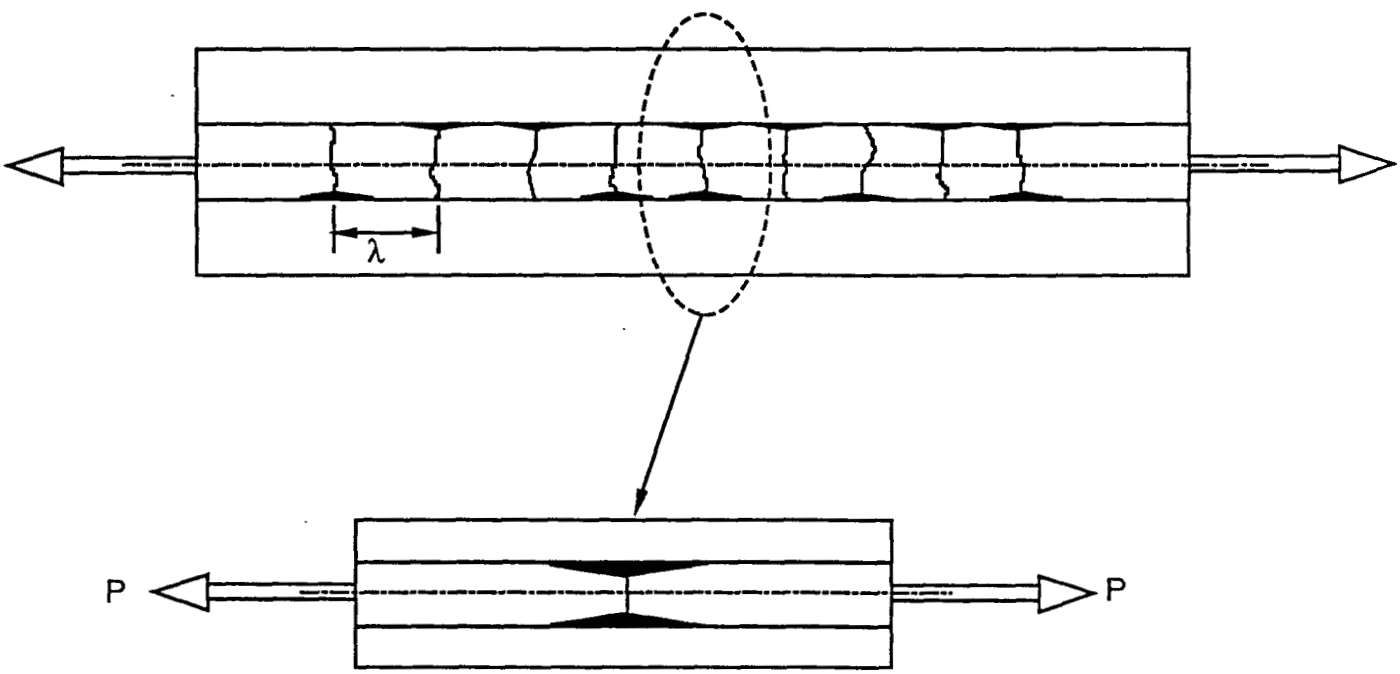

Fig. 1 Generic Crack-tip Delamination

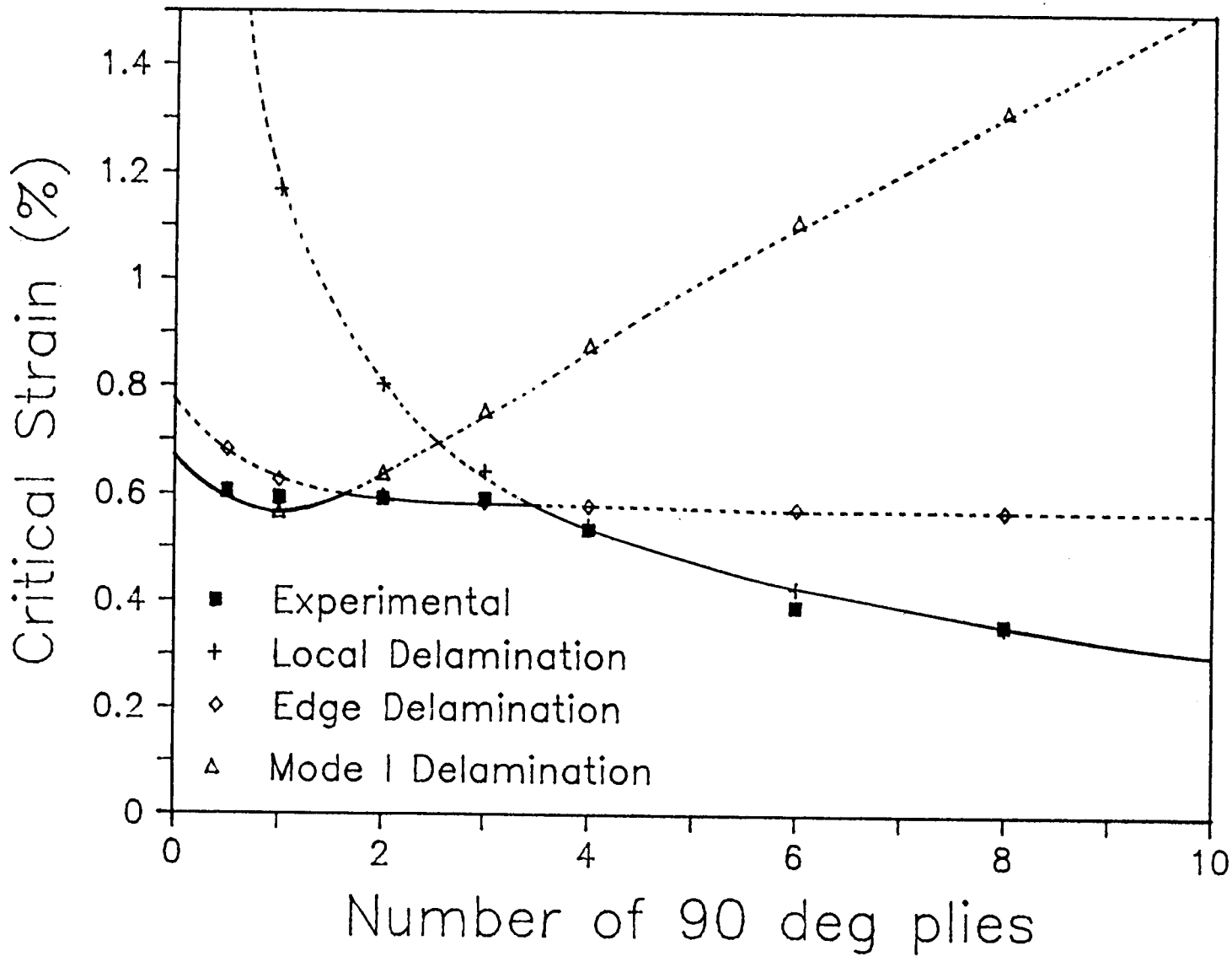

Fig. 2 Critical Strains and Associated Delamination Damage Modes

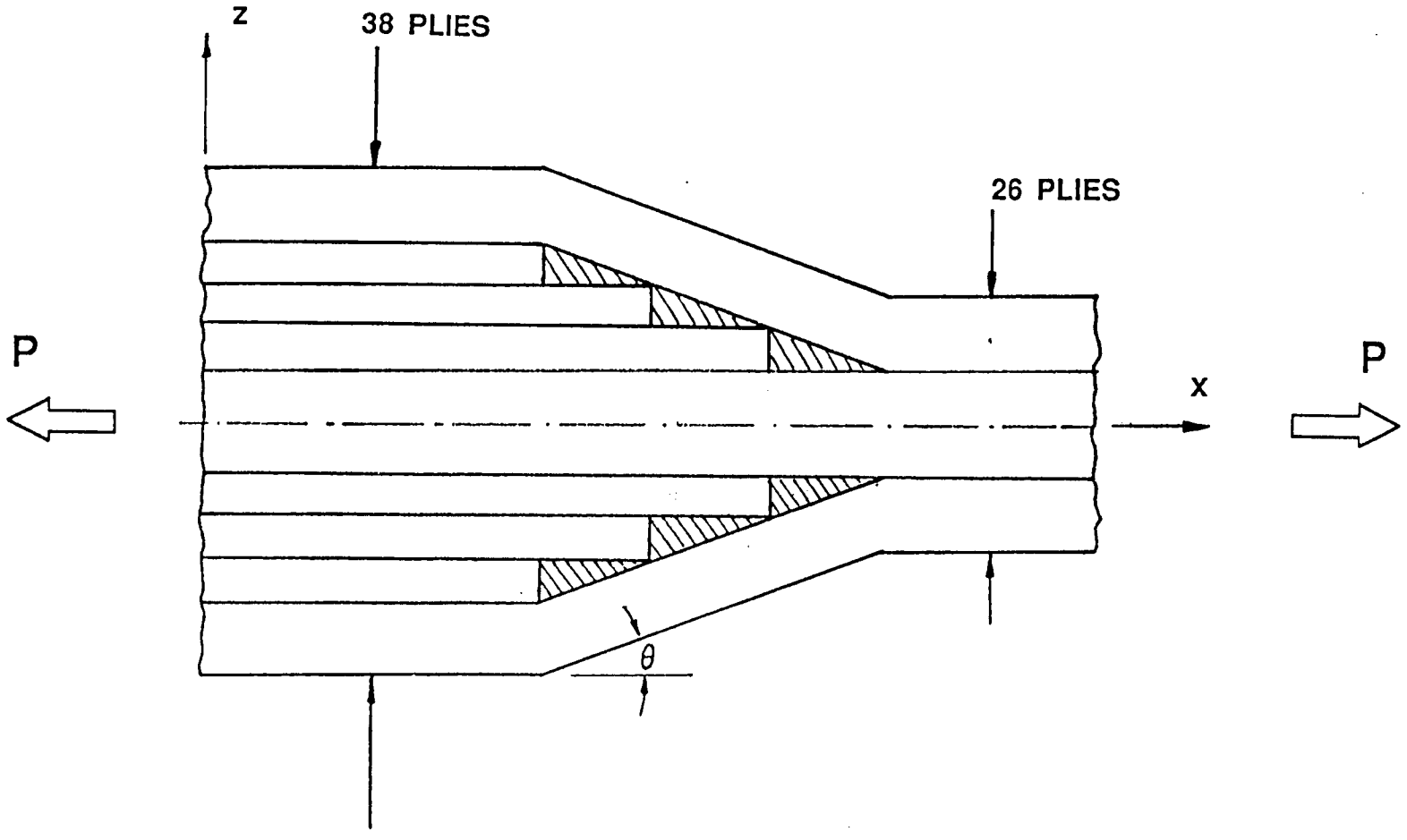

Figure 3. Edge View of the Tapered Structure

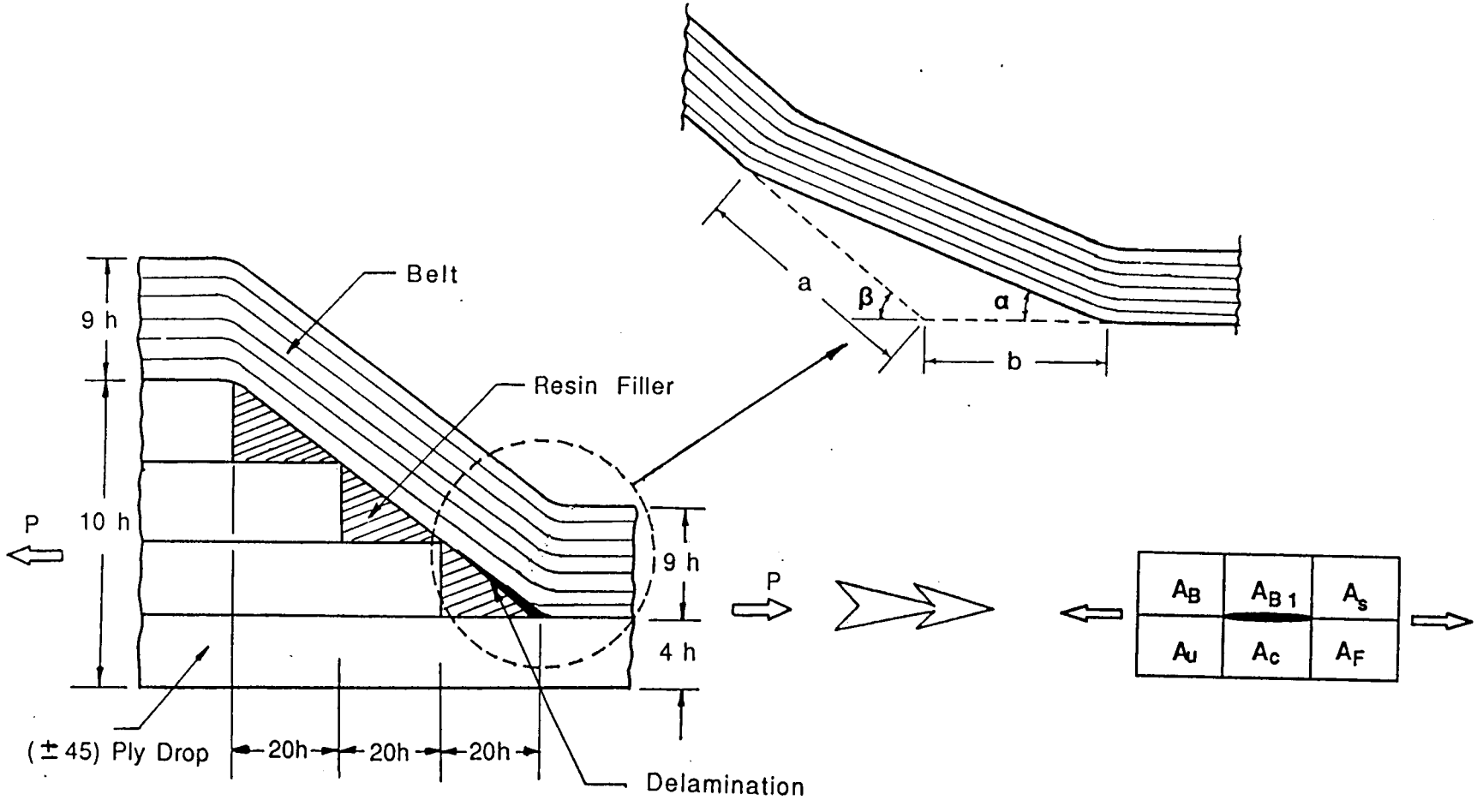

Figure 4. Modelling Approach

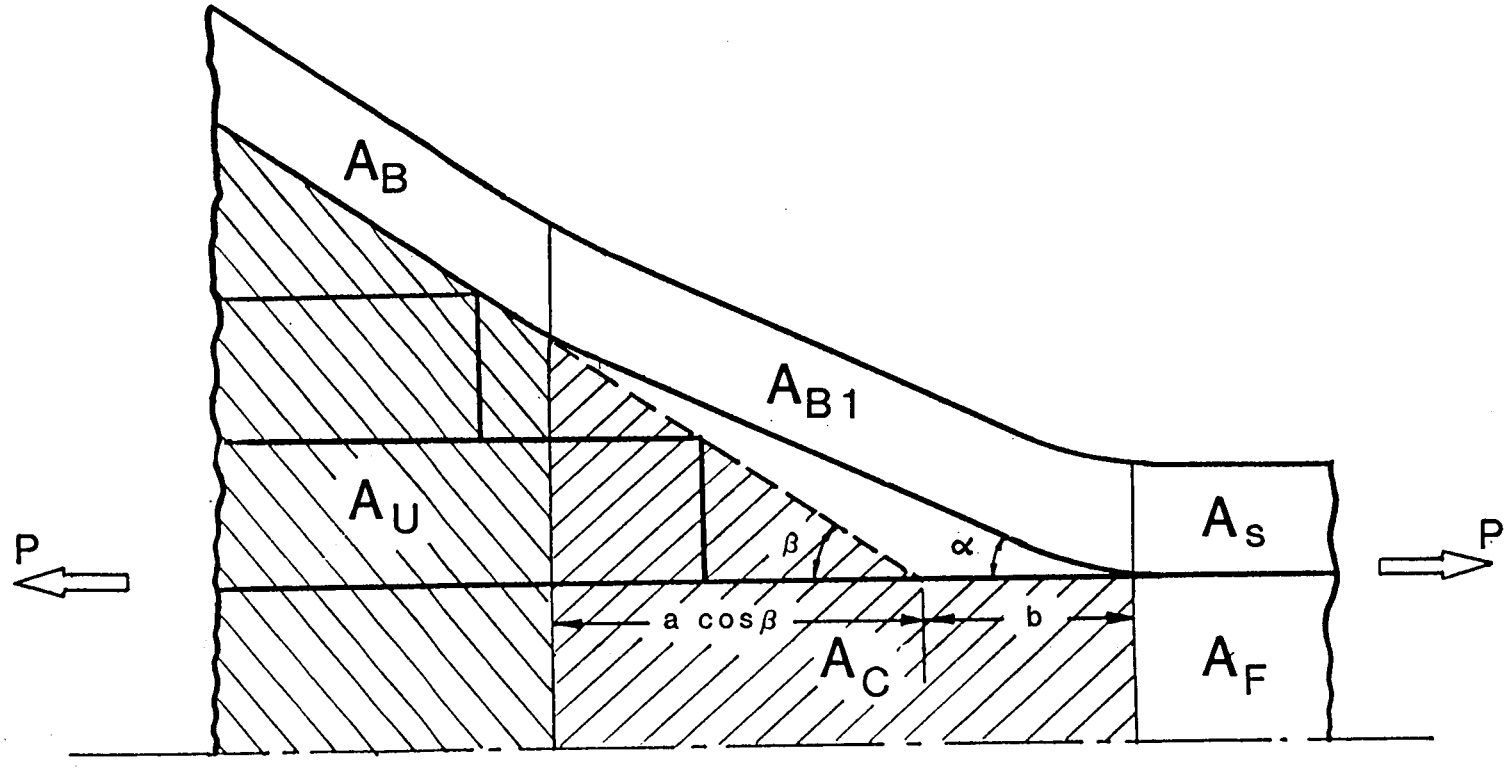

Figure 5. Dependency of Core and Belt Stiffnesses on Delamination

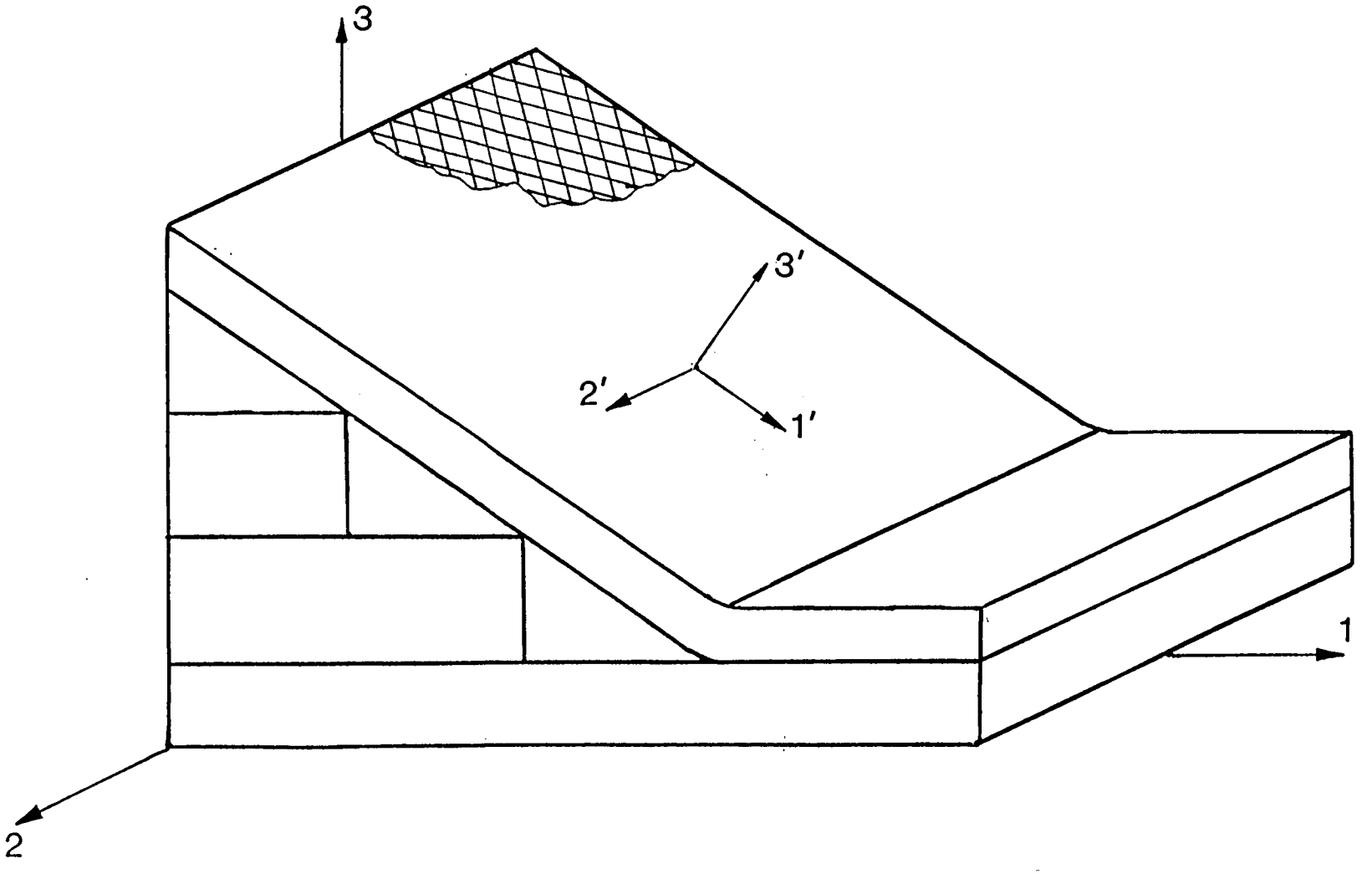

Figure 6. Three Dimensional Coordinates in the belt Region

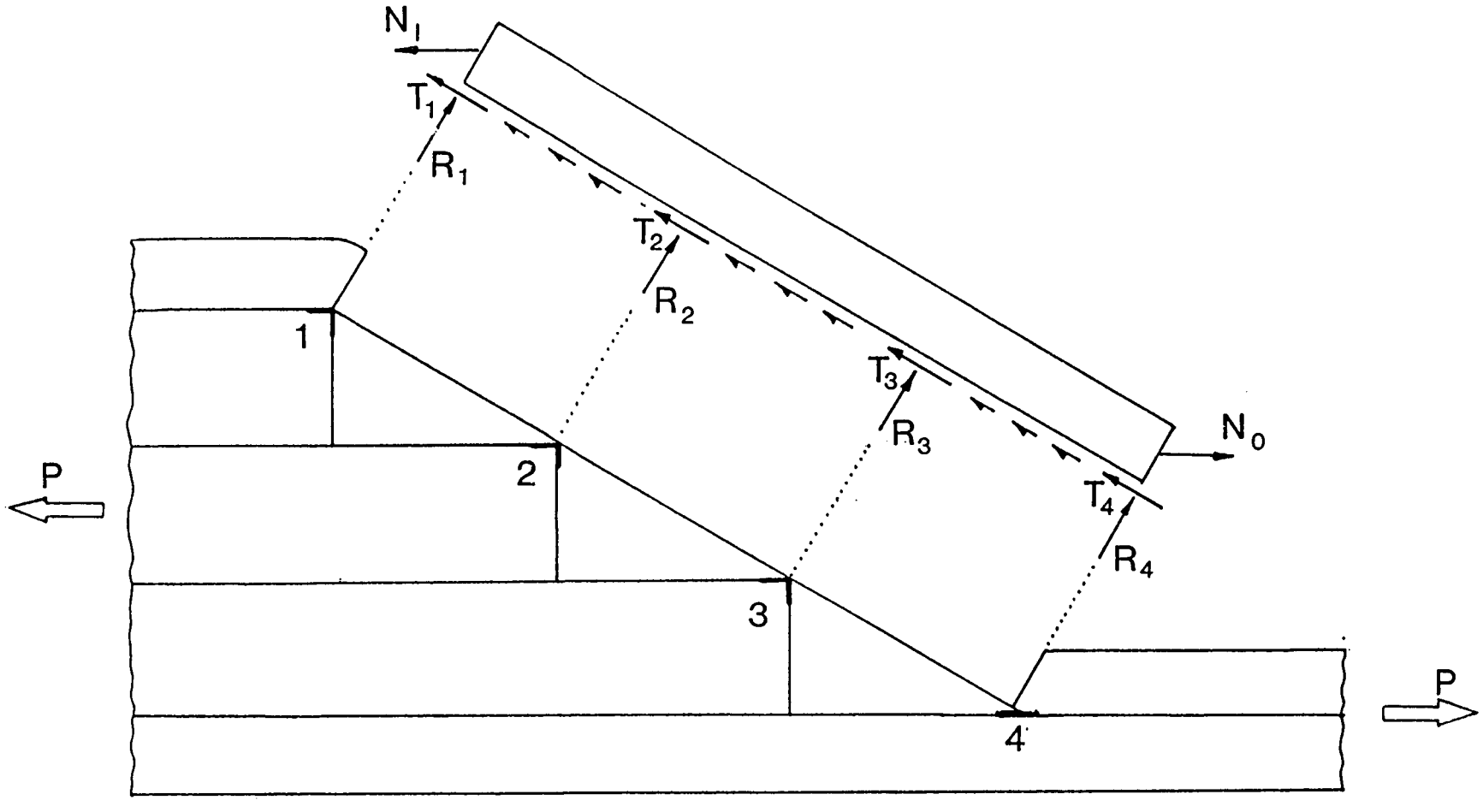

Figure 7. Interlaminar Stresses

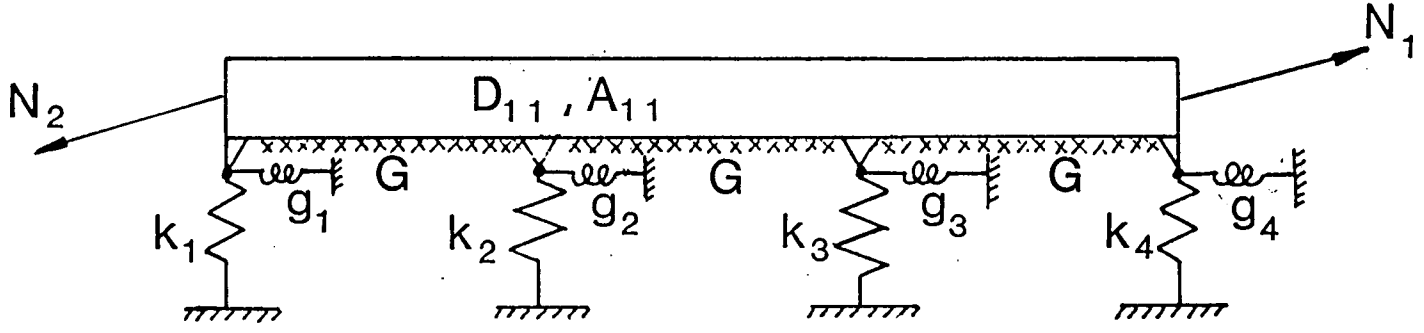

Figure 8. Elastic Stiffnesses and Supporting Conditions

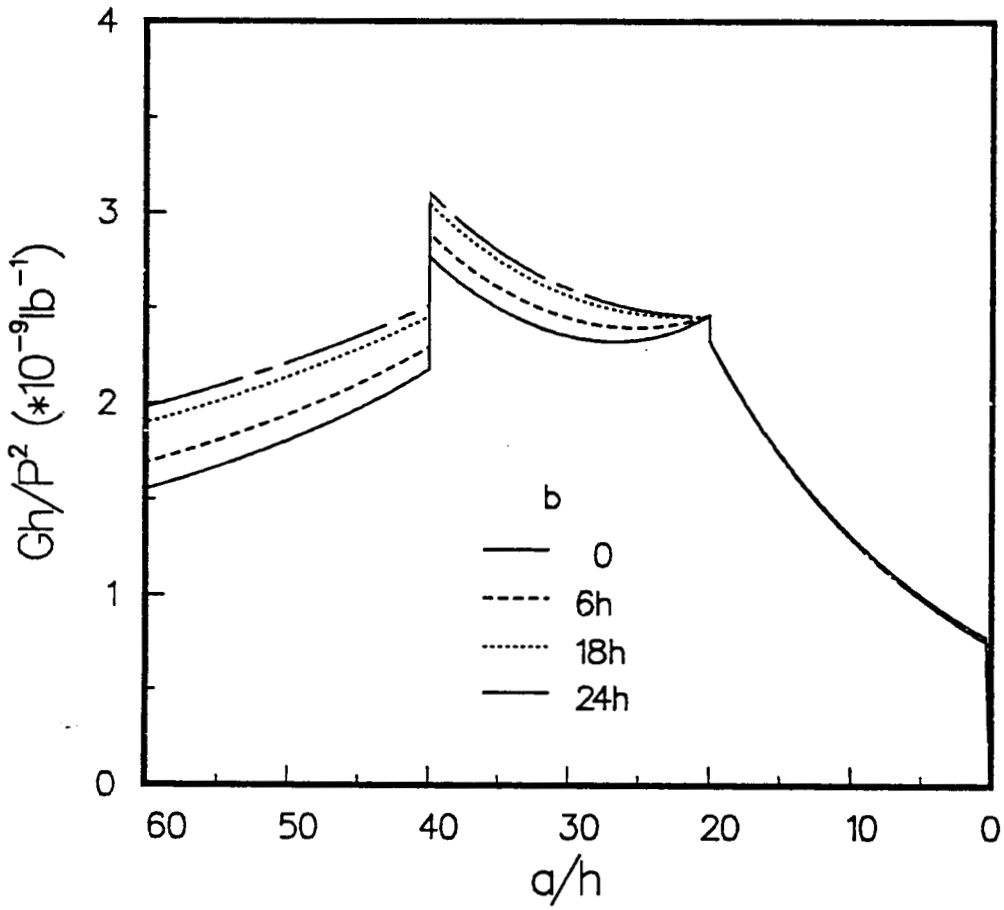

Figure 9. Variation of Total Strain Energy Release Rate with Delamination

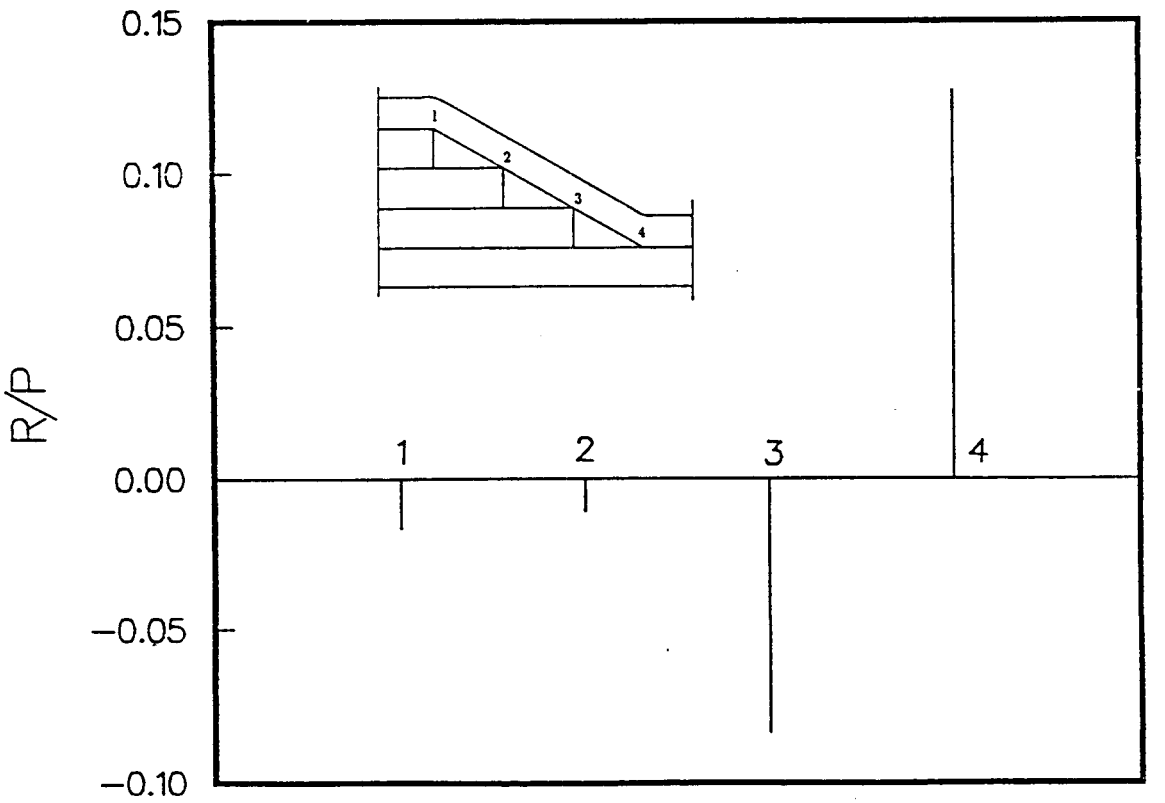

Figure 10 a. Distribution of Concentrated Normal Forces Along the Belt

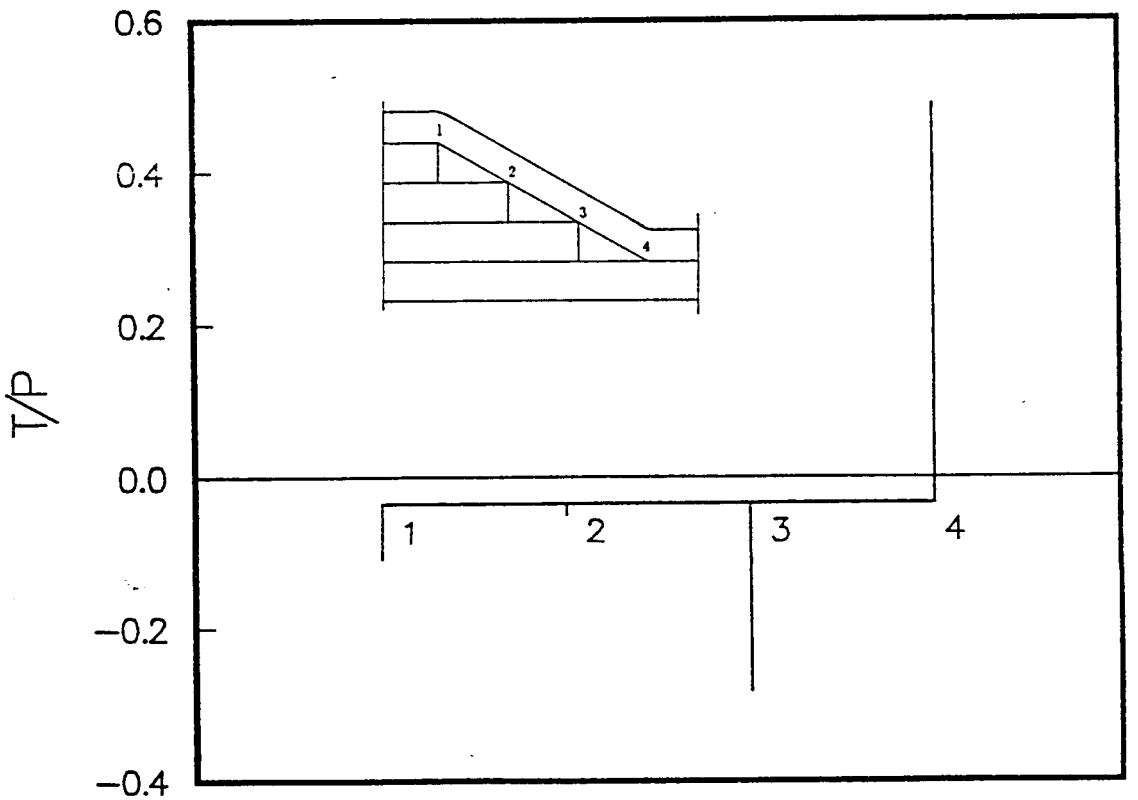

Figure 10 b. Distribution of Concentrated Shear Forces Along the Belt

APPENDIX I

A Study on the Thermal and Moisture Influences on the Free-Edge Delamination of Laminated Composites

By:

Mary A. Mahler

September 1987

A Special Problem Report:

Submitted in Partial Fulfilment for a

--- Master of Science ---

--- Aerospace Engineering Degree ---

Georgia Institute of Technology
School of Aerospace Engineering
Atlanta, Georgia 30332

Acknowledgments

It is with great pleasure that I express my deepest gratitude to my Advisor, Dr. Erian A. Armanios. Without his guidance, encouragement, and patience this work would not have been possible. Our enlightening discussions on delamination, composites, and related matters gave me the incentive to work harder. Throughout my graduate studies, I have learnt a great deal more from him then just the material presented in this report.

I am also indebted to Dr. Lawrence W. Rehfield for his classes and discussions with the Advance Composite Group. His talks about his past experiences were found to be very enhancing to my studies and research.

This research has been sponsored by the NASA Langley Research Center under Grant NAG-1-558. This support is gratefully acknowledged.

The patience of my roommate, Ruth Dolenga, for listening to my frustrations was sincerely appreciated. It was a privilege to have studied and worked with my officemates of the Advance Composites Group. Their words of encouragement, advise, and questions certainly enhanced my year at Georgia Institute of Technology.

At the foundation of all my work is the continuous support and encouragement from my parents, for which I am very grateful for.

Index

List of Figures

List of Tables

Abstract

Laminated composite structures exhibit a number of different failure modes. These include fiber-matrix debonding within individual layers, delamination or separation of the layers, transverse cracks through one or more layers and fiber fracture. These failures are influenced by enviromental conditions. Thermal and moisture conditions are significant factors in interlaminar delamination as well as the other modes of failures.

A simple delamination analysis method is presented here. It is based on a shear-type deformation theory and includes hygrothermal effects. These enviromental conditions are applied to the strain energy release rate and interlaminar shear stresses.

The method is applied to mixed mode edge delamination specimens made of T300/5208 graphite/epoxy material. Residual thermal and moisture stresses significantly influenced the strain energy release rate and interlaminar stresses. Both experienced large increases when thermal conditions were added to the mechanical strains. These effects were alleviated when moisture stresses were included. Thermal effects on the interlaminar shear stress and total energy release rate were totally alleviated for the same specific moisture content. Moreover, this value of moisture content was not significantly affected by the stacking sequence for the laminates considered.

Introduction

Composites have been used in the aircraft industry since 1969. One aspect of concern for using composites in structures is separation of plies or delamination. This occurs in regions of stress raisers such as holes, ply terminations, cut-outs and free edges. Delamination along the free edge of laminates have been observed during testing and service. The presence of delamination, initiated by interlaminar stresses, causes redistribution of the stresses among the plies in a laminate. Thus, it usually results in a reduction of stiffness and strength.

Figure 1 shows delamination in a rotor hub made of S2/SP250 glass/epoxy. The specimen has delaminated in two places that can be depicted by the dark lines. Figure 2 shows delamination in a single cracked-lap-shear test specimen made of AS4/3502 graphite/epoxy[1]. The specimen layup is $[\pm 45/0/90]_{6S}$ quasi-isotropic with 8 plies in the strap and 40 plies in the lap. The tests were performed on a displacement controlled machine. Fiber glass tabs were attached to the specimen ends. Multiple, isolated free edge delaminations occur in the neighborhood of the lap/strap junction and the tab. Figure 3 illustrates an I-beam section made of C3000/5225 graphite/epoxy woven cloth in the post-buckled regime. Free edge delamination depicted in the flanges precipitated the final failure in the specimen. Figure 4 shows how delamination can take place in single cracked-lap-shear specimens subjected to compressive and tensile loading. Specimens A and B delaminated under compressive loading while C experienced a

tensile loading. These examples illustrate the importance of investigating delamination problems in composites.

Thermal residual and moisture effects on a composite are practical enviromental conditions. Determining the response of these conditions on interlaminar stresses and energy release rates in laminated composites is the primary objective of this work.

Delamination analysis can be based on two approaches. They are the strain energy release rate and interlaminar stresses. The interlaminar stresses are due to Poisson's ratio mismatch and difference in the coefficients of thermal and moisture expansion between plies. Delamination occurs when these stresses reach the interlaminar strength of the material. An alternative approach is based on the actual process of fracture rather than the strength concept. Delamination can propagate when the strain energy release rate at the crack front is sufficient to overcome the material's fracture resistance or toughness.

The strain energy release rate can be obtained for three particular modes of crack action. These three modes are known as Mode I or opening mode, Mode II or forward shearing mode and Mode III or tearing mode. Several failure laws are formulated in terms of these modes [2].

A simple analysis predicting interlaminar shear stresses and total energy release rate with the influence of thermal and moisture effects is developed. This simple approach is useful in understanding the basic mechanics of the problem and predicting the factors controlling the behavior. The method is directed to the needs of a practical

design environment. It is not intended to compete with large-scale numerical approaches, but rather to serve as the means for selecting and screening candidate configurations and providing trend information. Simple codes for a desktop computer have been created to analyze laminate configurations.

Literature Summary

A historical discussion of previously developed work for predicting interlaminar stresses and energy release rates is presented to establish a basis for the proposed model and to permit the present work to be placed in proper perspective.

Earlier analyses have reflected the prediction of interlaminar stress and energy release rate without hygrothermal conditions. O'Brien[3,4] investigated delamination onset and growth in graphite/epoxy laminates under uniform extension. A simple expression was developed for the total energy release rate based on classical lamination theory. Whitney and Knight[5] used classical laminated plate theory to develop an edge delamination specimen analysis. This work was limited to Mode I behavior.

An analysis based on a shear deformation theory and a sublaminate formulation [6] was developed by Armanios and Rehfield[7,8]. This method provides good estimates for the interlaminar shear stresses. Energy release rate components are estimated based on these stresses. However, this method does not provide reliable estimates of peel stress since thickness strain is neglected. This analysis was limited to mechanical strain only.

O'Brien[9] modified his analysis to include thermal and moisture conditions. The influence of thermal effects was considered by Whitney[10].

The work of Reference 9 was based on a classical laminated plate theory. It was applied to mixed-mode edge delamination specimens.

The results were limited to strain energy release rate. Finite element modeling was used to determine the strain energy release rate components. O'Brien's results reflected an increase in the strain energy release rate due to thermal effects. It decreased with the addition of moisture considerations. For a T300/5208 graphite/epoxy laminate with $[\pm 30/\pm 30/90/\overline{90}]_s$ layup, the thermal effect increased the total energy release rate by 170 percent when compared to mechanical loading alone. However, a specific moisture level of 0.75 percent completely alleviated this increase. In calculating the total strain energy he showed that bending and coupling effects became important at high levels of moisture content.

In Reference 10 a higher-order plate theory with transverse normal strain effects was developed. Peel as well as interlaminar shear stresses could be predicted by this method. The thermal influence on total energy release rate and interlaminar stresses was investigated using a Mode I specimen. Residual thermal effects showed a significant influence on the stresses and release rates. For a graphite/epoxy laminate of $[0_3, 90_3]_s$ layup, thermal effects increased the maximum peel stress by a factor of 2.7 over that of pure mechanical strains.

In the present work both thermal and moisture influences are studied in a mixed-mode delamination specimen. The analysis includes total energy release rate as well as interlaminar stresses. Similarities between the interlaminar stesses and total energy release predictions with hygrothermal effects is investigated.

In the subsequent sections, the analytical approach is developed.

The method is then applied to six graphite/epoxy laminates. A discussion of the hygrothermal effects on interlaminar shear stress and total energy release rate predictions is provided. Recommendations for further investigations are proposed. Appendices are included for completeness. The first provides detailed expressions of the governing equations. Appendix II defines the hygrothermal expressions and their use in the analysis. The last appendix shows a listing of the program used and sample output.

Analytical Approach

Overview

The sublaminate modeling approach describes the essential features of the laminate behavior in a simple way. A free edge delamination specimen is shown in Figure 5. A uniform strain , ϵ, is applied in the axial direction. From symmetry, only one quarter of the specimen is considered. In Figure 6, the specimen is modeled as if it were composed of four distinct sublaminates. Sublaminates 2 and 3 represent the group of plies above and below the crack, respectively in the cracked portion of the laminate, while sublaminates 1 and 0 denote the same group of plies in the uncracked portion of the laminate.

The use of sublaminates -- groups of plies that are conveniently treated as laminated units -- simplifies the analysis considerably. This approach is applied with confidence when the characteristic length of the response is large compared to the individual sublaminate thickness[6]. This sublaminate modeling approach has been verified in Reference 7 by comparison with a ply-by-ply finite element solution. These sublaminates are connected by enforcing the proper continuity conditions on stresses and displacements at their interfaces.

Displacement fields within each sublaminate are defined as:

$$u = x\epsilon + U(y) + z\beta_x(y)$$

$$v = V(y) + z\beta_y(y) \qquad (1)$$

$$w = W(y)$$

where u,v, and w denote the displacements relative to the x, y, and z axes, respectively. Shear deformation is recognized through the rotations β_x and β_y. The governing equations for each sublaminate are derived using a virtual work approach. The derivation of the governing equations used in the development appears in Appendix I. The derivation is an extension of the work of Reference 8 with hygrothermal effects included.

The constituitive relationships in terms of these force and moment resultants can be written as

$$N_i = A_{ij}\,\epsilon_j + B_{ik}\,\kappa_k - N_i^{NM} \qquad (i,j,k = 1,2,6)$$

$$M_i = B_{ij}\,\epsilon_j + D_{ik}\,\kappa_k - M_i^{NM} \qquad (i,j,k = 1,2,6) \qquad (2)$$

$$Q_i = A_{ij}\,\epsilon_j \qquad (i,j = 4,5)$$

where the subscripts x, y, z, yz, xz, and xy are replaced by the subscripts 1-6 respectively. The force and moment resultants are denoted by N_i and M_i, respectively. Non-mechanical forces and moments resulting from the hygrothermal effects are labeled with a superscript NM. They are defined as:

$$(N_i^{NM},\ M_i^{NM}) = \int_{-h/2}^{h/2} Q_{ij}(1,z)\ (\alpha_j\,\Delta T + b_j\,C)\ dz \qquad (3)$$

The swelling coefficient is denoted by b_j in Equation (3), the thermal coefficient by α_j. The change in temperature is denoted by ΔT and moisture weight gain by C.

The elastic stiffnesses A_{ij} , B_{ij} , and D_{ij} are defined in terms of the sublaminate reduced stiffness Q_{ij} for a plane stress situation. These bear the classical definition.

$$(A_{ij} , B_{ij} , D_{ij}) = \int_{-h/2}^{h/2} (1,z,z^2) Q_{ij} \, dz \qquad (4)$$

The equilibrium equations are:

$$\begin{aligned} &N_{xy,y} + (t_{2x} - t_{1x}) = 0 \\ &N_{y,y} + (t_{2y} - t_{1y}) = 0 \\ &Q_{y,y} + (p_2 - p_1) = 0 \qquad (5) \\ &M_{xy,y} - Q_x + h/2 \, (t_{2x} + t_{1x}) = 0 \\ &M_{y,y} - Q_y + h/2 \, (t_{2x} + t_{1x}) = 0 \end{aligned}$$

where t_{2x}, t_{2y}, p_2 and t_{1x}, t_{1y}, p_1 denote the interlaminar stress components in the x-z, y-z and z directions at the sublaminate upper and lower surfaces, respectively. These stress components appear in Figure 7.

The displacements, resultant forces and moments, and interlaminar shear stresses in each sublaminate is governed by the displacement distribution (1), constituitive (2), and equilibrium (5) equations. These equations are applied to each sublaminate. The variables associated with each sublaminate are coupled through the continuity requirements at their interfaces. Enforcement of the boundary conditions lead to a solution for these variables. This procedure

discussed in general terms above is applied to the analysis of the edge delamination specimen shown in Figure 2 in the following sections.

The response associated with sublaminates 1 and 0 shown in Figure 2 is coupled through the continuity conditions at their common interface. The situation is different with sublaminate 2 and 3 where the continuity conditions are relaxed due to the presence of the crack.

Uncracked Region: Sublaminates 0 and 1

From symmetry conditions at the sublaminate bottom surface the shear stresses are zero. Interlaminar stresses at the top surface of sublaminate 0 are equal to those on the bottom of sublaminate 1. Substituting these conditions into the equilibrium and constitutive relations and enforcing continuity of displacements at their common interface yields a homogeneous system of ordinary differential equations. These can be expressed in terms of the sublaminate rotations β_x and β_y. Assuming an exponential solution of the form

$$(\beta_{1x}, \beta_{0x}, \beta_{1y}, \beta_{0y}) = (\beta^*_{1x}, \beta^*_{0x}, \beta^*_{1y}, \beta^*_{0y})\, e^{sy} \quad (6)$$

results in a characteristic equation of the form

$$E_8 s^8 + E_6 s^6 + E_4 s^4 + E_2 s^2 + E_0 = 0 \quad (7)$$

Parameter E_0 depends only on the stiffness coefficients A_{44}, A_{55} and A_{45} for both sublaminates while E_8 is predominantly influenced by the bending and coupling coefficients D_{ij} and B_{ij}. Thus, its

numerical value can be orders of magnitude smaller than the other coefficients. This results in the presence of a boundary zone in the response.

The characteristic roots controlling the behavior of the laminate are determined from Equation 7 which has a closed-form solution.

Crack Region of the Laminate: Sublaminates 2 and 3

With this group of laminates, there are free surfaces at both the top and bottom of sublaminates 0 and 1 respectively. This is due to the presence of the crack. With the crack dividing the sublaminates, continuity conditions are not enforced at the boundary interface. This results in zero shear stresses at the surfaces of each sublaminate. Thus, the equilibrium and constitutive relations combine to produce a second order differential equation in terms of the sublaminate rotations β_{2X} for sublaminate 2 and β_{3X} for sublaminate 3.

Interlaminar Stresses

The arbitrary constants that are obtained from the eighth degree polynomial are determined by enforcing the stress free boundary conditions at the free edges of sublaminates 2 and 3, and the continuity of force, moment, displacement and rotations between sublaminates 0 and 3, as well as between 1 and 2. This yields the following expression for the interlaminar shear stresses.

$$t_X = N_{XY_1,Y} = G_j \, e^{-s_j y} \tag{8}$$

$$t_Y = N_{Y_1,Y} = T_j \, e^{-s_j y} \qquad (j = 1 - 4) \tag{9}$$

Parameters T_j and G_j represent the amplitude of the response.

Energy Release Rate

A complete formulation of the strain energy release rate appears in Appendix II. The total energy release rate can be determined by considering the work done by external forces.

$$G = -1/2 * dW/da \tag{10}$$

The total energy release rate is denoted by G and the crack length by a. The work done is defined as

$$W = L/2\int_0^b N_{xi}\epsilon_{mi}\, dy \tag{11}$$

where subscript i denotes the sublaminate being referenced. The term ϵ_{mi} represents the mechanical strain in each ply. This is defined as the difference between the total strain and the strain corresponding to free expansion for each ply. This strain is estimated by using a procedure similar to Reference 5. However, in Reference 5 the free expansion strain was determined by considering groups of plies in the cracked and uncracked regions of a Mode I edge delamination specimen. This approach is valid for a limited class of laminates. A ply-by-ply analysis rather than a sublaminate modeling should be used. In the following analysis, free expansion strains are determined on a ply-by-ply basis.

From the symmetric conditions that exist in the uncracked section of the laminate, there exist no curvature. In the cracked portion,

the moment about the y-axis is assumed to be zero. Using both of these boundary conditions in Equation (2) yields the following.

$$N_{x1} = A_{11}\epsilon + A_{12}\epsilon_y + A_{16}\epsilon_z - N_{x1}^{NM} \qquad (12)$$

$$N_{x1} = A_{11}\epsilon + A_{12}\epsilon_y + A_{16}\epsilon_z + B_{12}\kappa_y - N_{x2}^{NM}$$

Strain components ϵ_y and ϵ_z in Equation 12 are expressed in terms of the applied strain by

$$\epsilon_y = C_v\,\epsilon + C_v^{NM} \qquad (13)$$

$$\epsilon_z = C_u\,\epsilon + C_u^{NM}$$

The terms C_v, C_u, C_v^{NM} and C_u^{NM} are functions of the extensional stiffness components A_{ij} of sublaminates 1 and 0.

Using these expressions, Equation 12 can be re-written in the form.

$$N_{xc}^k = (E_c^k \epsilon_c^k + T_c^k) \qquad (14)$$

$$N_{xu}^k = (E_u^k \epsilon_u^k + T_u^k)$$

Parameters E_c^k, T_c^k, E_u^k and T_u^k are defined in Appendix II. Superscript k denotes the individual ply. Subscripts u and c represent the uncracked and cracked portions, respectively. The non-mechanical strain in each ply corresponding to a state of free

expansion is obtained by allowing the stress in each ply to vanish. This yields the following.

$$\epsilon_u^k = -T_u^k / E_u^k \qquad (15)$$

$$\epsilon_c^k = -T_c^k / E_c^k$$

The strain corresponding to free expansion of the entire laminate is obtained by letting the resultant force vanish. The non-mechanical strain is

$$\epsilon^{NM} = \left\{ T_u^* - (T_u^* - T_c^*)\ 2a/b \right\} / \left\{ E_u^* - (E_c^* - E_u^*)\ 2a/b \right\} \qquad (16)$$

The terms T_u^*, T_c^*, E_u^* and E_c^* represent the summation of T_u^k, T_c^k, E_u^k and E_c^k over their respective sublaminates. These strain definitions for the effects of moisture and temperature can now be used in the general expression for the strain energy. The strain field is altered to represent the hygrothermal effects. The total strain for a sublaminate is expressed as:

$$\epsilon^T = \epsilon + \epsilon^{NM} \qquad (17)$$

The strain energy expression is given below showing the use of Equations (13) and (17).

$$W = \frac{L}{2}\left[\sum (E_c^k \epsilon^T + T_c^k)\ (\epsilon^T - \epsilon_c^k) + (E_u^k \epsilon^T + T_u^k)\ (\epsilon^T - \epsilon_u^k) \right] \qquad (18)$$

Substituting this into Equation (11) yields the total strain energy release rate per crack.

Results and Discussion

Benchmark Study

The analytical model is applied to the edge delamination specimen shown in Figure 5. The material considered is T300/5208 graphite/epoxy. Its mechanical properties are listed in Table I. The coefficients of swelling and thermal expansions are also stated. The geometry of the specimen is given in Table II. Cure temperature for this material is 350°F. The ambient operating temperature is 70°F. The moisture level for all cases was allowed to vary from 0 to 1.2 percent of the laminate weight. This moisture level reflects feasible conditions. The mechanical strain is taken as 0.00254. This particular value of strain was taken from test experiments[9]. It is considered a practical value for the material.

Six laminates have been analyzed. They can be divided into two groups. The first group is composed of laminates $[35/-35/0/\underset{\uparrow}{90}]_s$, $[35/0/-35/\underset{\uparrow}{90}]_s$, and $[0/35/-35/\underset{\uparrow}{90}]_s$. These laminates are prone to delaminate at the interfaces indicated by the arrow[9]. The Mode III in these laminates is negligible. This is due to the fact that relative sliding at the crack front and the interlaminar shear stress in the x-z direction, τ_{xz}, is neglegible. The second group of laminates is $[30/-60/\underset{\uparrow}{75}/15]_s$, $[-35/55/\underset{\uparrow}{10}/-80]_s$, and $[35/80/\underset{\uparrow}{-55}/-10]_s$. In these laminates Mode I, Mode II, and Mode III are finite. The Mode III strain energy release rate component due to mechanical loading in these laminates are significantly large, ranging from 60 to 90

percent[7].

Interlaminar Shear Stresses

The interlaminar stress τ_{yz} at the delamination interface appear in Figure 8 - 10, for the first group of laminates. The interlaminar shear stresses τ_{xz} and τ_{yz} for the second group of laminates appear in Figures 11 - 13. The labels M, M+T, and M+T+H stand for mechanical, mechanical and thermal, and mechanical, thermal and moisture respectively.

The boundary layer of decay for all laminates ranged from 0.85 to 0.93 of the laminate semi-width. In this context the boundary layer decay length is defined as the distance where the stress decays to 5 percent of its maximum value. The stress boundary zone is not significantly influenced by the environmental conditions.

The magnitude of shear stress however showed a strong dependency on thermal and moisture conditions. At the delamination front, the ratio of stress with thermal effects as compared to pure mechanical loading ranged from 3.22 to 3.36 for the first group of laminates. This maximum was experienced at the crack tip. For the laminates where Mode III was present, this ratio ranged from 4.16 to 5.23 for τ_{yz}. The shear in the x-z direction showed a ratio of 1.4 to 2.16 for the maximum stresses. The maximum τ_{yz} stress for the second group of laminates was experienced at the crack front. However, the maximum τ_{xz} stress occured slightly ahead of the crack. This can be seen in Figures 11 - 13.

The addition of moisture alleviated the thermal effect. A moisture content of 0.4 has reduced the stress of thermal influence by approximatly 40 percent as compared to thermal influences alone. This trend is similar to the results of Reference 9.

Numerical values of interlaminar shear stress at various moisture levels are provided in the sample output of Appendix III. Interlaminar shear stresses show numerical decrease with increase of moisture levels.

Energy Release Rate

The hygrothermal effect on total energy release rate appears in Figures 14 -15. The hygrothermal effects on total energy release rate show a similar trend to that of interlaminar shear stresses. Residual thermal stress tends to increase total energy release rate while residual moisture alleviates this effect. The figures show that for total alleviation of the thermal effect, the specific moisture content ranges between 0.70 and 0.77 for all laminates. This indicates there exist a weak dependency on the stacking sequence.

The effects of thermal conditions alone on the energy release rate does not correspond to the same numerical value as the interlaminar shear stresses. The total energy release rate of layups where Mode III was negligible showed a ratio of 5.1 for mechanical and thermal compared to mechanical conditions only. For the laminates where Mode III is finite, this ratio varied from 1.6 in the $[30/-60/75/-15]_s$ layup to 3.37 in the $[35/80/-55/-10]_s$ layup.

The total energy release rate in the first group of laminates is approximately the same for mechanical loading as shown in Figure 14. The influence of thermal and moisture does not appear to alter this trend. The energy release rate for the $[35/-35/\underset{\uparrow}{0}/90]_s$ laminate is indistinguishable from the $[0/35/\underset{\uparrow}{-35}/90]_s$ layup. The rate of alleviation due to moisture is the same for the three laminates. This is in contrast with the alleviation rate of the laminates where Mode III is finite as shown in Figure 15. For this class of laminates, the rate of alleviation due to moisture is different for each laminate.

In some of the laminates, the rate of alleviation is not constant. There is a steep gradient in the rate of alleviation until the moisture content approaches the totally alleviated state. After such moisture content, the decrease in total energy release rate with respect to moisture addition is not as significant.

It is worth noting there is a similarity between the strain energy release rate prediction and the interlaminar stresses for the totally alleviated state. This is shown in Figure 16 for a $[-35/55/\underset{\uparrow}{10}/-80]_s$ layup. The specific moisture percent producing complete alleviation of the total energy release rate from the thermal effect is 0.76 as seen in Figure 15. The interlaminar shear stress distribution corresponding to this level of moisture is indistinguishable from the mechanical loading alone. The same conclusion was reached studying the other laminates.

Conclusions

A simple analysis was developed that predicted the influence of thermal and moisture effects on the interlaminar shear stresses and strain energy release rate. The analysis was applied to six mixed-mode edge delamination specimens. The results provide several significant findings.

1. Residual thermal strain has a significant influence on the interlaminar shear stress and total energy release rate. The interlaminar stress and total energy release rate increased by 330 and 510 percent respectively over that of pure mechanical loading.

2. Moisture tends to alleviate the thermal effect for both the interlaminar stress and energy release rate. At a specific moisture content of approximately 0.75 percent, the thermal influence is totally alleviated.

3. The moisture content for total alleviation found from the total energy release rate analysis also produced an interlaminar stress distribution similar to pure mechanical loading conditions.

The first two findings are in agreement with the results of previous investigators. The third finding is new. It establishes a similarity in behavior between a delamination analysis expressed in terms of the energy release rate and the strength approach expressed

by the interlaminar stresses.

These findings point to new directions for further inquiry. These are discussed in the following section.

Recommendations

The thermal effects on the laminates showed a large increase in both the interlaminar shear stresses and strain energy release rate. The analysis should be supplemented with experimental tests to verify the result. Several fracture laws are expressed in terms of the strain energy release components, as well as the total strain energy. Further analysis should include predictions of these components in the presence of hygrothermal conditions.

Throughout this work the temperature is assumed to be uniform through the thickness of the laminate. The same is true with the moisture. An approach corresponding to a practical environment method should account for temperature and moisture gradients in the laminate. In this situation, the hygrothermal gradients through the thickness may create an unbalance effect in an originally balanced construction. This consideration is of significant importance in aerospace structural components subjected to a large temperature difference between the upper and lower surface.

The loading considered here is uniaxial extension. However, it is known that the load transfer points are not always in the plane of the laminate. Therefore, investigating laminate response under combined loads is of great practical importance. It is recommended that bending, torsion as well as their combined effect be addressed.

Findings by previous investigators suggested that delamination behavior in laminates subjected to fatigue loading follows static loading conditions. Further work is needed to investigate the

influence of hygrothermal conditions on the delamination of laminates under fatigue loading.

Finally, the present analysis is applied to the mixed-mode edge delamination specimen. Extension of this work to other specimens such as the single- and double-crack-lap shear and the Mode II edge notch flexure specimen is recommended.

When accomplished, these recommendations, together with the present research will provide a better understanding of the delamination problem in composites. Consequently, this will enable predicting, managing and ultimately preventing interlaminar fracture in laminated composites.

References

1. Armanios, E.A., Rehfield, L.W., and Reddy, A.D., "Design Analysis and Testing for Mixed-Mode and Mode II Interlaminar Fracture of Composites," Composite Materials: Testing and Design (Seventh Conference), ASTM STP 893, J.M. Whitney, Ed., American Society for Testing and Materials, Philadelphia, 1986, pp. 232-255.

2. Russel, A.J. and Street, K.N., "Moisture and Temperature Effects on the Mixed-Mode Delamination Fracture of Unidirectional Graphite/Epoxy", Delamination and Debonding of Materials, ASTM STP 876, W.S. Johnson, Ed., American Society for Testing and Materials, 1985, pp. 349-370.

3. O'Brien, T.K., "Characterization of Delamination Onset and Growth in a Composite Laminate," Damage in Composite Materials, ASTM STP 775, K.L. Reifsnider, Ed., American Society for Testing and Materials, 1982, pp. 140-167.

4. O'Brien, T.K., "Mixed-Mode Strain-Energy-Release Rate Effects on Edge Delamination of Composites," Effects of Defects in Composite Materials, ASTM STP 836, American Society for Testing and Materials, 1984, pp. 125-142.

5. Whitney, J.M. and Knight, M., "A Modified Free-Edge Delamination Specimen," Delamination and Debonding of Materials, ASTM STP 876. W.S. Johnson. Ed., American Society for Testing and Materials, Philadelphia, 1985, pp. 298-314.

6. Armanios, E.A., "New Methods of Sublaminate Analysis for Composite Structures and Applications to Fracture Processes," Ph.D. Thesis, Georgia Institute of Technology, March 1985.

7. Armanios, E.A. and Rehfield, L.W., "Interlaminar Analysis of Laminated Composites Using a Sublaminate Approach," Proceedings of the AIAA/ ASME/ASCE/ASH 27th Structures, Structural Dynamics, and Materials (SDM) Conference, San Antonio, Texas, 19-21 May 1986. AIAA Paper No. 86-0969CP, Part 1, pp. 442-452.

8. Armanios, E.A. and Rehfield, L.W., "Sublaminate Analysis of Interlaminar Fracture in Composites," Final Report, NASA Grant NAG-1-558, March 1986. Also to be published as a NASA Contractor Report.

9. O'Brien, T.K., Raju, I.S., and Garber, D.P., "Residual Thermal and Moisture Influences on the Strain Energy Release Rate Analysis of Edge Delamination," Journal of Composites Technology and Research, Vol. 8, No. 2, Summer 1986, pp. 37-47.

10. Whitney, J.M. "Stress Analysis of a Mode I Edge Delamination Specimen for Composite Materials," AIAA Paper 85-0611, presented at the 26th AIAA/ASME/ASCE/AHS Structures, Structural Dynamics and Materials Conference, April 15-17, 1985, Orlando, Florida.

TABLE I - T300/5208 GRAPHITE/EPOXY PROPERTIES

E_{11} = 18.7 MSI

E_{22} = 1.23 MSI

G_{12} = 0.832 MSI

Poisson Ratio = 0.292

Swelling Coefficients of the Material direction:

b(1-direction) = 0

b(2-direction) = 5560 με/%weight

Thermal Coefficients of the Material direction:

α(1-direction) = -.23 με/°F

α(2-direction) = 14.9 με/°F

TABLE II - GEOMETRIC DIMENSIONS OF SPECIMEN

Ply thickness = 0.0054 inch

Width = 1.5 inch

Crack length = 6 x ply thickness = 0.0324 inch

FIGURES 1-16

FIGURE 1 - GLASS/EPOXY ROTOR HUB AFTER DELAMINATION

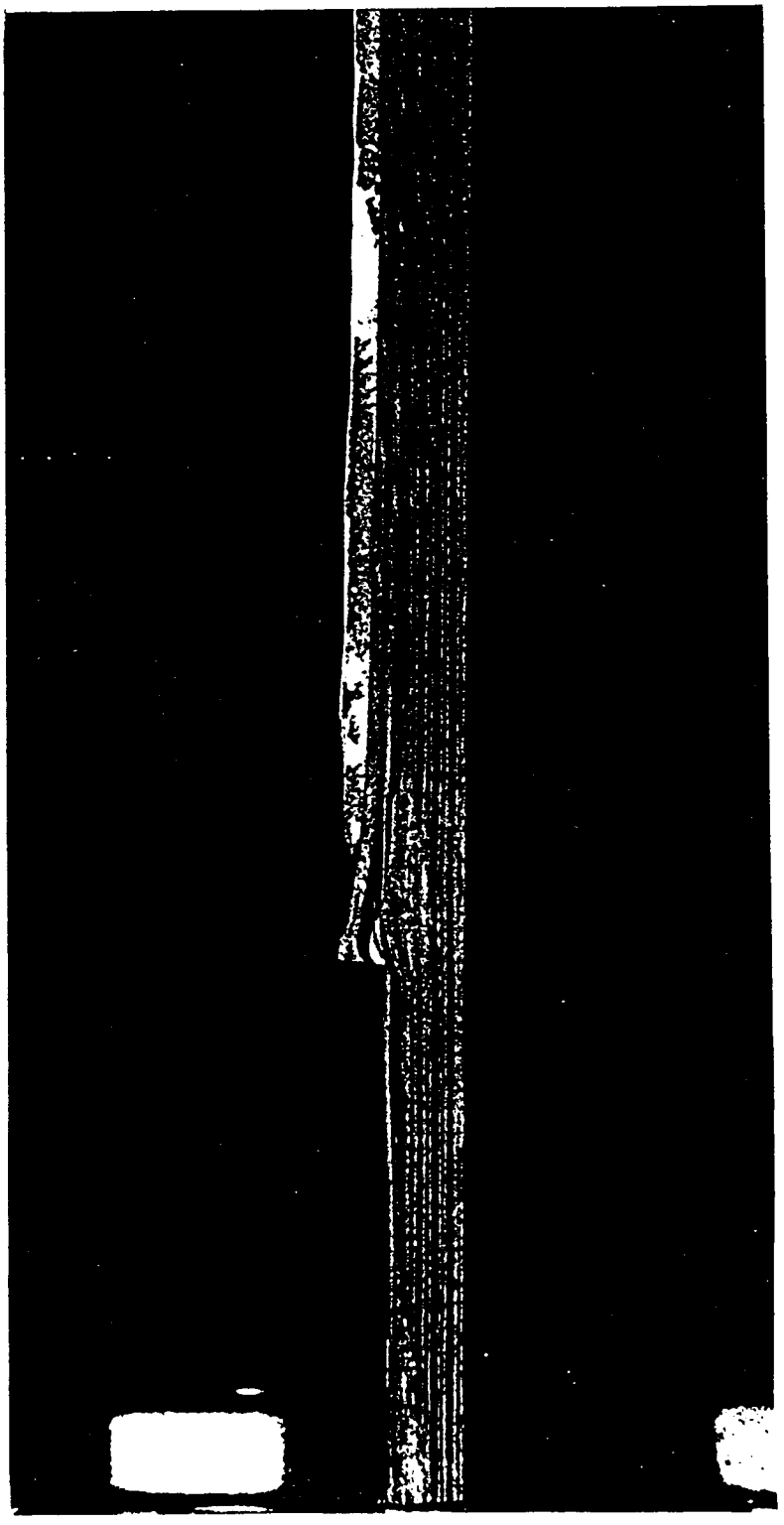

FIGURE 2 - GRAPHITE/EPOXY SINGLE CRACK-LAP-SHEAR SPECIMEN

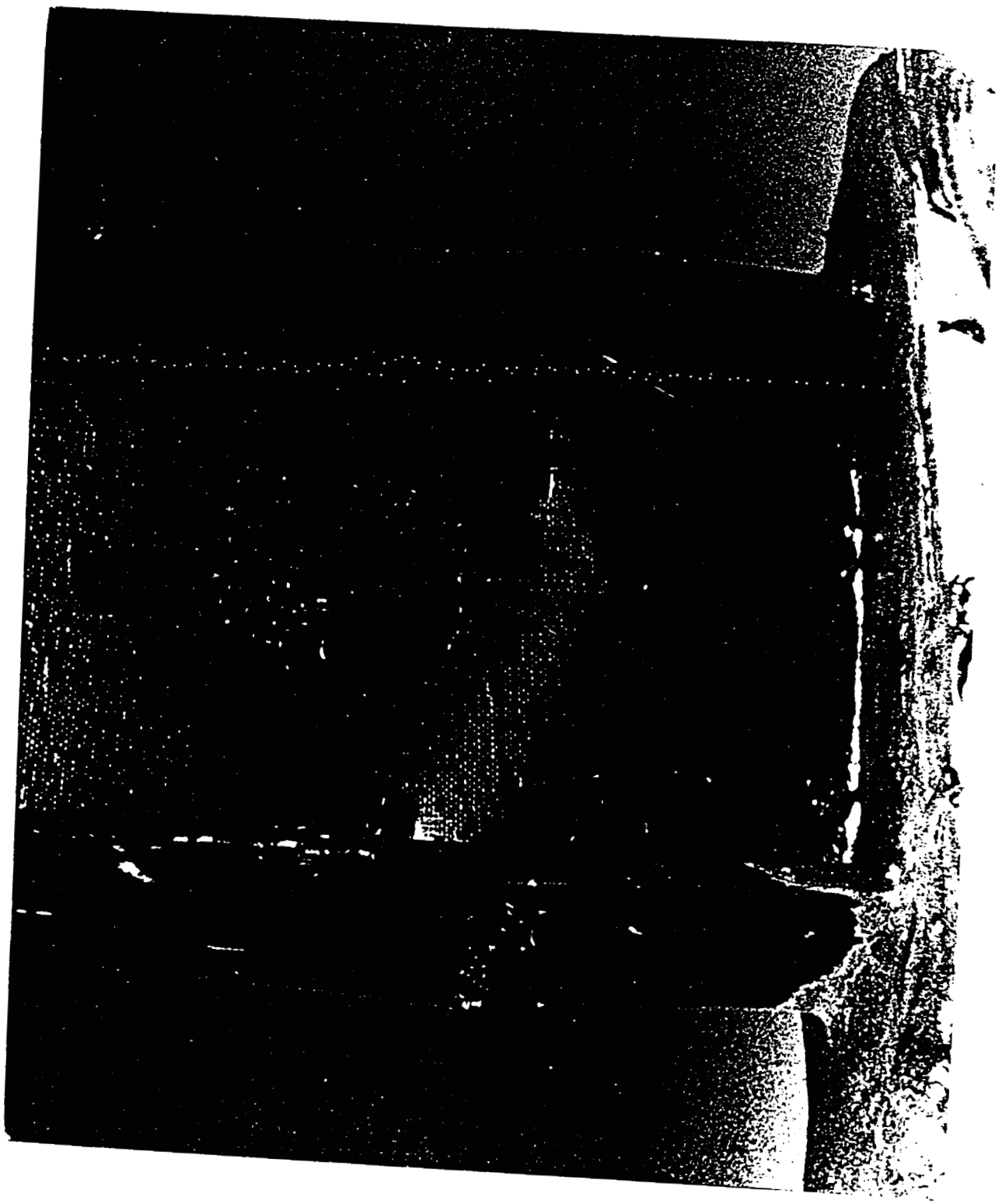

FIGURE 3 - GRAPHITE/EPOXY POST-BUCKLED I-BEAM

FIGURE 4 - COMPRESSIVE AND TENSILE DELAMINATION SPECIMENS

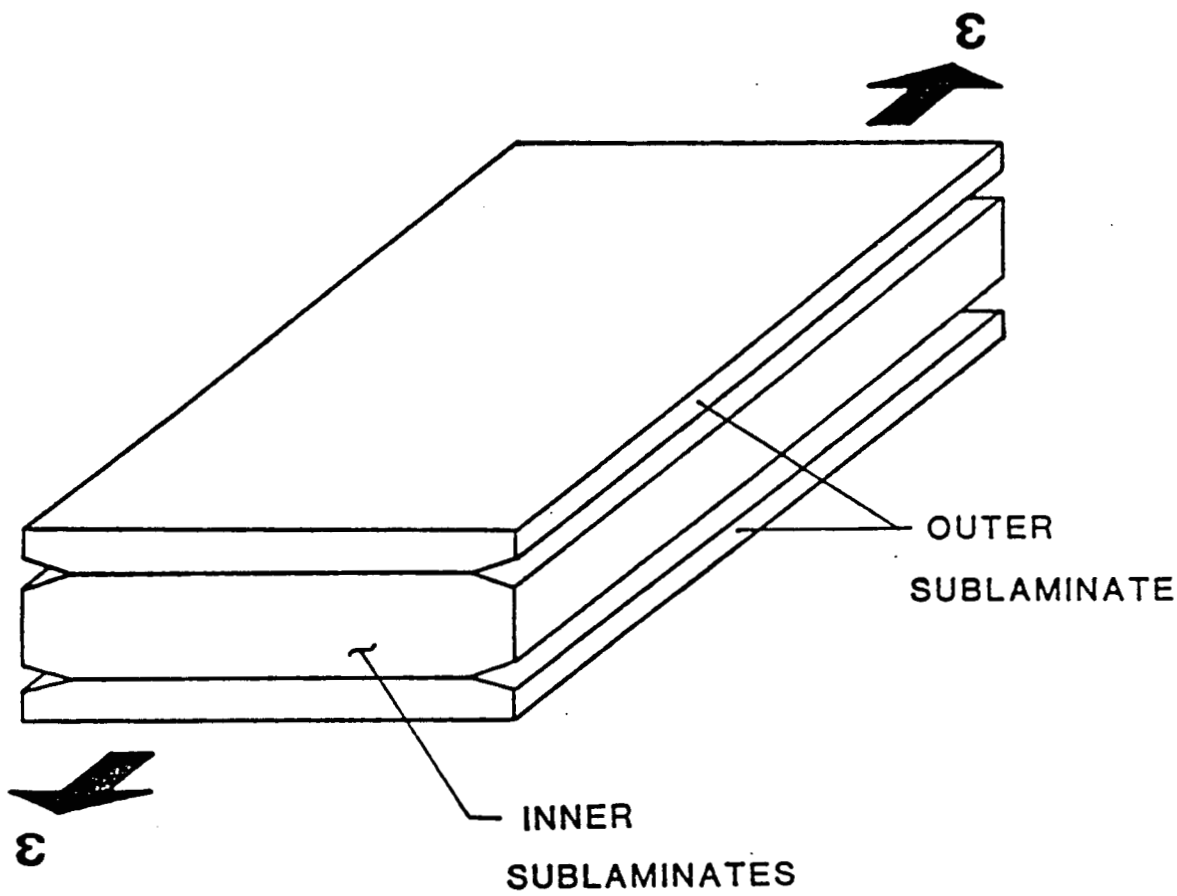

FIGURE 5 - FREE EDGE DELAMINATION SPECIMEN

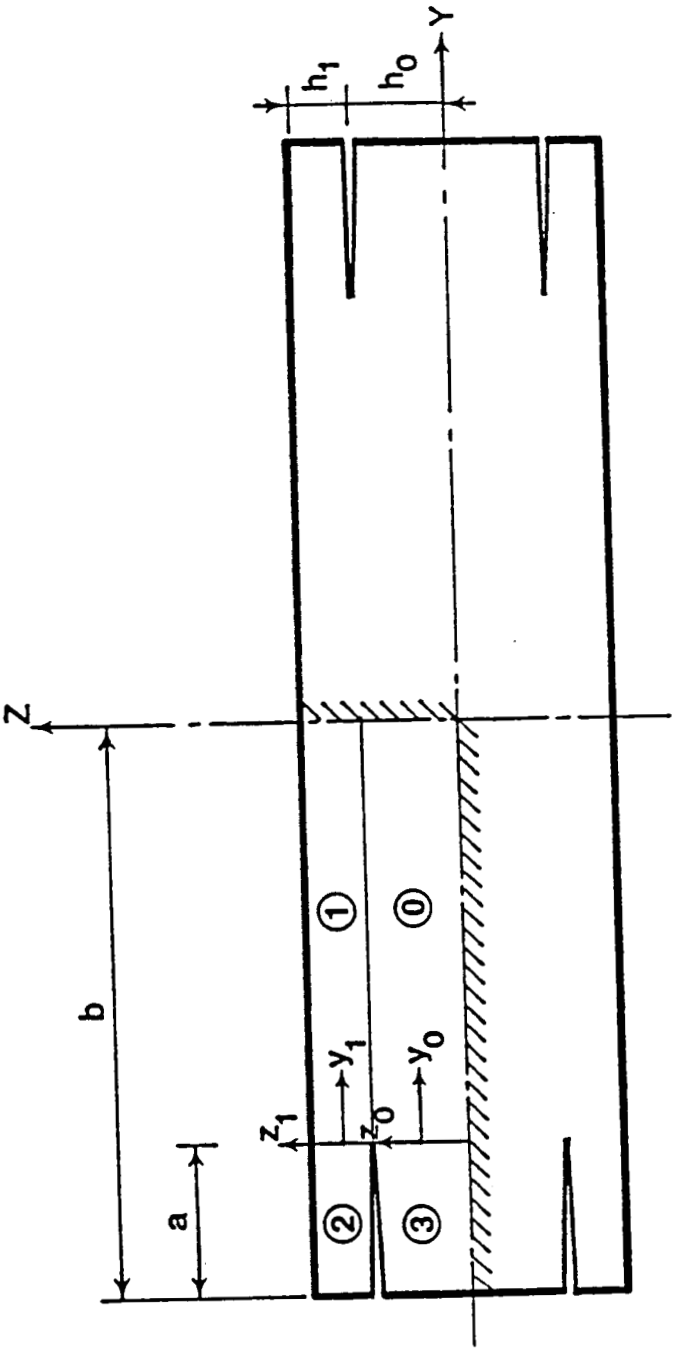

FIGURE 6 - SUBLAMINATE DESCRIPTION AND COORDINATE SYSTEM

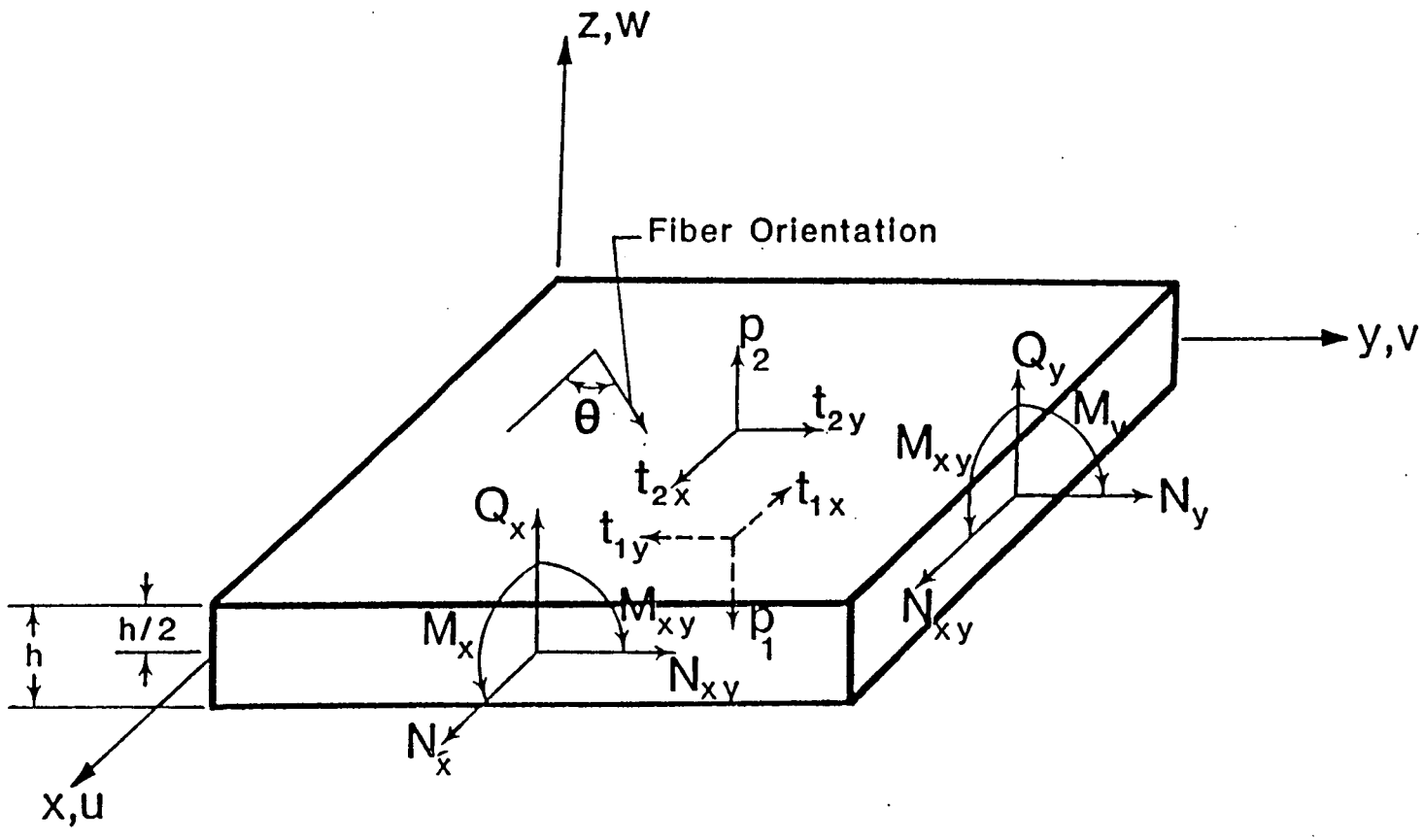

FIGURE 7 - NOTATIONS AND SIGN CONVENTION FOR GENERIC SUBLAMINATE

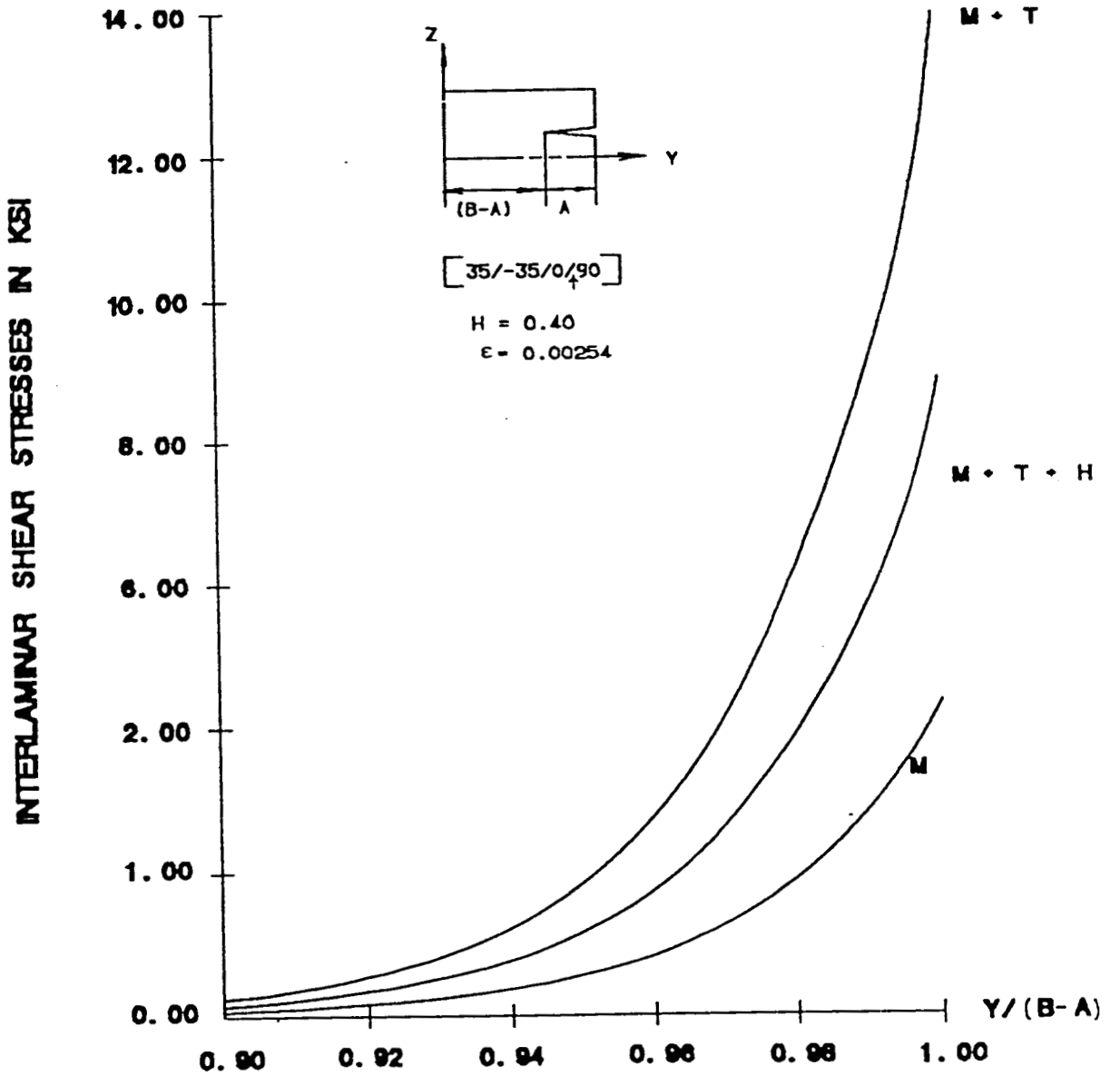

FIGURE 8 - COMPARISON OF INTERLAMINAR STRESS

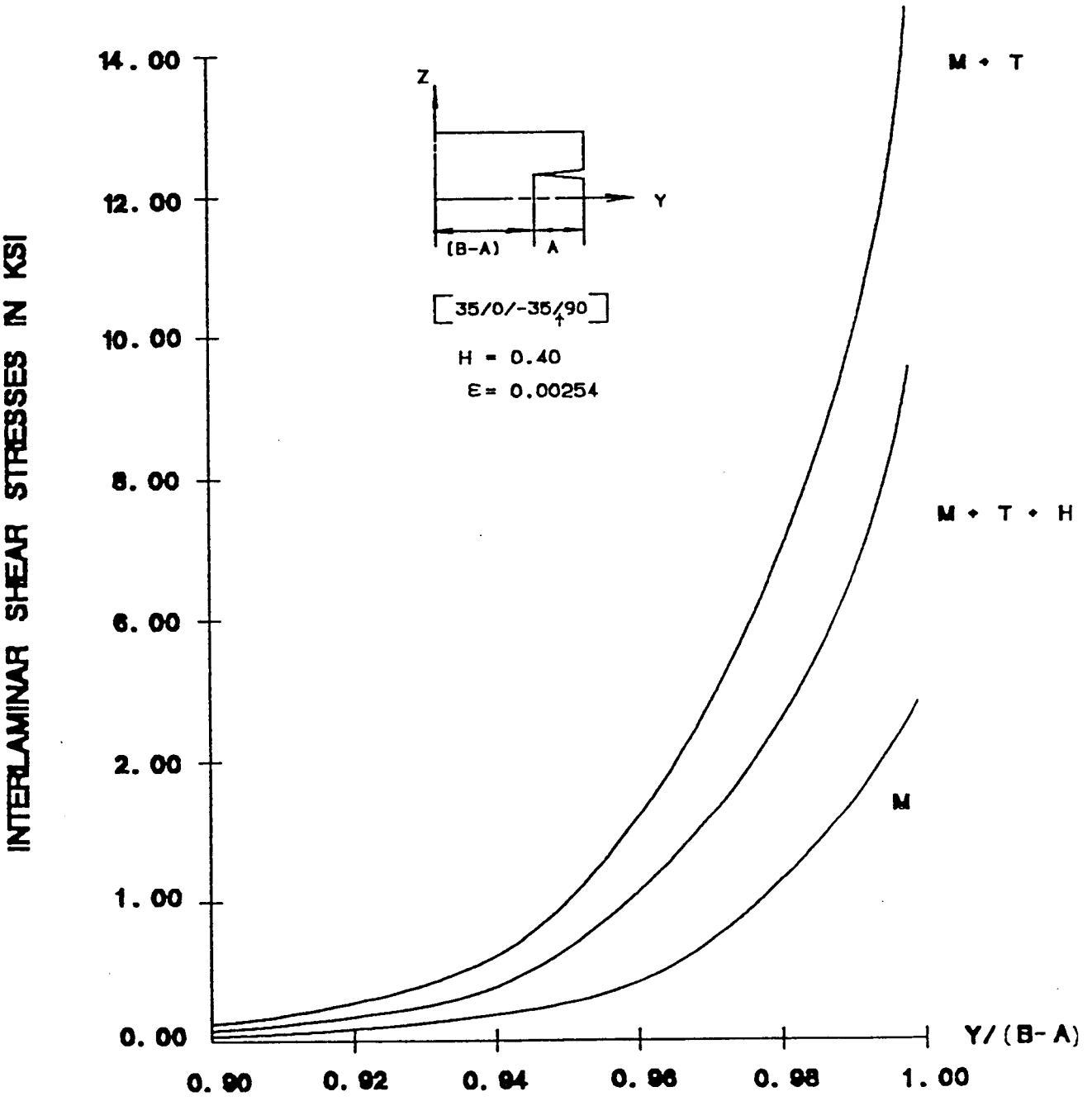

FIGURE 9 - COMPARISON OF INTERLAMINAR STRESS

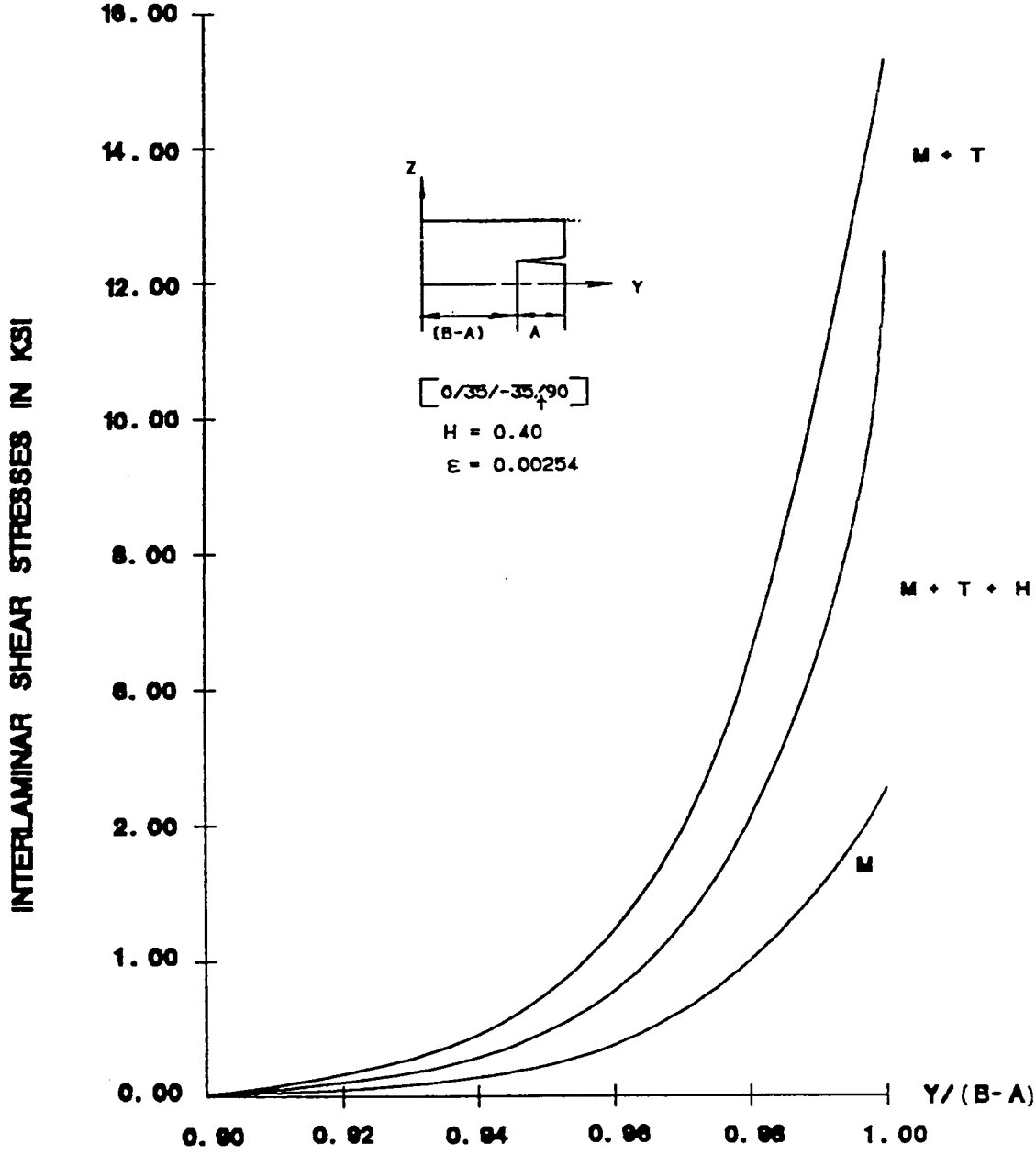

FIGURE 10 - COMPARISON OF INTERLAMINAR STRESS

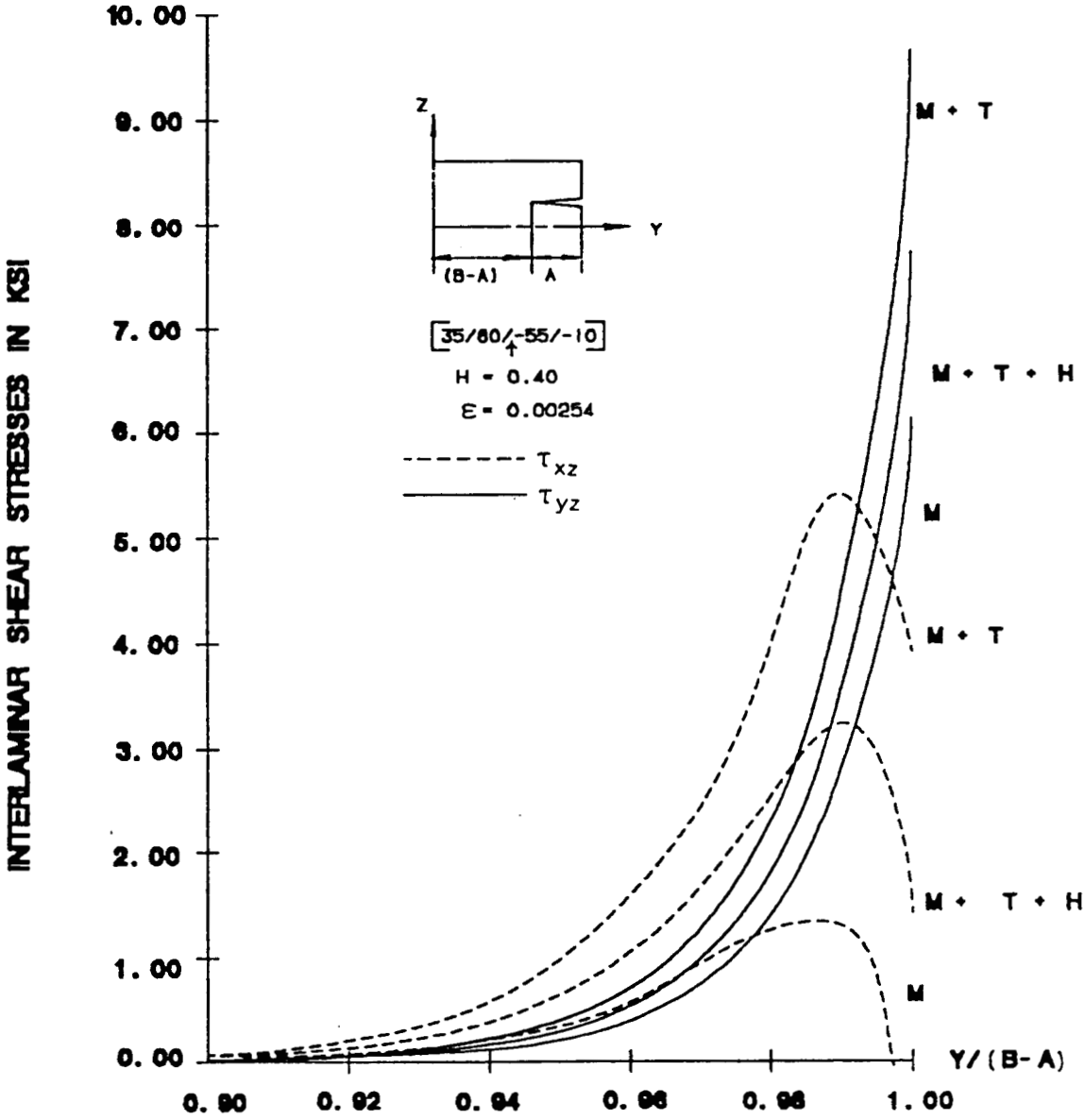

FIGURE 11 - COMPARISON OF INTERLAMINAR STRESSES

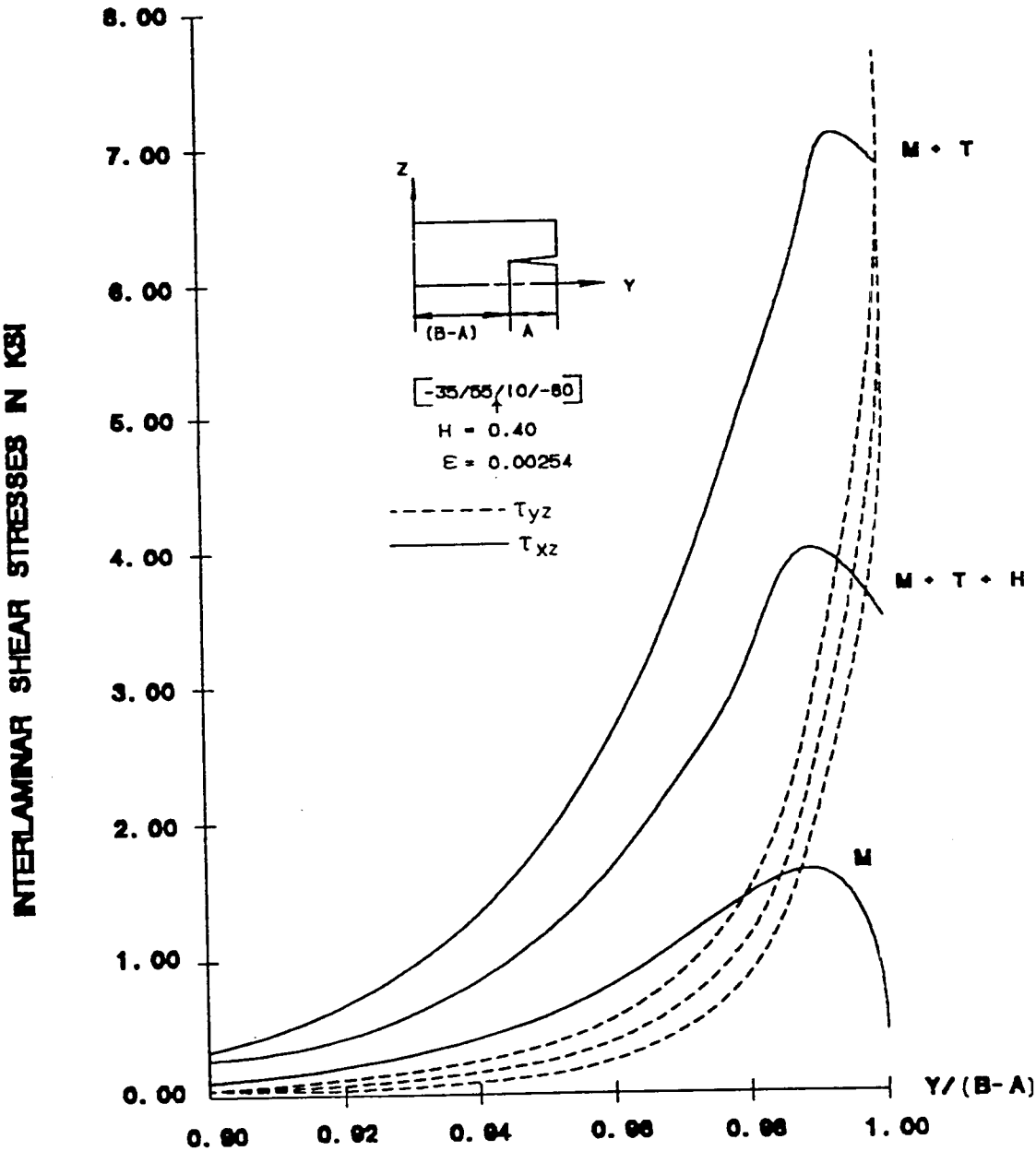

FIGURE 12 - COMPARISON OF INTERLAMINAR STRESSES

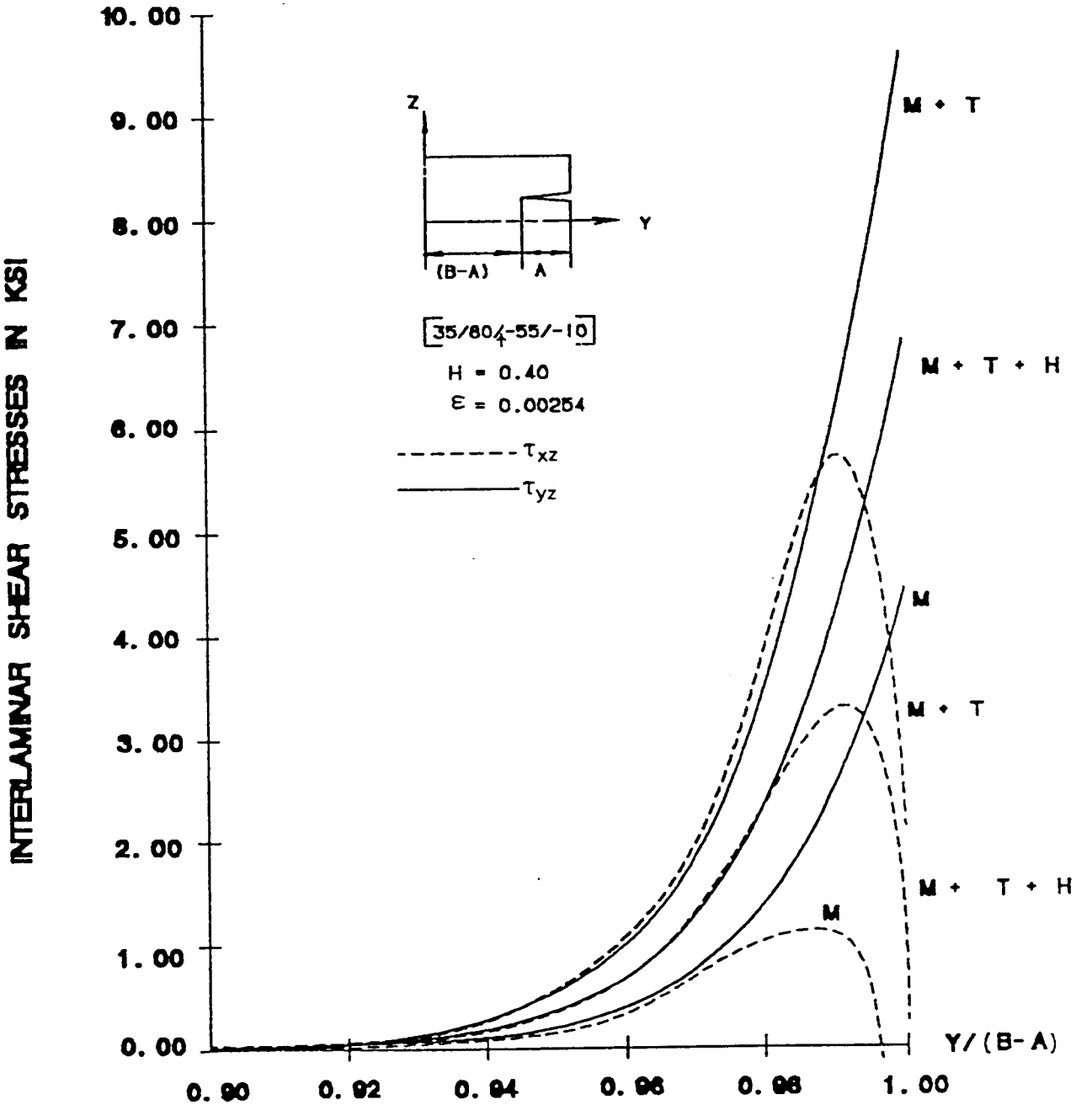

FIGURE 13 - COMPARISON OF INTERLAMINAR STRESSE

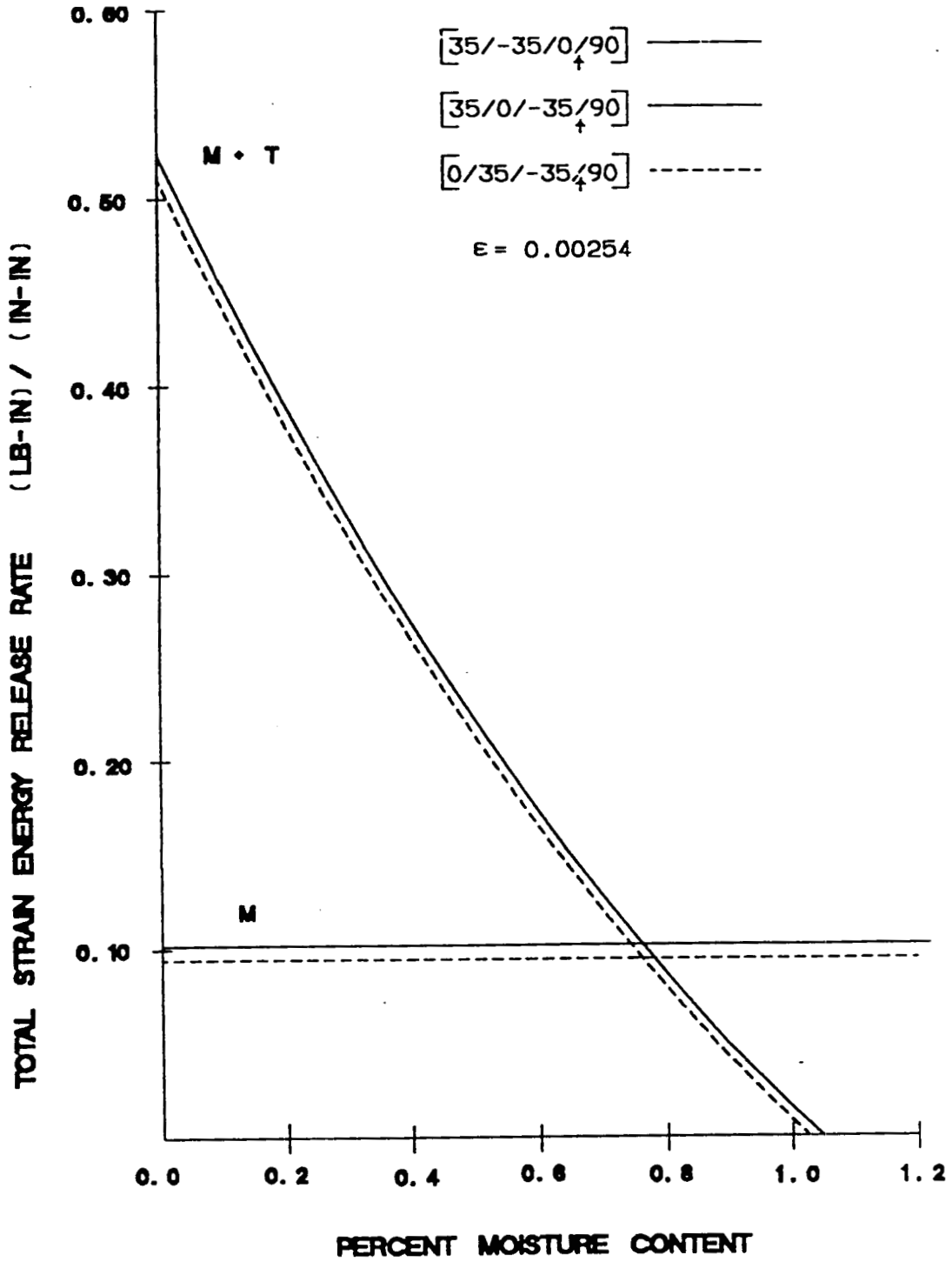

FIGURE 14 - ENERGY RELEASE RATE DISTRIBUTION FOR LAMINATES WITHOUT MODE III

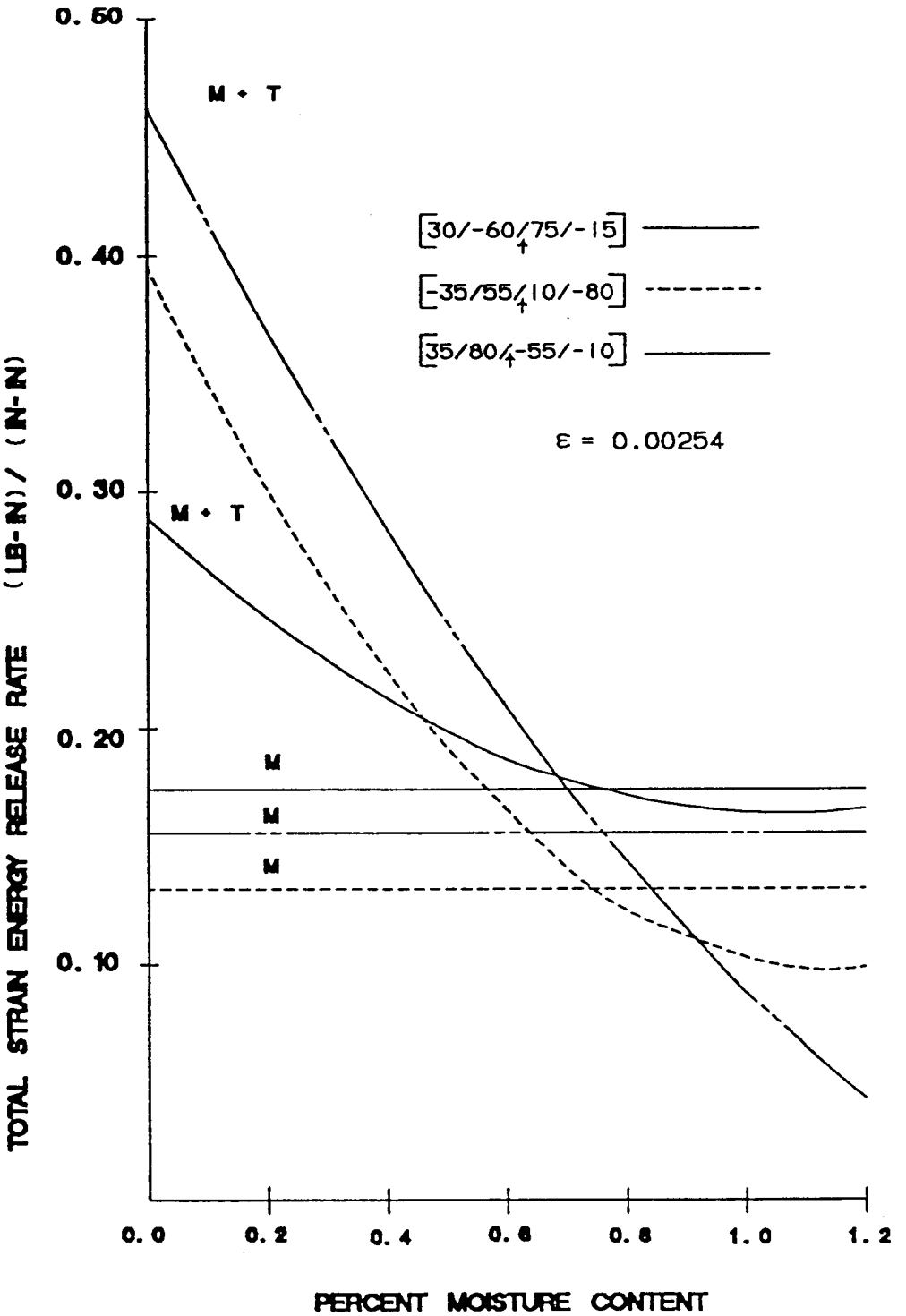

FIGURE 15 - ENERGY RELEASE RATE DISTRIBUTION FOR LAMINATES WITH MODE III

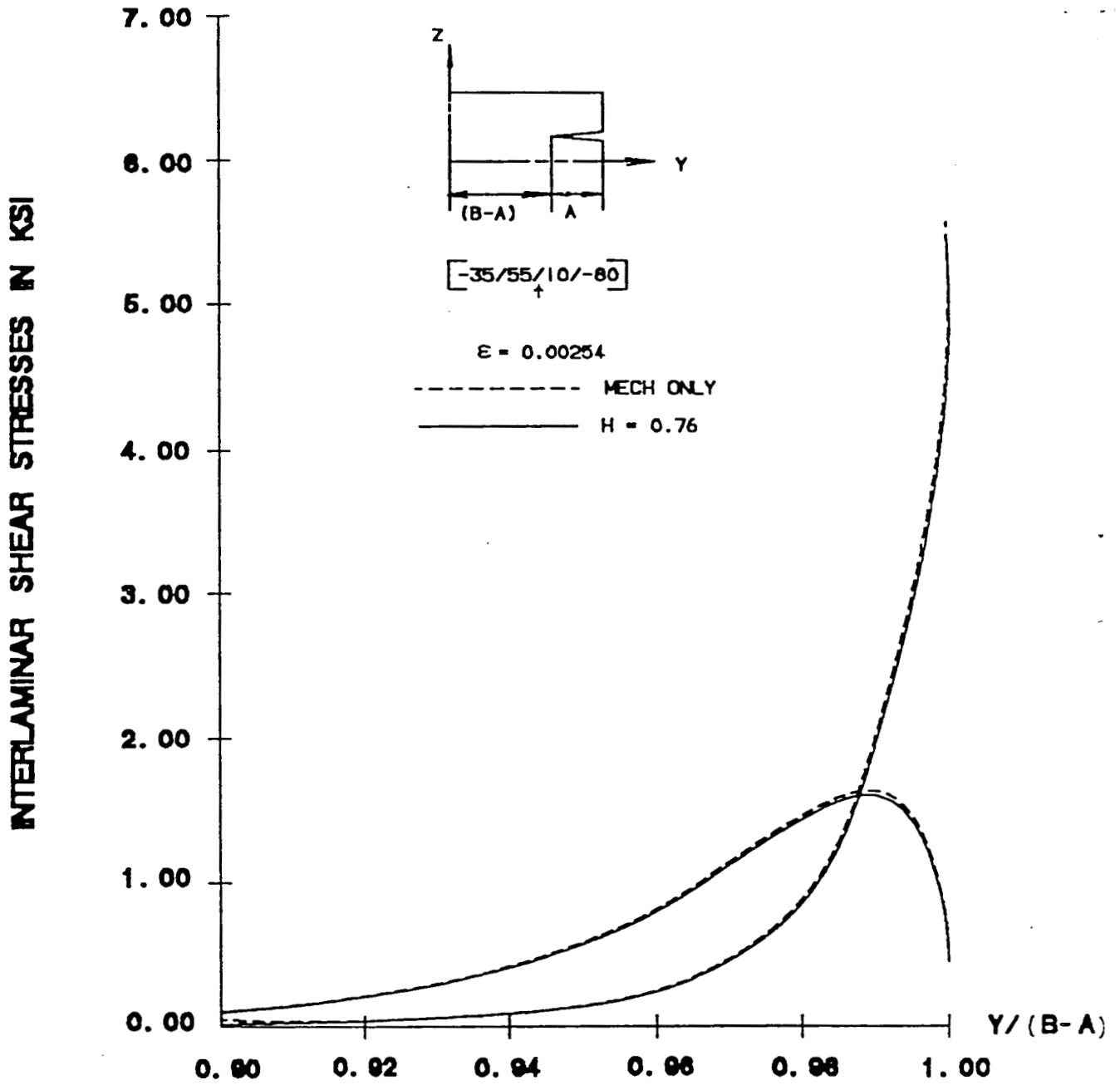

FIGURE 16 - TOTAL ALLEVIATED STATE STRESS DISTRIBUTION

APPENDIX I

Derivation of the Governing Equations

In this Appendix the governing equations for the sublaminate shown in Figure 7 are derived using the principle of virtual work.

Consider a sublaminate of thickness h. The origin of a cartesian coordinate system is located within the central plane (x-y) with the z-axis being normal to this plane. The material of each ply is assumed to possess a plane of elastic symmetry parallel to xy as shown in Figure 6.

Stress and moment resultants are given below.

$$(N_x,\ N_y,\ N_{xy},\ Q_x,\ Q_y) = \int_{h/2}^{h/2} (\sigma_x,\ \sigma_y,\ \tau_{xy},\ \tau_{xz},\ \tau_{yz})\ dz$$

$$(M_x,\ M_y,\ M_{xy}) = \int_{h/2}^{h/2} (\sigma_x,\ \sigma_y,\ \tau_{xy}) z dz \qquad \text{(I-1)}$$

Because of the existence of a plane of elastic symmetry, the constitutive relations are given by

$$\begin{bmatrix} \sigma_x \\ \sigma_y \\ \sigma_z \\ \tau_{xy} \end{bmatrix} = \begin{bmatrix} C_{11} & & & \\ C_{12} & C_{22} & \text{SYM} & \\ C_{13} & C_{23} & C_{33} & \\ C_{16} & C_{26} & C_{36} & C_{66} \end{bmatrix} \begin{bmatrix} \varepsilon_x \\ \varepsilon_y \\ \varepsilon_z \\ \gamma_{xy} \end{bmatrix}_M$$

$$\begin{bmatrix} \tau_{yz} \\ \tau_{xz} \end{bmatrix} = \begin{bmatrix} C_{44} & \text{SYM} \\ C_{45} & C_{55} \end{bmatrix} \begin{bmatrix} \gamma_{yz} \\ \gamma_{xz} \end{bmatrix}_M \qquad \text{(I-2)}$$

where C_{ij} are components of the anisotropic stiffness matrix and γ_{xy}, γ_{yz} and γ_{xz} are engineering shear strains.

The displacements are assumed to be of the form

$$\begin{aligned} u &= U(x,y) + z\beta_x(x,y) \\ v &= V(y) + z\beta_y(x,y) \\ w &= W(x,y) \end{aligned} \qquad \text{(I-3)}$$

where u,v and w are the displacement components in the x, y and z directions, respectively. Equation (I-3) in conjunction with the strain-displacement relations of classical theory of elasticity leads to the following kinematic relations

$$
\begin{aligned}
\epsilon_{xx} &= U_{,x} + z\beta_{x,x} \\
\epsilon_{yy} &= V_{,y} + z\beta_{y,y} \\
\epsilon_{zz} &= 0 \\
\gamma_{xy} &= U_{,y} + V_{,x} + z(\beta_{x,y} + \beta_{y,x}) \\
\gamma_{xz} &= \beta_x + W_{,x} \\
\gamma_{yz} &= \beta_y + W_{,y}
\end{aligned}
\qquad \text{(I-4)}
$$

Substitute Equation (I-4) into Equation (I-2) and put the results into Equation (I-1). This yields the following constitutive relations:

$$
\begin{bmatrix} N_x \\ N_y \\ N_{xy} \\ M_x \\ M_y \\ M_{xy} \end{bmatrix} = \begin{bmatrix} A_{11} & A_{12} & A_{16} & B_{11} & B_{12} & B_{16} \\ A_{12} & A_{22} & A_{26} & B_{12} & B_{22} & B_{26} \\ A_{16} & A_{26} & A_{66} & B_{16} & B_{26} & B_{66} \\ B_{11} & B_{12} & B_{16} & D_{11} & D_{12} & D_{16} \\ B_{12} & B_{12} & B_{26} & D_{11} & D_{12} & D_{26} \\ B_{16} & B_{26} & B_{66} & D_{16} & D_{26} & D_{66} \end{bmatrix} \begin{bmatrix} U_{,x} \\ V_{,y} \\ U_{,y}+V_{,x} \\ \beta_{x,x} \\ \beta_{y,y} \\ \beta_{x,y}+\beta_{y,x} \end{bmatrix} - \begin{bmatrix} N_x \\ N_y \\ N_{xy} \\ M_x \\ M_y \\ M_{xy} \end{bmatrix}^{NM}
$$

$$
\begin{bmatrix} Q_y \\ Q_x \end{bmatrix} = \begin{bmatrix} A_{44} & A_{45} \\ A_{45} & A_{55} \end{bmatrix} \begin{bmatrix} \beta_y + W_{,y} \\ \beta_x + W_{,x} \end{bmatrix}
$$

where

$$
(A_{ij},\ B_{ij},\ D_{ij}) = \int_{h/2}^{h/2} C_{ij}\ (1,\ z,\ z^2)dz \qquad \text{(I-5)}
$$

and the non-mechanical terms are defined in Appendix II.

The variation of the strain energy due to virtual displacements δu, δv and δw is

$$\delta\bar{V} = \int_V (\sigma_x\ \delta\varepsilon_x + \sigma_y\delta\varepsilon_y + \sigma_z\delta\varepsilon_z + \tau_{xy}\ \delta\gamma_{xy} + \tau_{yz}\delta\gamma_{yz} + \tau_{xz}\delta\gamma_{xz})dV \qquad \text{(I-6)}$$

where $\delta\varepsilon_x$, $\delta\varepsilon_y$, $\delta\varepsilon_z$. $\delta\gamma_{xy}$, $\delta\gamma_{xz}$ are the strains associated with the virtual displacements. Using Equations (I-3) and (I-1) then integrating through the thickness gives

$$\delta\bar{V} = \int_A [N_x\ \delta U,_x + N_y\delta V,_y + N_{xy}\ \delta U,_y + Q_x\ \delta\beta_x + Q_y\ (\delta\beta_y + \delta W,_y) + M_x\delta\beta_{x,x} + M_y\ \delta\beta_{y,y} + M_{xy}\ \delta\beta_{x,y}]\ dA \qquad \text{(I-7)}$$

The variation of the work done by the external forces and by the surface tractions is

$$\delta\bar{W} = \int_A (n_x\ \delta U + n_y\ \delta V + q\delta W + m_x\delta\beta_x + m_y\ \delta\beta_y)\ dA$$

$$+ \int_S (\bar{N}_n\ \delta\bar{U}_n + \bar{N}_{ns}\ \delta\bar{U}_s + \bar{M}_n\ \delta\bar{\beta}_n + \bar{M}_{ns}\delta\bar{\beta}_s)ds \qquad \text{(I-8)}$$

where a bar denotes values on the boundary. Variables n and s are coordinates normal and tangential to the edge, and

$$n_x = t_{2x} - t_{1x}$$

$$n_y = t_{2y} - t_{1y}$$

$$q = p_2 - p_1$$

$$m_x = \frac{h}{2}\ (t_{2x} + t_{1x})$$

$$m_y = \frac{h}{2}\ (t_{2y} + t_{1y}) \qquad \text{(I-9)}$$

where n_x and n_y can be regarded as effective distributed axial forces. Terms m_x and m_y are effective distributed moments and q is an effective lateral pressure.

From the principle of virtual work the equations of equilibrium and boundary conditions are determined from the Euler equations and boundary conditions of the variational equation.

$$\delta\bar{V} = \bar{\delta W} \qquad \text{(I-10)}$$

Substitution of Equations (I-7) and (I-8) into Equation (I-10) leads the following equations of equilibrium:

$$N_{x,x} + N_{xy,y} + n_x = 0$$

$$N_{xy,x} + N_{y,y} + n_y = 0$$

$$Q_{x,x} + Q_{y,y} + q = 0$$

$$M_{x,x} + M_{xy,y} - Q_x + m_x = 0$$

$$M_{xy,x} + M_{y,y} - Q_y + m_y = 0 \qquad \text{(I-11)}$$

and one member of the following five products must be prescribed on the sublaminate edges

$$N_n U_n,\ N_{ns}U_s,\ M_n\beta_n,\ M_{ns}\beta_s \text{ and } Q_n W \qquad \text{(I-12)}$$

For the ED specimen under uniform extension, U(x,y) in Equation (I-3) is given by

$$U(x,y) = U^*(y) + x\epsilon \qquad \text{(I-13)}$$

and the response is a function of y and z coordinates only. For this case the equilibrium equations (I-11) take the form

$$N_{xy,y} + n_x = 0$$

$$N_{y,y} + n_y = 0$$

$$Q_{y,y} + q = 0$$

$$M_{xy,y} - Q_x + m_x = 0$$

$$M_{y,y} - Q_y + m_y = 0 \qquad \text{(I-14)}$$

Substitution of the constitutive relations in Equation (I-5) into Equation (I-14) yields the following equilibrium equations in terms of kinematic variables.

$$\begin{bmatrix} A_{66}L_{yy} & & & & \\ A_{26}L_{yy} & A_{22}L_{yy} & & \text{SYM} & \\ 0 & 0 & -A_{44}L_{yy} & & \\ B_{66}L_{yy} & B_{26}L_{yy} & -A_{45}L_{yy} & (D_{66}L_{yy} - A_{55}) & \\ B_{26}L_{yy} & B_{22}L_{yy} & -A_{44}L_{y} & (D_{26}L_{yy} - A_{45} & (D_{22}L_{yy} - A_{44}) \end{bmatrix} \begin{bmatrix} U^* \\ V \\ W \\ \beta_x \\ \beta_y \end{bmatrix} = - \begin{bmatrix} n_x \\ n_y \\ -q \\ m_x \\ m_y \end{bmatrix} \tag{I-15}$$

where the operators

$$L_{yy} = d^2/dy^2$$

$$L_y = d/dy$$

From these governing equations the basis of the work presented in this paper is formed. Appendix II gives a detailed formulation of the hygrothermal terms and the formulation of the total strain energy release rate and interlaminar stresses.

APPENDIX II

Hygrothermal Effects on Edge Delamination

The displacement field and constitutive relations governing the free edge ply separation were presented in Appendix I. The hygrothermal expressions, represented with the superscript NM for non-mechanical, are defined as follows

$$(N_i^{NM},\ M_i^{NM}) = \int_{h/2}^{h/2} (1,z)\ \bar{Q}_{ij} \left\{ \bar{\alpha}_j\ (T-T_r) + \bar{\beta}_j\ C \right\} dz \qquad \text{(II-1)}$$

where

$\bar{\alpha}_j$ - Coefficient of thermal expansion

$\bar{\beta}_j$ - Swelling coefficient

T - Local temperature

T_r - Reference temperature

C - Specific moisture concentration

$\bar{Q}_{ij}$ - Reduced stiffness coefficient

The terms $\bar{\alpha}_j$ and $\bar{\beta}_j$ are transformed as second order tensors with the assumption of no thermal or swelling shear strain.

The concept of sublaminates is used when enforcing the boundary conditions.

Cracked Sublaminates

Sublaminate 2:

The boundary conditions for this sublaminate are expressed as:

$$N_{y2} = N_{xy2} = M_{y2} = Q_{y2} = 0 \qquad \text{(II-2)}$$

$$M_{xy2,y} - Q_{x2} = 0$$

Using the first three conditions in the governing equations, one can express V_2, U_2 and β_{2y} in terms of β_{2x} to obtain:

$$\begin{bmatrix} A^1_{12} & B^1_{26} \\ A^1_{16} & B^1_{66} \\ B^1_{12} & D^1_{26} \end{bmatrix} \begin{bmatrix} \epsilon \\ \beta_{2x,y} \end{bmatrix} + \begin{bmatrix} A^1_{22} & A^1_{26} & B^1_{22} \\ A^1_{26} & A^1_{66} & A^1_{26} \\ B^1_{22} & B^1_{26} & D^1_{22} \end{bmatrix} \begin{bmatrix} V_{2,y} \\ V_{2,y} \\ \beta_{2y,y} \end{bmatrix} - \begin{bmatrix} N_{y1} \\ N_{xy1} \\ M_{Y1} \end{bmatrix}^{NM} = 0 \qquad \text{(II-3)}$$

Sublaminate 3:

The boundary conditions for this sublaminate are given as:

$$N_{y3} - N_{xy3} - 0$$

$$M_{y3,y} - Q_{y3} - 0$$

$$M_{xy3,y} - Q_{x3} - 0 \qquad \text{(II-4)}$$

These are used in a similar manner (as in sublaminate 2) to obtain

$$\begin{bmatrix} A^o_{22} \\ A^o_{26} \end{bmatrix} \begin{bmatrix} V_{3,Y} \\ U_{3,Y} \end{bmatrix} + \begin{bmatrix} A^o_{12} & B^o_{22} & B^o_{26} \\ A^o_{16} & B^o_{26} & B^o_{66} \end{bmatrix} \begin{bmatrix} \epsilon \\ \beta_{3,y} \\ \beta_{3x,Y} \end{bmatrix} \begin{bmatrix} N_{yo} \\ N_{xyo} \end{bmatrix} - 0 \qquad \text{(II-5)}$$

These equations are then substituted back into the governing equations to obtain expressions for the force and moment resultants. They can be expressed in terms of the strain plus non-mechanical effects.

UNCRACKED SUBLAMINATES

Sublaminates 0 and 1:

The boundary conditions of continuity at the interfaces must be satisfied.

$$N_{y1}(0) - N_{xy1}(0) - N_{yo}(0) - N_{xyo}(0) = 0 \qquad \text{(II-6)}$$

$$M_{xy1}(0) - M_{xy2}(0)$$

$$M_{yo}(0) - M_{y3}(0)$$

$$M_{xy0}(0) - M_{xy3}(0) \tag{II-7}$$

and

$$\begin{aligned} &M_{xy1}(0) - M_{xy2}(0) \\ &\beta_{1x}(0) - \beta_{2x}(0) \\ &M_{y0}(0) - M_{y3}(0) \\ &\beta_{0y}(0) - \beta_{3y}(0) \\ &M_{xy0}(0) - M_{xy3}(0) \\ &\beta_{0x}(0) - \beta_{3x}(0) \end{aligned} \tag{II-8}$$

Enforcing equations (II-6) and (II-7) in the governing equations yields the following:

$$\begin{bmatrix} A^1_{12} & A^1_{22} & A^1_{26} \\ A^1_{16} & A^1_{26} & A^1_{66} \\ A^o_{12} & A^o_{22} & A^o_{26} \\ A^o_{16} & A^o_{26} & A^o_{66} \end{bmatrix} \begin{Bmatrix} \varepsilon \\ \varepsilon_y \\ \gamma_{xy} \end{Bmatrix} - \begin{Bmatrix} N_{y1} \\ N_{xy1} \\ N_{yo} \\ N_{xyo} \end{Bmatrix}^{NM} + \begin{Bmatrix} -N_{y1j} \\ -N_{xy1j} \\ N_{y1j} \\ N_{xy1j} \end{Bmatrix} s_j G_j = 0 \tag{II-9}$$

$$\begin{bmatrix} B^1_{12} & B^1_{22} & B^1_{26} \\ -A_1 & B^1_{26} & B_{66} \end{bmatrix} \begin{Bmatrix} \varepsilon \\ \varepsilon_y \\ \gamma_{xy} \end{Bmatrix} - \begin{Bmatrix} M^{NM}_{y1} \\ A^{NM}_1 \end{Bmatrix} - \begin{Bmatrix} M_{y1j} s_j \\ M_{xy1j} s_j + B_1 s_c \alpha_j \end{Bmatrix} \tag{II-10}$$

$$(j = 1 - 4)$$

The expressions in (II-9) and (II-10) are defined below

$$\begin{bmatrix} \epsilon_y \\ \gamma_{xy} \end{bmatrix} - \begin{bmatrix} C_v \\ C_u \end{bmatrix} \epsilon + \begin{bmatrix} C_v \\ C_u \end{bmatrix}^{NM} \qquad \text{(II-11)}$$

$$\Delta = A_{22}^{*} \; A_{66}^{*} - (A_{26}^{*})^2 \qquad \text{(II-12)}$$

$$\begin{bmatrix} C_v \\ C_u \end{bmatrix} = \frac{1}{\Delta} \begin{bmatrix} A_{26}^{*} \; A_{16}^{*} - A_{66}^{*} \; A_{12}^{*} \\ A_{26}^{*} \; A_{12}^{*} - A_{22}^{*} \; A_{16}^{*} \end{bmatrix} \qquad \text{(II-13)}$$

$$\begin{bmatrix} C_v \\ C_u \end{bmatrix}^{NM} = \frac{1}{\Delta} \begin{bmatrix} A_{66}^{*} \; (N_{y1} + N_{yo})^{NM} - A_{26}^{*} \; (N_{xy1} + N_{xyo})^{NM} \\ -A_{26}^{*} \; (N_{y1} + N_{yo})^{NM} + A_{22}^{*} \; (N_{xy1} + N_{xyo})^{NM} \end{bmatrix} \qquad \text{(II-14)}$$

A_1 and A_1^{NM} are functions of A_{ij}, B_{ij} and D_{ij}. The superscripts * implies a summation of the upper and lower sublaminates.

Continuing with the derivation one can substitute the expressions set forth into equation (I-7) as well as 10 and 11 in the report. This gives the following expression for the total energy release rate.

$$G = \frac{1}{2} \; \frac{d}{da} \int_0^b \left[\int_{h/2}^{h/2} N_x \; \epsilon_m \; dz \right] DY \qquad \text{(II-15)}$$

The concept of free-expansion in the x-direction is implemented to find the strain induced by the non-mechanical effects on the structure. Setting $N_x = 0$ for each ply in Equation (I-5) and using the boundary conditions of (II-2), (II-4) and (II-6) allows the following.

$$\epsilon_u^k = - \; T_u^k \; / \; E_u^k$$

$$\epsilon_c^k = - T_c^k \; / \; E_c^k \qquad \text{(II-16)}$$

where

$$T_u^k = h^k C_v^{NM} \bar{Q}_{12}^k + h^k C_u^{NM} \bar{Q}_{16}^k - (N_x^{NM})^k$$

$$E_u^k = h^k (\bar{Q}_{11}^k + C_v \bar{Q}_{12}^k + C_u \bar{Q}_{16}^k)$$

$$T_c^k = \bar{Q}_{12}^k F_1^{NM} h^k + \bar{Q}_{16}^k F_2^{NM} h^k + B_{12}^k F_3^{NM} - (N_x^{NM})^k$$

$$E_c^k = \bar{Q}_{11}^k h^k + \bar{Q}_{12}^k h^k Cd_{11} + \bar{Q}_{16}^k h^k Cd_{12}^k + B_{12}^k Cd_{31} \qquad \text{(II-17)}$$

Superscript k represents the ply. Expressions Cd_{ij} and F_i^{NM} are found by substituting the conditions of (II-2) into (II-3).

$$\left[Cd\right]_{3\times 2} = -\begin{bmatrix} A_{22}^1 & A_{26}^1 & B_{22}^1 \\ A_{26}^1 & A_{66}^1 & B_{26}^1 \\ B_{22}^1 & B_{26}^1 & D_{22}^1 \end{bmatrix}^{-1} \begin{bmatrix} A_{12}^1 & B_{26}^1 \\ A_{16}^1 & B_{66}^1 \\ B_{12}^1 & D_{26} \end{bmatrix} \qquad \text{(II-18)}$$

$$\left\{F^{NM}\right\}_{3\times 1} = -\begin{bmatrix} A_{22}^1 & A_{26}^1 & B_{22}^1 \\ A_{26}^1 & A_{66}^1 & D_{22}^1 \\ B_{22}^1 & B_{26}^1 & D_{22}^1 \end{bmatrix}^{-1} \begin{Bmatrix} N_y \\ N_{xy1} \\ M_{y1} \end{Bmatrix}^{NM} \qquad \text{(II-19)}$$

Sublaminate 3 has $B_{ij} = 0$ due to symmetry of the structure. When considering these plies, the term F_1^{NM} and F_2^{NM} are found by substituting the boundary conditions (II-4) into (II-5).

This gives a second expression of F^{NM} for this sublaminate

$$\begin{bmatrix} F^{NM} \end{bmatrix}_{2\times 1} - \begin{bmatrix} A^{o}_{22} & A^{o}_{26} \\ A^{o}_{26} & A^{o}_{66} \end{bmatrix}^{1} \begin{bmatrix} N_{y0} \\ N_{xy0} \end{bmatrix}^{NM} \qquad \text{(II-20)}$$

To find the total strain associated with the non-mechanical effects, it is necessary to sum the force over the entire structure and set it to zero. These are used in order to obtain Equation (16), (17) and (18) in the report on page 17. Substituting this in Equation (II-15) gives the total strain energy release rate expression per unit length

$$G - \frac{1}{2} \sum_{K} - (E^{k}_{c}\, \epsilon^{T} + T^{k}_{c})\ (\epsilon^{T} - \epsilon^{k}_{c}) + (E^{k}_{u}\, \epsilon^{T} + T^{k}_{u})\ (\epsilon^{T} - \epsilon^{k}_{u})$$

The expression $\epsilon^{T} - \epsilon^{k}_{c,u}$ is in essence the total mechanical strain of that ply.

INTERLAMINAR STRESSES

The interlaminar stresses of the structure are defined in Equations (8) and (9)

$$t_x - N^{1}_{xy,y} - N_{xy1j}\, s_j^{2}\, G_j \quad e^{-s_j y}$$

$$t_y - N^{1}_{y,y} - N_{y1j}\, s_j^{2}\, G_j\, e^{-s_j y} \qquad (j = 1\text{-}4) \qquad \text{(II-21)}$$

While s_j, the positive roots reulsting from the ploynominal

$$E_8 s^{8} + E_6 s^{6} + E_4 s^{4} + E_2 s^{2} + E_o - 0, \qquad \text{(II-22)}$$

are independent of the hygrothermal effects, the rest of the terms are not.

Solving Equations (II-9) and (II-10) gives the term G_j while N_{xy1j} and N_{y1j} are found from

$$\begin{Bmatrix} N_{y1j} \\ N_{xyj} \end{Bmatrix} - \begin{bmatrix} A^1_{22} & A^1_{26} & B^1_{22} & B^1_{26} \\ A^1_{26} & A^1_{66} & B^1_{26} & B^1_{66} \end{bmatrix} \begin{Bmatrix} v_j \\ u_j \\ \alpha_j \end{Bmatrix} \qquad (II\text{-}23)$$

$$(j = 1,2,3,4)$$

where v_j, U_j and α_j are found by imposing the boundary conditions on the mode shapes. They are dependent on the four values of s_j as well as the sublaminate stiffness matrices.

APPENDIX III

```
      PROGRAM START (INPUT, OUTPUT, TAPE5=INPUT, TAPE6=OUTPUT)

    THIS  PROGRAM IS FOR THE FINAL PAPER   8-16-87
   DIMENSION STATEMENTS

      REAL BG(4),E(9),GG(4,4), MATR32(3,2), MATR33(3,3), MATR3(3),
     C STRAIN(25), SAVE3(3), SAVE33(3,3), WKAREA(99), ZR
      COMPLEX SJ(8)
      DOUBLE PRECISION BNEG, A, C, DIFF1, DIFF2, UNSY(2), UNSX(2),
     C  SSSS, SSSC, SSCC, SCCC, ZZZ0(0:50),J22,J26,FNM(3),S1NM,S2NM,
     C  MEMSY, MEMSX, F11M, F22M, SS1, SS2, SSY, SSX, ZZZ1(0:50),
     C  THICK(40),THETA(50), E1(50), E2(50), CCCC, HSS(5),HSN1,HSN2,
     C  Q(6,6,50), Z0(0:40), A0(6,6), A1(6,6), U13, U14, BG1, BG2,
     C  NX0(4), E15,E16,E17, E18, E19, ZTT(0:40),
     C  NY1(4), X(2), Y(3), CV, CU, W(2), ZZ(3), VV11, VV12
      DOUBLE PRECISION  ALPHA(4), PHI(4), GAMMA(4), NX1(4),
     C  B1(6,6), B0(6,6), D0(6,6), D1(6,6), F(4,4), VV13, VV14, J66,
     C  RDLT, RTA1, RTA2, RSB1, RSB2, U12, U11, A1NM,
     C  NXY1(4), MY1(4), MXY1(4), WD(2,3), CD(3,2), WIDTH,
     C  V12(50), V21(50),  SS, CC, K66, K26, K22,
     C  Z1(0:40), FX, FY, G1(2,35), K16,K12, H66
      DOUBLE PRECISION  SV(5), SU(5), AL, SC, S(8), DY,
     C  G12(50), G31(50), C2, C1, THETV, THETU, G111(2,35), CS,
     C  DEL, H0, H1, H22, HE, HG, HNY(50), HNXY(50), HM3,CVNM,
     C  C11, C12, C22, C26, C44, D, C55, C66, H26, SQ, DUM,CUNM,
     C  CONY, CONXY, SMNY, SMNXY,
     C  SB1,SB2,TA1,TA2,ATHM1(40),ATHM2(40),ATHM6(40),BSW2(40),
     C  NMNY0,NMNXY0,G11(2,35),
     C  DVV11, DVV12, DU13, DU14, DF(4,4), DX, ATH,CCONY,CCONXY,
     C  BSW6(40), DELTEMP, BSW1(40), CM0IST(35),
     C  SIGX(0:40,79:120),
     C  NMNY1,NMNXY1,NMMX1,NMMY1,SIGY(0:40,79:120)
      DOUBLE PRECISION   NMST0(50), NMST2(50),NMST3(50), TNC,UNCL,
     C  T1(50), T12(50), T13(50),EX(50),EXX(50),EX3(50), JY,
     C  EXNC,ESTAR, TSTAR, TNMST, GLC(0:50), NXNM(50),B12(50)
      DATA  Q/1800*0.0/,   ZR/0.00/
*******************************************************************************
*******************************************************************************

      DATE OF PROGRAM : SEPT. 1, 1987

     THIS IS THE FINAL PROGRAM FOR PREDICTING THE ENERGY RELEASE RATE OF
      COMPOSITE LAMINATES INCLUDING HYGROTHERMAL EFFECTS ..........
      HOWEVER, IT ONLY CONSIDERS EXTENSION EFFECTS OF STRAIN WHEN DEALING
      WITH HYGRALTHERMAL EFFECTS.... LIKE WHITTNEY'S PAPER.....
      EXCEPT ON A PLY BY PLY ANALYSIS BASIS OF THE HYGRALTHERMAL EFFECTS


       THE INPUT ALLOWS FOR: THE LAMINATE LAY-UP TO CHANGE AND POSITION
                 OF THE CRACK, DIFFERENT STRAIN VALUES TO BE EVALUATED,
                 (UP TO 40 LAMINATES AND 25 DIFFERENT STRAIN VALUES)
                 AND FOR THE EVALUATION OF ONE MOISTURE CONSTANT OR A
                 RANGE OF THE MOISTURE CONSTANT FROM 0 TO 1.2.

      THIS PROGRAM IS FOR THE GIVEN DATA TO BE IN ENGLISH UNITS.

       ALL LAMINATES ARE EVALUATED WITHOUT THRMAL EFFECTS AUTOMATICALLY

*******************************************************************************
*******************************************************************************
         LZQ IS THE NUMBER OF DIFFERENT LAMINATE (OR CRACK POSITIONS)
           TO BE EVALUATED.

      READ(5,*)   LZQ
       DO 400     LZZ = 1,LZQ
```

```
      READ(5,*)  WIDTH, NPLYO, NPLY1, AL
        NEXTPL = NPLYO + 1.
        TPLY = NPLYO + NPLY1

  FOR EACH PLY IN THE SUBLAMINATE, THE MATERIAL CHARACTERISTICS
  MUST BE READ IN.

          PI = 4. * ATAN(1.)
          HO = 0.0
          ATH = 0.0
          H1=0.0
          DO 3  LK = 1, TPLY
          ZO(LK) = 0.0
3         Z1(LK) = 0.0


        DO 5   I = 1,NPLYO
          READ(5,*) THICK(I), THETA(I), E1(I), E2(I)
          READ(5,*) V12(I)
          READ(5,*) G12(I), G31(I)
          THETA(I) = THETA(I) * PI / 180.
5       HO = HO + THICK(I)

        DO 10  I = NEXTPL, TPLY
          READ(5,*) THICK(I), THETA(I), E1(I), E2(I)
          READ(5,*) V12(I)
          READ(5,*) G12(I), G31(I)
          THETA(I) = THETA(I) * PI / 180.
10      H1 = H1 + THICK(I)

*************************************************************************
*************************************************************************
   THESE ARE WRITE STATEMENTS TO CHECK THE INITIAL CONDITIONS OF THE
                SUBLAMINATE  AND VALUES READ IN
*************************************************************************
*************************************************************************

    EACH PLY MAY HAVE DIFFERNT PROPERTIES SO THE PROPERTY OF EACH

      WRITE(6,289)
CC
      WRITE(6,201)  WIDTH
      WRITE(6,202) NPLY1, NPLYO

          WRITE(6,204)
            DO 15 J = 1, TPLY
            JJ = TPLY + 1 - J
            WRITE(6,206) J
            WRITE(6,207) THICK(JJ), THETA(JJ)*180/PI
            WRITE(6,208) E1(JJ)/1E+06 , E2(JJ)/1E+06
            WRITE(6,209) V12(JJ)
15          WRITE(6,214) G12(JJ)/1E+06, G31(JJ)/1E+06


 *************************************************************************
 *************************************************************************
      DETERMINE THE Z COMPONENT OF ALL LAMINATES

       CHECK = 0.00000001
       ZTT(0) = 0.0
       ZO(0) = -HO / 2.0
        DO 20 I = 1, NPLYO
          ZTT(I) = THICK(I) + ZTT(I-1)
20        ZO(I) = THICK(I) +  ZO(I-1)

       Z1(NPLYO) = -H1 / 2.0
```

```
        DO 25 I = NEXTPL,TPLY
          ZTT(I) = THICK(I) + ZTT(I-1)
25        Z1(I) = THICK(I) +  Z1(I-1)

*************************************************************************
FIRST READ IN THE NUMBER OF STRAINS TO BE EVALUATED AND THEIR VALUE
THEN READ IN IF THE MOISTURE CONTENT SHOULD VARY OVER 0 TO 1.2 OR
 BE A CONSTANT.

            NSTRA =  ..... NUMBER OF VARIOUS STRAIN VALUES
          IF MOISTV = 1 ... CMOIST VARIES OVER 0 TO 1.2
          IF MOISTV = 0 ... CMOIST IS A SPECIFIC VALUE
*************************************************************************
        READ(5,*) NSTRA
         DO 27  J=1,NSTRA
27      READ(5,*) STRAIN(J)

          DO 400 LST = 1,NSTRA
           READ(5,*) RDLT,RSB1,RSB2,RTA1,RTA2
           WRITE(6,231) STRAIN(LST),RDLT, RSB1, RSB2, RTA1, RTA2

          READ(5,*) MOISTV
          IF (MOISTV.EQ.0) READ(5,*) CM
          IF (MOISTV.EQ.0)  MMC = 1
          IF (MOISTV.EQ.0) WRITE(6,232) CM
          IF (MOISTV.EQ.1)  MMC = 25
          IF (MOISTV.EQ.1)  WRITE(6,233)
*************************************************************************
          DO 300  JM = 1,MMC +1

 FIND Q'S AS WELL AS Q-BAR ,  SAVING Q-BAR
 AND READ AND CALCULATE THE HYGRO THERMO EFFECTS

*************************************************************************
       DO 200  IZZ = 1,2
         LIL = 0
         IF (IZZ.EQ.1) JMM = JM
         IF (IZZ.EQ.2) JMM = 0
         IF(JM.EQ.1. AND .IZZ.EQ.1) LIL = 1
    IF (JM.GT.1 .AND. IZZ.EQ.2) GO TO 200

          NMNY1 = ZR
          NMNXY1 = ZR
          NMMX1 = ZR
          NMMY1 = ZR

          NMNYO = ZR
          NMNXYO = ZR
          HM3 = ZR
          SMNY = ZR
          SMNXY = ZR

        DO 24 I=1,5
           E(I)  = ZR
           E(I+4) = ZR
24         HSS(I) = ZR
         DO 26 I=1,6
         DO 26 J= 1,6
            NXNM(I)= ZR
          DF(I,J) = ZR
          AO(I,J) = ZR
          BO(I,J) = ZR
          DO(I,J) = ZR
          A1(I,J) = ZR
          B1(I,J) = ZR
26        D1(I,J) = ZR
```

```
          DO 28  MM = 1,TPLY
28        IF( THICK(MM) .GT. ATH ) ATH = THICK(MM)

    IZZ = 2 IS FOR LAMINATE WITHOUT ANY HYGROTHERMAL EFFECTS
    IZZ = 1 IS FOR HYGROTHERMAL EFFECTS CONSIDERED

        DO 30  I = 1, TPLY

  READ THE HYGROTHERMO EFFECTS, BOTTOM PLY IS FIRST AND UPWARD

         IF (IZZ.EQ.2) GO TO 35
            IF (MOISTV.EQ.0) CMOIST(JM) = CM
            IF (MOISTV.EQ.1) CMOIST(JM) = 0.05 * (JM-1)
           DELTEMP = RDLT
            SB1 = RSB1
            SB2 = RSB2
            TA1 = RTA1
            TA2 = RTA2
            GO TO 40

35          DELTEMP = ZR
            CMOIST(JM) = ZR
            SB1 = ZR
            SB2 = ZR
            TA1 = ZR
            TA2 = ZR

40          V21(I) = V12(I) * E2(I) / E1(I)
            C11 = E1(I) / (1 - V12(I) * V21(I) )
            C12 = E2(I) * V12(I) / ( 1 - V12(I) * V21(I) )
            C22 = E2(I) / ( 1 - V12(I) * V21(I) )
            C44 = G31(I)
            C55 = G31(I)
            C66 = G12(I)

      SS = DSIN(THETA(I)) * DSIN(THETA(I))
      CC = 1 - SS
      CS = 0.5 * DSIN(2*THETA(I))


      SSSS = SS * SS
      SSSC = SS * CS
      SSCC = SS * CC
      SCCC = CC * CS
      CCCC = CC * CC

      Q(1,1,I) = C11 * CCCC + 2 * (C12 + 2 * C66 ) * SSCC
     C           + C22 * SSSS
      Q(1,2,I) = (C11 + C22 - 4 * C66) * SSCC + C12 * ( SSSS
     C         + CCCC )
      Q(2,2,I) = C11 *  SSSS + 2 * ( C12 + 2 * C66) * SSCC
     C        + C22 * CCCC
      Q(1,6,I) = (C11 - C12 - 2 * C66) * SCCC
     C             + (C12 - C22 + 2 * C66 ) * SSSC
      Q(2,6,I) = (C11 - C12 - 2 * C66 ) * SSSC
     C                + (C12 - C22 + 2 * C66 ) * SCCC
      Q(6,6,I) = (C11 + C22  - 2 * C12 - 2 * C66) * SSCC
     C           + C66 * ( SSSS + CCCC )
      Q(4,4,I)= C44 * CC+ C55 * SS
      Q(5,5,I) = C44 * SS + C55 * CC
      Q(4,5,I) = CS *  (C44 - C55)
       Q(6,2,I) = Q(2,6,I)
       Q(6,1,I) = Q(1,6,I)
       Q(2,1,I) = Q(1,2,I)

        HSS(I) = HSS(I) + Q(1,2,I)
```

```
          HSS(2) = HSS(2) + Q(2,2,I)
          HSS(3) = HSS(3) + Q(2,6,I)
          HSS(4) = HSS(4) + Q(1,6,I)
          HSS(5) = HSS(5) + Q(6,6,I)



        ATHM1(I) = TA1 * CC + TA2 * SS
        ATHM2(I) = TA1 * SS + TA2 * CC
        ATHM6(I) = CS * ( TA2 - TA1)
        BSW1(I) = SB1 * CC + SB2 * SS
        BSW2(I) = SB1 * SS + SB2 * CC
        BSW6(I) = CS * ( SB2 - SB1 )

30      CONTINUE

  FIND THE A, B, AND D MATRICES FOR THE LOWER AND UPPER SUBLAMINATE.
  ALSO FINDS HYGRALTHERMAL EXPRESSIONS ON A PER LAMINA AND PER
  SUBLAMINATE BASIS.


                ZZZO(0) = ZO(0) * ZO(0) * ZO(0)
          DO 45  I = 1,NPLYO


       NXNM(I) = (Q(1,1,I)*( ATHM1(I)*DELTEMP + BSW1(I)*CMOIST(JM))
     C                + Q(1,2,I)*( ATHM2(I)*DELTEMP + BSW2(I)*CMOIST(JM))
     C + Q(1,6,I)*( ATHM6(I)*DELTEMP + BSW6(I)*CMOIST(JM)) ) * THICK(I)


       NMNYO= NMNYO+(Q(1,2,I)*( ATHM1(I)*DELTEMP + BSW1(I)*CMOIST(JM) )
     C               + Q(2,2,I)*( ATHM2(I)*DELTEMP + BSW2(I)*CMOIST(JM) )
     C + Q(2,6,I)*( ATHM6(I)*DELTEMP + BSW6(I)*CMOIST(JM)) ) * THICK(I)

      NMNXYO= NMNXYO+(Q(1,6,I)*( ATHM1(I)*DELTEMP + BSW1(I)*CMOIST(JM) )
     C               + Q(2,6,I)*( ATHM2(I)*DELTEMP + BSW2(I)*CMOIST(JM) )
     C  + Q(6,6,I)*( ATHM6(I)*DELTEMP + BSW6(I)*CMOIST(JM)) ) * THICK(I)
C



          ZZZO(I) = ZO(I) * ZO(I) * ZO(I)
        B12(I) = Q(1,2,I)*0.5*((ZO(I)*ZO(I))-(ZO(I-1)*ZO(I-1)))
             DO 45 L =1,6
             DO 45  J = 1,6
                  IF( REAL( Q(J,L,I) ).EQ.ZR) GO TO 45
        AO(J,L) = AO(J,L) + Q(J,L,I) * THICK(I)
        BO(J,L) = BO(J,L)+Q(J,L,I)*0.5*((ZO(I)*ZO(I))-(ZO(I-1)*ZO(I-1)))
        DO(J,L) = DO(J,L)+Q(J,L,I)/3.0*( ZZZO(I) -  ZZZO(I-1)  )
45         CONTINUE

           ZZZ1(NPLYO) = Z1(NPLYO) * Z1(NPLYO) * Z1(NPLYO)


           DO 50  I = NEXTPL,TPLY
           ZZZ1(I) = Z1(I) * Z1(I) * Z1(I)


       NXNM(I) = ( Q(1,1,I)*( ATHM1(I)*DELTEMP + BSW1(I)*CMOIST(JM) )
     C               + Q(1,2,I)*( ATHM2(I)*DELTEMP + BSW2(I)*CMOIST(JM) )
     C   + Q(1,6,I)*( ATHM6(I)*DELTEMP + BSW6(I)*CMOIST(JM) ))* THICK(I)


       NMNY1= NMNY1+ ( Q(1,2,I)*( ATHM1(I)*DELTEMP + BSW1(I)*CMOIST(JM) )
     C               + Q(2,2,I)*( ATHM2(I)*DELTEMP + BSW2(I)*CMOIST(JM) )
     C   + Q(2,6,I)*( ATHM6(I)*DELTEMP + BSW6(I)*CMOIST(JM)) )* THICK(I)
```

```
C
      NMNXY1= NMNXY1+(Q(1,6,I)*( ATHM1(I)*DELTEMP + BSW1(I)*CMOIST(JM) )
     .C              + Q(2,6,I)*( ATHM2(I)*DELTEMP + BSW2(I)*CMOIST(JM) )
      C   + Q(6,6,I)*( ATHM6(I)*DELTEMP + BSW6(I)*CMOIST(JM)) )* THICK(I)


      NMMX1= NMMX1 + 0.5 * ( Z1(I)*Z1(I) - Z1(I-1)*Z1(I-1) ) *
     C       ( Q(1,1,I)*( ATHM1(I)*DELTEMP + BSW1(I)*CMOIST(JM) )
     C       + Q(1,2,I)*( ATHM2(I)*DELTEMP + BSW2(I)*CMOIST(JM) )
     C       + Q(1,6,I)*( ATHM6(I)*DELTEMP + BSW6(I)*CMOIST(JM) ) )

      NMMY1= NMMY1 + 0.5 * ( Z1(I)*Z1(I) - Z1(I-1)*Z1(I-1) ) *
     C       ( Q(1,2,I)*( ATHM1(I)*DELTEMP + BSW1(I)*CMOIST(JM) )
     C       + Q(2,2,I)*( ATHM2(I)*DELTEMP + BSW2(I)*CMOIST(JM) )
     C       + Q(2,6,I)*( ATHM6(I)*DELTEMP + BSW6(I)*CMOIST(JM) ) )


       B12(I) = Q(1,2,I)*0.5*((Z1(I)*Z1(I))-(Z1(I-1)*Z1(I-1)))
                DO  50   L=1,6
                DO  50   J=1,6
                     IF ( REAL( Q(J,L,I) ).EQ.0 ) GO TO 50
       A1(J,L) = A1(J,L) + Q(J,L,I) * THICK(I)
       B1(J,L) = B1(J,L)+Q(J,L,I)*0.5*((Z1(I)*Z1(I))-(Z1(I-1)*Z1(I-1)))
       D1(J,L) = D1(J,L)+Q(J,L,I)/3.0*( ZZZ1(I) -  ZZZ1(I-1)  )

50    CONTINUE


 ************************************************************************

 SEE IF COUPLING IS TAKING PLACE .........................

 ************************************************************************
              COUPL = 2
           DO 60  I=1,6
             DO 60 J=1,6
           IF  ( REAL(BO(I,J)).GT.CHECK ) COUPL=1
60         IF  ( REAL(B1(I,J)).GT.CHECK ) COUPL=1
           IF  ( REAL  (D1(2,6)).GT. CHECK ) COUPL=1
           IF  ( REAL  (DO(2,6))  .GT. CHECK ) COUPL=1

           IF  ( COUPL.EQ.1 .AND. LIL.EQ.1 ) WRITE(6,205)
           IF  ( COUPL.EQ.2 .AND. LIL.EQ.1 ) WRITE(6,210)
 ************************************************************************

       CHECK THE SIGN OF THE PEEL STRESS ***************************

            HSN1 = NMNY1 + NMNYO
            HSN2 = NMNXY1 + NMNXYO

 ************************************************************************
          HDD= HSS(2) * HSS(5) - HSS(3) * HSS(3)
          HE =   HSS(3) * HSS(4) - HSS(1) * HSS(5)
          HE = HE /HDD
          HG =   HSS(1) * HSS(3) - HSS(2) * HSS(4)
          HG = HG / HDD
          DO 65 I=1,TPLY
              HNY(I) = ATH * STRAIN(LST) * ( Q(1,2,I) + Q(2,2,I) * HE +
     C                   Q(2,6,I) * HG )
              HNXY(I) = ATH * STRAIN(LST) * ( Q(1,6,I) + Q(2,6,I) * HE +
     C                    Q(6,6,I) * HG)
65        CONTINUE


          DO 70 I = 1,NPLY1
```

```
          HM3 = HM3 + ATH * HNY(I) * ( NPLY1 - I + .5 )
          SMNY = SMNY + HNY(I)
 70       SMNXY = SMNXY  + HNXY(I)


          IF ( HM3.GT.ZR) GO TO 85
C
C       IF (LIL.EQ.1) WRITE(6,*)' CASE OF COMPRESSIVE PEEL STRESS
C       WRITE(6,218)
C         DO 75 I=1,TPLY
75      WRITE(6,220)THETA(I),HNY(I),HNXY(I)
C       WRITE(6,*)' THE MOMENT CALCULATED WAS = ',HM3
C
 85      DO 80 I=1,6
         DO 80 J=1,6
          IF( ABS( REAL(BO(I,J)) ).LT.CHECK) BO(I,J)=ZR
 80       IF( ABS( REAL(B1(I,J)) ).LT.CHECK) B1(I,J) = ZR
 ***********************************************************************
  ***************************************************

     DEFINE SOME PARAMETERS NEEDED IN THE PROGRAM

   ***********************************************************
         H22 = B1(2,2) + H1 / 2.00 * A1(2,2)
         H26 = B1(2,6) + H1 / 2.00 * A1(2,6)
         H66 = B1(6,6) + H1 / 2.00 * A1(6,6)

          C22 = BO(2,2) + HO / 2.00 * A1(2,2)
         C26 = BO(2,6) + HO / 2.00 * A1(2,6)
         C66 = BO(6,6) + HO / 2.00 * A1(6,6)

         K22 = A1(2,2) +  AO(2,2)
         K26 = A1(2,6) +  AO(2,6)
         K66 = A1(6,6) +  AO(6,6)
         K12 = A1(1,2) +  AO(1,2)
         K16 = A1(1,6) +  AO(1,6)

         D = K22 * K66 -( K26 * K26)

         E15 = DO(2,2)  - HO/2*BO(2,2)
         E16 = DO(2,6)  - HO/2*BO(2,6)
         E17 = DO(6,6)  - HO/2*BO(6,6)
         E18 = BO(1,2)  - HO/2*AO(1,2)
         E19 = BO(1,6)  - HO/2*AO(1,6)

           VV11 = ( K26 * H26 - K66 * H22 ) / D  + ( H1 / 2.00 )
           VV12 = ( K26 * C26 - K66 * C22 ) / D  + ( HO / 2.00 )
           VV13 = ( K26 * H66 - K66 * H26 ) / D
           VV14 = ( K26 * C66 - K66 * C26 ) / D

            U11 = ( K26 * H22 - K22 * H26 ) / D
            U12 = ( K26 * C22 - K22 * C26 ) / D
            U13 = ( K26 * H26 - K22 * H66 ) / D  + ( H1 / 2.00 )
            U14 = ( K26 * C26 - K22 * C66 ) / D  + ( HO / 2.00 )

        F(1,1) = D1(2,2) + B1(2,2) * H1 / 2.0 + H22*VV11 + H26 * U11
        F(2,1) = H22 * VV12  +  H26 * U12
        F(3,1) = D1(2,6) + B1(2,6) * H1 / 2.0 + H22*VV13 + H26 * U13
        F(4,1) = H22 * VV14 + H26 * U14

        F(2,2) = DO(2,2) - BO(2,2) * HO / 2.0 + C22 * VV12 + C26*U12
        F(3,2) = H26 * VV12 + H66 * U12
        F(4,3) = H26 * VV14 + H66 * U14

        F(3,3) = D1(6,6) + B1(6,6) * H1 / 2.0 + H26*VV13 + H66 * U13
        F(4,2) = DO(2,6) - BO(2,6) * HO / 2.0 + C22*VV14 + C26 * U14
```

C - 2

```
      F(4,4) = DO(6,6) - BO(6,6) * HO / 2.0 + C26*VV14 + C66 * U14

      DX  = K22 * K66

        DVV11 =  - K66 * H22  / DX  + ( H1 / 2.00 )
        DVV12 =  - K66 * C22  / DX  + ( HO / 2.00 )
         DU13 =  - K22 * H66  / DX  + ( H1 / 2.00 )
         DU14 =  - K22 * C66  / DX  + ( HO / 2.00 )

     DF(1,1) = D1(2,2) + B1(2,2) * H1 / 2.0 + H22*DVV11
     DF(2,1) = H22 * DVV12
     DF(2,2) = DO(2,2) - BO(2,2) * HO / 2.0 + C22 * DVV12
     DF(4,3) = H66 * DU14

     DF(3,3) = D1(6,6) + B1(6,6) * H1 / 2.0 +  H66 * DU13
     DF(4,4) = DO(6,6) - BO(6,6) * HO / 2.0 + C66 * DU14


    W(1) = F(3,3)*( F(2,2)*F(4,4)-F(4,2)*F(4,2) ) - F(3,2)*F(3,2)*
C          F(4,4) + 2*F(4,3)*F(4,2)*F(3,2) - F(2,2)*F(4,3)*F(4,3)

    W(2) = - F(3,3)*(F(2,2)*AO(5,5) + F(4,4)*AO(4,4) - 2*F(4,2)
C           * AO(4,5) ) -  A1(5,5) * ( F(2,2) * F(4,4) -
C          F(4,2) * F(4,2)) + F(3,2) * F(3,2) * AO(5,5) -
C       2.0 *F(4,3)*F(3,2)*AO(4,5) + F(4,3) * F(4,3) * AO(4,4)


   X(1) =F(3,1)*(F(2,2)*F(4,4)-F(4,2)*F(4,2))-F(3,2)*(F(2,1)*F(4,4)
C         - F(4,1)*F(4,2)) + F(4,3)*(F(2,1)*F(4,2) - F(4,1)*F(2,2))

    X(2) = - F(3,1) * ( F(2,2) * AO(5,5) + F(4,4) * AO(4,4)
C          - 2 * F(4,2) * AO(4,5) ) - A1(4,5) *  ( F(2,2) * F(4,4)
C           - F(4,2) * F(4,2) ) + F(3,2) * ( AO(5,5) * F(2,1) -
C      F(4,1)*AO(4,5)) - F(4,3)*( F(2,1)*AO(4,5) - F(4,1)*AO(4,4))


    Y(1) = F(3,1)*(F(3,2)*F(4,4) - F(4,3)*F(4,2)) - F(3,3)*(F(2,1)*
C     F(4,4) - F(4,1)*F(4,2))+F(4,3)*(F(2,1)*F(4,3)-F(4,1)*F(3,2))

    Y(2) = 0 - A1(4,5)*(F(3,2)*F(4,4) - F(4,2)*F(4,3))
C          - F(3,1) * (  F(3,2)*AO(5,5) - F(4,3) * AO(4,5) ) +
C          A1(5,5) * ( F(2,1) * F(4,4) - F(4,1) * F(4,2) ) +
C          F(3,3) * ( F(2,1) * AO(5,5) - F(4,1) * AO(4,5) )
    Y(3) = A1(4,5)*(F(3,2)*AO(5,5) - F(4,3)*AO(4,5)) - A1(5,5) *
C          ( F(2,1) * AO(5,5) - F(4,1) * AO(4,5) )


    ZZ(1) = F(3,1)*(F(3,2)*F(4,2) - F(4,3)*F(2,2)) - F(3,3)*(F(2,1)*
C        F(4,2)-F(4,1)*F(2,2))+F(3,2)*(F(2,1)*F(4,3)-F(4,1)*F(3,2))

    ZZ(2) = F(3,1)*(F(4,3)*AO(4,4) - F(3,2)*AO(4,5)) - A1(4,5)*
C         (F(3,2)*F(4,2) - F(4,3)*F(2,2))+ A1(5,5)*(F(2,1)* F(4,2) -
C         F(4,1)*F(2,2)) - F(3,3)*(F(4,1)*AO(4,4) - F(2,1)*AO(4,5))
    ZZ(3) = 0 - A1(4,5)*(F(4,3)*AO(4,4)-F(3,2)*AO(4,5))+A1(5,5)*
C           ( F(4,1) * AO(4,4) - F(2,1) * AO(4,5) )
*****************************************************************************

 NOW OBTAIN THE VALUES OF E SO THAT THE 8TH ORDER POLYNOMIAL MAY BE SOLVED

 *****************************************************************************
      E(1) = F(1,1)*W(1) - F(3,1)*X(1) + F(2,1)*Y(1) - F(4,1)*ZZ(1)
      E(3) = F(1,1)*W(2) - A1(4,4)*W(1) - F(3,1)*X(2) + A1(4,5)*X(1)
C             + F(2,1) * Y(2) - F(4,1) * ZZ(2)
      E(5) = (AO(4,4)*AO(5,5) - AO(4,5)*AO(4,5))*(F(1,1)*F(3,3)
C         - F(3,1)*F(3,1)) + (F(2,2)*AO(5,5) + F(4,4)*AO(4,4) -
C          2*F(4,2)*AO(4,5))*(F(1,1)*A1(5,5) - F(3,1)*A1(4,5) )
```

```
C         - A1(4,4)*W(2) + A1(4,5)*X(2)+ F(2,1)*Y(3) - F(4,1)*ZZ(3)

      E(7) = - (AO(4,4)*AO(5,5) - AO(4,5)*AO(4,5))*(F(1,1)*A1(5,5)
C          + F(3,3)*A1(4,4) - 2*F(3,1)*A1(4,5)) - (A1(4,4)*A1(5,5) -
C          A1(4,5)*A1(4,5))*(F(2,2)*AO(5,5) + F(4,4)*AO(4,4)
C           - 2 * AO(4,5) * F(4,2) )

      E(9) = (AO(4,4)*AO(5,5) - AO(4,5)*AO(4,5) ) *
C           (A1(4,4) * A1(5,5) - A1(4,5) * A1(4,5) )

       CALL UP SUBROUTINE TO SOLVE 8TH ORDER POLYNOMIAL

        NDEG = 8
        IER = 0
        CALL ZPOLR (E,NDEG,SJ,IER)

        KK = 0
*************************************************************************
*************************************************************************


        IF (LIL.EQ.1) WRITE(6,217)
        DO 90  L = 1, 8
        S(L) = REAL(SJ(L))
        IF (REAL(SJ(L)).GT.0) KK = KK + 1
90      IF (REAL(SJ(L)).GT.0) S(KK) = S(L)
           DO 95 KK = 1,4
95         IF (LIL.EQ.1) WRITE(6,221) KK, S(KK)


*************************************************************************

*************************************************************************
 NOW FIND THE UNCOUPLED S VALUES AND THOSE OF THE MEMBRANE

      BNEG= DF(1,1) * AO(4,4) + DF(2,2) * A1(4,4)
      A = DF(1,1) * DF(2,2) - DF(2,1) * DF(2,1)
      C = AO(4,4) * A1(4,4)
       SQ = DSQRT (BNEG * BNEG - ( 4.0 * A * C))
       DIFF1 = DABS ( BNEG - SQ )
       DIFF2 = DABS ( BNEG + SQ )
        IF (DIFF1.GT.DIFF2) GO TO 100
        UNSY(1) = DSQRT ( (BNEG+SQ) / 2.0 / A  )
        GO TO 105
100     UNSY(1) = DSQRT ( (BNEG-SQ) / 2.0 / A  )
105     UNSY(2) = DSQRT( (BNEG/A) - UNSY(1)* UNSY(1) )

      BNEG= DF(3,3) * AO(5,5) + DF(4,4) * A1(5,5)
      A = DF(3,3) * DF(4,4) - DF(4,3) * DF(4,3)
      C = AO(5,5) * A1(5,5)
       SQ = DSQRT (BNEG * BNEG - ( 4.0 * A * C) )
       DIFF1 = DABS ( BNEG - SQ )
       DIFF2 = DABS ( BNEG + SQ )
        IF (DIFF1.GT.DIFF2) GO TO 110
        UNSX(1) = DSQRT ( (BNEG+SQ) / 2.0 / A )
        GO TO 115
110     UNSX(1) = DSQRT ( (BNEG-SQ) / 2.0 / A )
115     UNSX(2) = DSQRT ( (BNEG/A) - UNSX(1) * UNSX(1) )

*************************************************************************
      IF (LIL.EQ.1) WRITE(6,224)  UNSX(1), UNSX(2)
      IF (LIL.EQ.1) WRITE(6,223)  UNSY(1), UNSY(2)

*************************************************************************

      NOW THE S FOR THE MEMBRANE ONLY
```

```
      F11M = H1/2. * ( A1(2,2) * (DVV11 + DVV12*HO/H1*A1(4,4)/AO(4,4))
     C      + B1(2,2) )

      F22M = H1/2. * ( A1(6,6) * (U13 + U14*HO/H1*A1(5,5)/AO(5,5))
     C       + B1(6,6) )

        MEMSY = DSQRT ( A1(4,4) / F11M )
        MEMSX = DSQRT ( A1(5,5) / F22M )

*************************************************************************

      IF (LIL.EQ.1) WRITE(6,219) MEMSX, MEMSY

*************************************************************************

      DUM = AO(2,2) * AO(6,6) - AO(2,6) * AO(2,6)
      S1NM = ( AO(6,6)*NMNYO - AO(2,6)*NMNXYO ) / DUM
      S2NM = ( AO(2,2)*NMNXYO - AO(2,6)*NMNYO ) / DUM
        IF (LIL.EQ.1) WRITE(6,288) S1NM,S2NM

        IF ( COUPL.EQ.2)GO TO 130

 SOLVE FOR WD, CD, CU AND CV

      WD(1,1) = (AO(2,6) * AO(1,6) - AO(6,6) * AO(1,2) ) / DUM
      WD(1,2) = (AO(2,6) * BO(2,6) - AO(6,6)*BO(2,2) ) / DUM
      WD(1,3) = (AO(2,6)*BO(6,6) - AO(6,6)*BO(2,6) ) / DUM
      WD(2,1) = (AO(2,6) * AO(1,2) - AO(2,2) * AO(1,6) )/DUM
      WD(2,2) = (AO(2,6)*BO(2,2) - AO(2,2)* BO(2,6) ) / DUM
      WD(2,3) = (AO(2,6) * BO(2,6) - AO(2,2)*BO(6,6) ) / DUM


        MATR33(1,1) = A1(2,2)
        MATR33(1,2) = A1(2,6)
        MATR33(1,3) = B1(2,2)

        MATR33(2,1) = MATR33(1,2)
        MATR33(2,2) = A1(6,6)
        MATR33(2,3) = B1(2,6)

        MATR33(3,1) = MATR33(1,3)
        MATR33(3,2) = MATR33(2,3)
        MATR33(3,3) = D1(2,2)


        MATR32(1,1) =  - A1(1,2)
        MATR32(1,2) =  - B1(2,6)

        MATR32(2,1) =  - A1(1,6)
        MATR32(2,2) =  - B1(6,6)

        MATR32(3,1) =  - B1(1,2)
        MATR32(3,2) =  - D1(2,6)
        IF (IZZ.EQ.2) GO TO 122

         DO 120 I=1,3
         DO 120 K=1,3
120      SAVE33(I,K) = MATR33(I,K)
          SAVE3(1) = NMNY1
          SAVE3(2) = NMNXY1
          SAVE3(3) = NMMY1
             IRR = 0
       CALL LEQT2F(SAVE33,1,3,3,SAVE3,0,WKAREA,IRR)

122     M=2
```

```
            N=3
            IA=3
            IRR=0
            IDD=0                                                          72

          CALL LEQT2F(MATR33,M,N,IA,MATR32,IDD,WKAREA,IRR)

              DO  125 I=1,3
             IF (IZZ.EQ.2)  SAVE3(I) = ZR
              FNM(I) = SAVE3(I)
                DO 125  L=1,2
125           CD(I,L) = MATR32(I,L)


          SC = DSQRT(  ( A1(5,5) - A1(4,5) * A1(4,5) / A1(4,4) )
     C       / ( D1(6,6) + B1(2,6)*CD(1,2) + B1(6,6)*CD(2,2)
     C                 + D1(2,6) * CD(3,2) ) )
          GO TO 135
*********************************************************************

            IN CASE THE LAYERS ARE UNCOUPLED

 ********************************************************************
 130      DY = -1/ ( A1(2,2)*A1(6,6) -  A1(2,6) * A1(2,6) )
          CD(1,1) = ( A1(6,6)*A1(1,2) - A1(2,6)*A1(1,6) ) / DY
          CD(2,1) = ( A1(2,2)*A1(1,6) - A1(2,6)* A1(1,2) ) / DY
          CD(3,2) = ( A1(2,2)*A1(6,6) + A1(2,6)*A1(2,6) ) *
     C               D1(2,6) / D1(2,2)/ DY
          CD(1,2) = ZR
          CD(2,2) = ZR
          CD(3,1) = ZR

          DR = -1 / (  AO(2,2)*AO(6,6) - AO(2,6)*AO(2,6) )
          WD(1,1) = ( AO(6,6)*AO(1,2) - AO(2,6)*AO(1,6) ) / DR
          WD(2,1) = ( AO(2,2)*AO(1,6) - AO(2,6)*AO(1,2) ) / DR
          WD(1,2) = ZR
          WD(1,3) = ZR
          WD(2,2) = ZR
          WD(2,3) = ZR
          SSY = DSQRT( AO(5,5) / DO(6,6) )
          SSX = DSQRT( AO(4,4) / DO(2,2) )

           FNM(1) = (A1(2,6)*NMNXY1 - A1(6,6)*NMNY1) / DY
           FNM(2) = (A1(2,6)*NMNY1 - A1(2,2)*NMNXY1 ) / DY
        FNM(3)=(A1(2,6)*A1(2,6) - A1(2,2)*A1(6,6))/DY * NMMY1/D1(2,2)

             SC = DSQRT(  (A1(5,5)* A1(6,6)) / (A1(6,6)*D1(6,6)
     C            - (B1(6,6)*B1(6,6)) ) )


 ********************************************************************
  ********************************************************************


 135       C1 = B1(1,6) + CD(1,1)*B1(2,6) + CD(2,1)*B1(6,6)
     C                  + CD(3,1) * D1(2,6)
           C2 = D1(6,6) + CD(1,2)*B1(2,6) + CD(2,2)*B1(6,6) +
     C                  CD(3,2) * D1(2,6)


           J22 = DO(2,2) + BO(2,2) * WD(1,2) + BO(2,6) * WD(2,2)
           J66 = DO(6,6) + BO(2,6) * WD(1,3) + BO(6,6) * WD(2,3)
           J26 = DO(2,6) + BO(2,2) * WD(1,3) + BO(2,6) * WD(2,3)

          BNEG = J22 * AO(5,5) + J66 * AO(4,4) - 2. * J26 * AO(4,5)
          A = J22 * J66 - J26 * J26
```

```
          C = AO(4,4) * AO(5,5) - AO(4,5) * AO(4,5)

          SQ = DSQRT ( (BNEG * BNEG) - 4.0 * C * A )                    73
          DIFF1 = DABS( BNEG + SQ )
          DIFF2 = DABS( BNEG - SQ )
          IF (DIFF1.GT.DIFF2) GO TO 140
          SS1 = DSQRT ((BNEG + SQ) / 2. / A )
          GO TO 145
140       SS1 = DSQRT ( (BNEG-SQ) / 2. / A )
145       SS2 = DSQRT ( (BNEG/A) - SS1 * SS1 )

           SSY = DSQRT ( AO(4,4) * J22 )
           SSX = DSQRT ( AO(5,5) * J66 )

 **********************************************************************

         IF (LIL.EQ.1) WRITE(6,*)'     S1 AND S2 = ',SS1, SS2
         IF (LIL.EQ.1) WRITE(6,*)'     SX AND SY = ',SSX, SSY

 **********************************************************************

       CVNM = ( K66 * (NMNY1 + NMNYO) - K26 * (NMNXY1 + NMNXYO) ) / D
       CUNM = ( K22 * (NMNXY1 + NMNXYO) - K26 * (NMNY1 + NMNYO) ) / D

        CV = STRAIN(LST) / D * ( K26 * K16 - K66 * K12 ) + CVNM
        CU = STRAIN(LST) / D * ( K26 * K12 - K22 * K16 ) + CUNM

 **********************************************************************

        NOW FIND SOME OF THE NEEDED CONSTANTS.....
         FIRST DO LOOP IS TO VARY THE VALUES OF S

            DO 150  I = 1,4

  FORM THE A MATRIX (MATR32) AND ITS B (MATR3)

            MATR33(1,1) =  - ( F(3,1) * S(I) * S(I) - A1(4,5) )
            MATR33(1,2) =  - ( F(2,1) * S(I) * S(I) )
            MATR33(1,3) =  - ( F(4,1) * S(I) * S(I) )
            MATR33(2,1) =  - ( F(3,3) * S(I) * S(I) - A1(5,5) )
            MATR33(2,2) =  - ( F(3,2) * S(I) * S(I) )
            MATR33(2,3) =  - ( F(4,3) * S(I) * S(I) )
            MATR33(3,1) =  - ( F(3,2) * S(I) * S(I) )
            MATR33(3,2) =  - ( F(2,2) * S(I) * S(I) - AO(4,4) )
            MATR33(3,3) =  - ( F(4,2) * S(I) * S(I) - AO(4,5) )

            MATR3(1) = (F(1,1) * S(I) * S(I) ) - A1(4,4)
            MATR3(2) = F(3,1) * S(I) * S(I)  - A1(4,5)
            MATR3(3) = F(2,1) * S(I) * S(I)


       CALL UP  ROUTINE  TO FIND THE VALUES OF ALPHA, PHI AND GAMMA

            M=1
            N=3
            IRR=0
            IDD=0
            IA=3
            CALL LEQT2F(MATR33,M,N,IA,MATR3,IDD,WKAREA,IRR)
             ALPHA(I) = MATR3(1)
             PHI(I) = MATR3(2)
             GAMMA(I) = MATR3(3)

       SV(I) = VV11 + ALPHA(I)*VV13 + PHI(I)*VV12 + GAMMA(I)*VV14
150    SU(I) = U11 + ALPHA(I)*U13 + PHI(I)*U12 + GAMMA(I)*U14
```

```
      DO 155 I = 1,4

      NX1(I)=A1(1,2)*SV(I) + A1(1,6)*SU(I) + B1(1,2) + B1(1,6)*ALPHA(I)
      NY1(I)=A1(2,2)*SV(I) + A1(2,6)*SU(I) + B1(2,2) + B1(2,6)*ALPHA(I)
     NXY1(I)=A1(2,6)*SV(I) + A1(6,6)*SU(I) + B1(2,6) + B1(6,6)*ALPHA(I)
      MY1(I)=B1(2,2)*SV(I) + B1(2,6)*SU(I) + D1(2,2) + D1(2,6)*ALPHA(I)
     MXY1(I)=B1(2,6)*SV(I) + B1(6,6)*SU(I) + D1(2,6) + D1(6,6)*ALPHA(I)
     NXO(I) =AO(1,2)*SV(I) + AO(1,6)*SU(I) + E18*PHI(I) + E19*GAMMA(I)
            GG(1,I) = NY1(I)
            GG(2,I) = NXY1(I)
            GG(3,I) = MY1(I)
                FTH = C2 * SC
155         GG(4,I) = MXY1(I) + FTH * ALPHA(I)/ S(I)


      A1NM = B1(2,6)* FNM(1) + B1(6,6)*FNM(2) + D1(2,6) * FNM(3)

                                                                      **
      BG(1) = A1(1,2)*STRAIN(LST) + CV * A1(2,2) + A1(2,6) * CU-NMNY1
      BG(2) = A1(1,6)*STRAIN(LST) + CV * A1(2,6) + A1(6,6) * CU-NMNXY1
      BG(3) = B1(1,2)*STRAIN(LST) + B1(2,2) * CV + B1(2,6) * CU-NMMY1
      BG(4) = B1(1,6)*STRAIN(LST) + B1(2,6) * CV + B1(6,6) * CU-A1NM
C           - C1 * STRAIN(LST)

            BG1= BG(1)
            BG2 = BG(2)

        M=1
        N=4
        IA=4
        IDD=0
        IRR=0
            CALL LEQT2F(GG,M,N,IA,BG,IDD,WKAREA,IRR)

*************************************************************************

       TVNM =   S1NM - FNM(1) + H1 / 2.0 * FNM(3)
       TUNM =   S2NM - FNM(2)

       THETV =  -CD(1,1) + WD(1,1) + H1/2.0*CD(3,1)
       THETU =  -CD(2,1) + WD(2,1)
        THETV = THETV  + TVNM
        THETU = THETU  + TUNM

     IF (LIL.EQ.1) WRITE(6,215) THETV, THETU
     IF (LIL.EQ.1) WRITE(6,216)  SMNY, SMNXY

*************************************************************************
THE STEPS USED TO FIND THE TOTAL ENERGY RELEASE FROM USING A PURE
EXTENSION ANALYSIS FOR THE HYGRALTHERMAL EFFECTS.  (SIMILAR TO
WHITNEY'S). ANALYSIS IS CARRIED OUT ON A PLY BY PLY BASIS


       ZV = ( K26 * K16 - K66 * K12 ) / D
       ZU = ( K26 * K12 - K22 * K16 ) /D
C
        DO 162  LL = 1,TPLY
C
C
       EX(LL) = THICK(LL) * ( Q(1,1,LL) + ZV*Q(1,2,LL) +
C              ZU*Q(1,6,LL) )
       T1(LL) = NXNM(LL) - CVNM*THICK(LL)*Q(1,2,LL) -
C               CUNM * THICK(LL) * Q(1,6,LL)
       EXX(LL) = Q(1,1,LL)*THICK(LL) + Q(1,2,LL)*THICK(LL)*CD(1,1)
```

```
C           + Q(1,6,LL)*THICK(LL)*CD(2,1) + B12(LL)*CD(3,1)
      T12(LL) = NXNM(LL) - FNM(1)*Q(1,2,LL)*THICK(LL) -
C           FNM(2)*Q(1,6,LL)*THICK(LL) - FNM(3)*B12(LL)
      EX3(LL) = Q(1,1,LL)*THICK(LL) + WD(1,1)*Q(1,2,LL)*THICK(LL)
C            + WD(2,1)*Q(1,6,LL)*THICK(LL)
      T13(LL) = NXNM(LL) - Q(1,2,LL)*THICK(LL)*S1NM - Q(1,6,LL)
C            * THICK(LL) * S2NM

          IF (IZZ.EQ.2) NMSTO(LL) = 0.0
          IF (IZZ.EQ.2) NMST2(LL) = 0.0
          IF (IZZ.EQ.2) NMST3(LL) = 0.0
          IF (IZZ.EQ.2) GO TO 162


       NMSTO(LL) =  T1(LL)  / EX(LL)
       NMST2(LL) =  T12(LL) / EXX(LL)
       NMST3(LL) =  T13(LL) / EX3(LL)

162    CONTINUE

         WRITE(6,*)' JMM, NMSTO,2,3 OF ALL PLYS ',( NMSTO(JP),
C      NMST2(JP),NMST3(JP),' ---  ',JP=1,TPLY)

         WRITE(6,*)' EX, EXX EX3  OF ALL PLYS ',( EX(JP),
C      EXX(JP),EX3(JP),' ---  ',JP=1,TPLY)

          TNC = 0.0
          EXNC = 0.0
          TSTAR = 0.0
          ESTAR = 0.0
          DO 163  LK = 1,TPLY
           TNC =  TNC  + T1(LK)
           EXNC = EXNC + EX(LK)
           IF (LK.LE.NPLYO) TSTAR = TSTAR + T13(LK)
           IF (LK.GT.NPLYO) TSTAR = TSTAR + T12(LK)

           IF (LK.LE.NPLYO) ESTAR = ESTAR + EX3(LK)
163        IF (LK.GT.NPLYO) ESTAR = ESTAR + EXX(LK)

          IF(IZZ.EQ.2) TNMST = 0.0
          IF (IZZ.EQ.2) GO TO 89

      TNMST = (  TNC -(TNC-TSTAR)*2*AL/WIDTH ) / ( EXNC -
C           (EXNC-ESTAR)*2*AL/WIDTH )
89    WRITE(6,*)'  TNMST EQUALS ',TNMST


      DO 164   LL = 1,TPLY

       IF (LL.LE.NPLYO) WWC =  (EX3(LL) *
C        (STRAIN(LST) + TNMST) - T13(LL) )
C *   ( STRAIN(LST) - NMST3(LL) + TNMST )

       IF (LL.GT.NPLYO) WWC =  (EXX(LL) *
C        (STRAIN(LST) + TNMST) - T12(LL) )
C *   ( STRAIN(LST) - NMST2(LL) + TNMST )

     WWO = ( EX(LL)* (STRAIN(LST) + TNMST) - T1(LL) )
C         *  ( STRAIN(LST) - NMSTO(LL) + TNMST )


164    GLC(JMM) =  GLC(JMM) + WWO - WWC

          GLC(JMM) = GLC(JMM) / 2.0
*****************************************************************************
```

```
      THIS IS TO CALCULATE THE INTERLAMINAR SHEAR STRESSES.

     ************************************************************************
             UNCL =(WIDTH / 2.0)- AL
               DO 180  JX = 80,100
                JY =(  1.0 -  JX /100.0)  * UNCL
                SIGX(JMM,JX) = 0
                SIGY(JMM,JX) = 0
                   DO 180  JS = 1,4
                   SIGX(JMM,JX) =  BG(JS) * S(JS) * DEXP ( -S(JS)* JY )
        C                         * NXY1(JS) + SIGX(JMM,JX)

                   SIGY(JMM,JX) =  BG(JS) * S(JS) * DEXP ( -S(JS)* JY )
        C                         * NY1(JS) + SIGY(JMM,JX)

      180          CONTINUE

          THE PROGRAM CONTINUES AND FINDS THE VARIOUS STRAIN ENERGY RELEASE
          COMPONENTS .....


              IF (COUPL.EQ.1) GO TO 165

              THIS  IS  FOR A SYSTEM THAT IS COUPLED, THE  CRACK LENGTH IS

              DEL = S(4) * S(2) * ATH * ATH
              DEL = DEL * DEL * 0.6144
              GO TO 170

           THIS IS FOR AN UNCOUPLED SYSTEM.....................

      165     SSW = .65 * ( S(1) + S(2) + S(3) )
              DEL = 18.7 * S(4) * SSW * ATH * ATH
              DEL = DEL * DEL / 571.00
      170     DEL = 135.7 * DEL * ATH

     C        IF (LIL.EQ.1)  WRITE(6,211) DEL

              FY = ZR
              FX = ZR


              DO 175   JP=1,4

               CONY= NY1(JP)*BG(JP)*( DEXP  ( -S(JP) * DEL ) - 1 )
               CONXY= NXY1(JP)* BG(JP)*( DEXP( -S(JP) *DEL)- 1 )
               CCONXY = CCONXY + CONXY/S(JP)
      175      CCONY = CCONY + CONY/S(JP)

     ************************************************************************
     ************************************************************************

               FY = BG1 + CCONY / DEL
               FX = BG2 + CCONXY / DEL

              GII(IZZ,JM) =   FY / 2.0  * THETV *STRAIN(LST)
              GIII(IZZ,JM) =   FX / 2.0 * THETU * STRAIN(LST)

             DIFFG= GII(IZZ,JM) - GIII(IZZ,JM)
             CON = 2
               IF (DIFFG.GT.REAL(GLC(JMM))) CON=1
               IF (DIFFG.GT.REAL(GLC(JMM))) DEL = DEL * .9
               IF (DIFFG.GT.REAL(GLC(JMM))) WRITE(6,*)' IT EXPLODES

                GI(IZZ,JM) = GLC(JMM)-GII(IZZ,JM)-GIII(IZZ,JM)
```

```
200      CONTINUE

   RESULTS ARE PRINTED FOR EACH RUN.                                    77


300          CONTINUE
       WRITE(6,266)  STRAIN(LST)
       WRITE(6,267)
       WRITE(6,269)  GLC(0)  , GI(2,1), GII(2,1), GIII(2,1),
   C    GI(2,1)/GLC(0)

          DO 350 I=1,MMC +1
      WRITE(6,268)  CMOIST(I),GLC(I), GI(1,I),GII(1,I),
   C    GIII(1,I), GI(1,I)/GLC(I)
350      CONTINUE

     WRITE(6,287)

          DO 360  NS = 80,90,2
360        WRITE(6,285)NS/100., SIGX(0,NS),( SIGX(KL,NS),KL=1,22,4)

          DO 365  NS = 91,100
365        WRITE(6,285)NS/100.,SIGX(0,NS),  ( SIGX(KL,NS),KL=1,22,4)

     WRITE (6,286)
          DO 370  NS = 80,90,2
370        WRITE(6,285)  NS/100.,SIGY(0,NS),( SIGY(KL,NS),KL=1,22,4)

          DO 375  NS = 91,100
375        WRITE(6,285)  NS/100.,SIGY(0,NS),( SIGY(KL,NS), KL=1,22,4)


400          CONTINUE

201  FORMAT(//,'  THE WIDTH OF THE LAMINATE IS ',F8.5)
287  FORMAT(/////,' THESE ARE THE IN-PLANE  INTERLAMINAR SHEAR ',
   C 'STRESSES -- SIGMA XY  ',/,'  THEY ARE FOUND AT VARIOUS',
   C '- MOISTURE CONTENTS ',//,'  Y LOCATION',7X,' MECH ONLY',8X,
   C  'H=0.0',10X,'H=0.2',10X,'H=0.4',10X,
   C    'H=0.6',10X,'H=0.8',10X,'H=1.0',//)
285  FORMAT(3X,F7.2,4X,7F15.8)
202  FORMAT(' THE NUMBER OF LAMINATES ABOVE AND BELOW THE CRACK IS'
   C     ,I3,5X,I3)
204       FORMAT(///,'  THE PLYS ARE INPUTTED FROM BOTTOM TO TOP',/,
   C  ' BUT THE PLY CHARACTERISTICS FROM TOP TO BOTTOM ARE ')
206  FORMAT(//,' FOR PLY',I5,' THE SUBLAMINATE HAS THESE PROPERTIES')
205   FORMAT(//,'  WITH THIS LAYUP, THE PLYS ARE COUPLED ',//)
210   FORMAT(//,'  WITH THIS LAYUP, THE PLYS ARE DECOUPLED ',//)
286  FORMAT(//,' THESE ARE THE OUT-OF-PLANE  INTERLAMINAR SHEAR ',
   C 'STRESSES -- SIGMA YZ  ',/,'  THEY ARE FOUND AT VARIOUS',
   C ' MOISTURE CONTENTS ',//,' Y LOCATION',8X,' MECH ONLY',8X,
   C  'H=0.0',10X,'H=0.2',10X,'H=0.4',10X,
   C    'H=0.6',10X,'H=0.8',10X,'H=1.0',//)
208  FORMAT(' E1 AND E2 ARE (MSI)                ',F8.4,10X,F8.4)
289  FORMAT(//,'  THE LAMINA PLY CHARACTERISTICS INITIALLY ARE ',/)
288  FORMAT(/,'  S1NM AND S2NM ARE EQUAL TO ',F14.10,4X,F14.10)
211  FORMAT(//,'  THE CRACK LENGTH STEP SIZE IS ',F12.8)
266    FORMAT('0','1','   THE STRAIN IS EQUAL TO ',F12.7,/,
   C '  THE VALUES OF GT,  GI,  GII,  AND  GIII  ARE  IN  IN-LB/IN/IN
   C  ')
267    FORMAT (/,3X,'% CMOIST',8X,'GGG(WHITNEY)',6X,'GI',9X,
   C   ' GII',8X,'GIII',6X,' GI/G(W-T)',//)
269  FORMAT(/,'  MECH. ONLY ',3X,F12.9,4(2X,F11.7),/)
268  FORMAT(5X,F8.3,3X,F12.9,4(2X,F11.7) )
215  FORMAT(////,'  THETA V IS ',F15.10,' THETA U IS ',F24.19)
216  FORMAT(//,'  NY IS ',F23.11,'  NXY IS ',F23.18)
```

```
207  FORMAT(/,' THE THICKNESS AND THETA VALUES ARE ',F9.6,5X,F8.3)
209  FORMAT(' THE POISSON RATIO (1,2) IS     ',F10.5)
214  FORMAT(' G OF (1-2),  AND (3-1) ARE -MSI ', 2(F9.4,2X))
217  FORMAT('0',////,8X,'THE FOUR CHARACTERISTIC VALUES ASSOCIATED'
   C ,/,8X,' WITH THE 8 DEGREE POLYNOMIAL FOR THE COUPLED CASE ARE')
218  FORMAT(//,5X,' THETA ',6X,' NY ',8X,' NXY ',//)
219  FORMAT(///,' THE S VALUES OF THE MEMBRANE ARE ',F15.5,3X,F15.5)
220  FORMAT(/,4X,F9.4,3X,F9.2,3X,F9.2)
221  FORMAT(/,'  S OF ',I2,' IS EQUAL TO ',F20.10)
223  FORMAT(/,'  THE UNCOUPLED SY (1,2) VALUES ARE ',F15.5,3X,F15.5)
224  FORMAT(/,'  THE UNCOUPLED SX (1,2) VALUES ARE ',F15.5,3X,F15.5)
231  FORMAT(//,'  THE STRAIN IS EQUAL TO ',F12.8,/,
   C '  THE CHANGE IN TEMPERATURE IS ',F12.5,/,
   C '  THE COEFFICIENTS SWELLING DUE TO MOISTURE ARE ',2(2X,F12.8)
   C ,/,'  THE COEFFICIENTS OF THERMAL EXPANSION ARE ',2(2X,F15.9))

232  FORMAT(/,'  THE MOISTURE COEFFICENT IS ',F15.8)
233  FORMAT(/,'  THE MOISTURE COEFFICIENT VARIES FROM 0 TO 1.2 ')

       STOP
       END
```

THE LAMINA PLY CHARACTERISTICS INITIALLY ARE

THE WIDTH OF THE LAMINATE IS 1.51200
THE NUMBER OF LAMINATES ABOVE AND BELOW THE CRACK IS 3 1

FOR PLY 1 THE SUBLAMINATE HAS THESE PROPERTIES
THE THICKNESS AND THETA VALUES ARE .005400 35.000
E1 AND E2 ARE (MSI) 18.7000 1.2300
THE POISSON RATIO (1,2) IS .29200
G OF (1-2), AND (3-1) ARE -MSI .8320 .8320

FOR PLY 2 THE SUBLAMINATE HAS THESE PROPERTIES
THE THICKNESS AND THETA VALUES ARE .005400 -35.000
E1 AND E2 ARE (MSI) 18.7000 1.2300
THE POISSON RATIO (1,2) IS .29200
G OF (1-2), AND (3-1) ARE -MSI .8320 .8320

FOR PLY 3 THE SUBLAMINATE HAS THESE PROPERTIES
THE THICKNESS AND THETA VALUES ARE .005400 .000
E1 AND E2 ARE (MSI) 18.7000 1.2300
THE POISSON RATIO (1,2) IS .29200
G OF (1-2), AND (3-1) ARE -MSI .8320 .8320

FOR PLY 4 THE SUBLAMINATE HAS THESE PROPERTIES
THE THICKNESS AND THETA VALUES ARE .005400 90.000
E1 AND E2 ARE (MSI) 18.7000 1.2300
THE POISSON RATIO (1,2) IS .29200
G OF (1-2), AND (3-1) ARE -MSI .8320 .8320

THE STRAIN IS EQUAL TO .00254000
THE CHANGE IN TEMPERATURE IS -280.00000
THE COEFFICIENTS SWELLING DUE TO MOISTURE ARE .00000000 .00556000
THE COEFFICIENTS OF THERMAL EXPANSION ARE -.000000230 .000014900

THE MOISTURE COEFFICIENT VARIES FROM 0 TO 1.2

WITH THIS LAYUP, THE PLYS ARE COUPLED

THE FOUR CHARACTERISTIC VALUES ASSOCIATED
WITH THE 8 DEGREE POLYNOMIAL FOR THE COUPLED CASE ARE

S OF 1 IS EQUAL TO 407.0573682744

S OF 2 IS EQUAL TO 141.1197780418

S OF 3 IS EQUAL TO 116.7332723860

S OF 4 IS EQUAL TO 55.5544207729

THE UNCOUPLED SX (1,2) VALUES ARE 392.22478 106.21737

THE UNCOUPLED SY (1,2) VALUES ARE 134.68589 56.25754

THE S VALUES OF THE MEMBRANE ARE 177.38945 66.26466

S1NM AND S2NM ARE EQUAL TO -.0000157292 .0000000000
S1 AND S2 = 134.93247116395780394312025 7 641.50029909958418278794308 9
SX AND SY = 7.00358208142090671392409983 33.29665543989595725571430 52

THETA V IS .3932559441 THETA U IS -.0981017742335529623

NY IS -38.32041690358 NXY IS -61.959633961712929972

THE STRAIN IS EQUAL TO .0025400
THE VALUES OF GT, GI, GII, AND GIII ARE IN IN-LB/IN/IN

% CMOIST	GGG (WHITNEY)	GI	GII	GIII	GI/G (W-T)
MECH. ONLY	.101653935	.0670191	.0346174	.0000174	.6592868
.000	.522939955	.4084740	.1144151	.0000509	.7811106
.050	.488576635	.3794622	.1090658	.0000486	.7766688
.100	.455156902	.3513864	.1037241	.0000464	.7720115
.150	.422680755	.3242463	.0983903	.0000442	.7671187
.200	.391148194	.2980421	.0930641	.0000420	.7619672
.250	.360559220	.2727737	.0877458	.0000397	.7565296
.300	.330913832	.2484412	.0824351	.0000375	.7507731
.350	.302212031	.2250445	.0771323	.0000353	.7446576
.400	.274453816	.2025836	.0718371	.0000331	.7381338
.450	.247639187	.1810586	.0665497	.0000308	.7311387
.500	.221768145	.1604694	.0612701	.0000286	.7235909
.550	.196840689	.1408161	.0559982	.0000264	.7153809
.600	.172856820	.1220986	.0507341	.0000242	.7063566
.650	.149816537	.1043169	.0454777	.0000220	.6962975
.700	.127719840	.0874710	.0402291	.0000197	.6848665
.750	.106566730	.0715610	.0349882	.0000175	.6715139
.800	.086357206	.0565869	.0297550	.0000153	.6552653
.850	.067091269	.0425486	.0245296	.0000131	.6341891
.900	.048768918	.0294461	.0193120	.0000109	.6037875
.950	.031390154	.0172794	.0141021	.0000087	.5504724
1.000	.014954976	.0060486	.0088999	.0000064	.4044538
1.050	-.000536616	-.0042464	.0037055	.0000042	7.9132595
1.100	-.015084621	-.0136055	-.0014811	.0000020	.9019465
1.150	-.028689040	-.0220288	-.0066600	-.0000002	.7678481
1.200	-.041349872	-.0295163	-.0118312	-.0000024	.7138182

THESE ARE THE IN-PLANE INTERLAMINAR SHEAR STRESSES -- SIGMA XZ
THEY ARE FOUND AT VARIOUS MOISTURE CONTENTS

Y LOCATION	MECH ONLY	H=0.0	H=0.2	H=0.4	H=0.6	H=0.8	H=1.0
.80	.06513504	.21416031	.17460962	.13505894	.09550826	.05595758	.01640689
.82	.14545604	.47814372	.38984949	.30155526	.21326102	.12496679	.03667255
.84	.32456173	1.06633353	.86946804	.67260256	.47573707	.27887159	.08200610
.86	.72279559	2.37175315	1.93411286	1.49647257	1.05883228	.62119200	.18355171
.88	1.60209840	5.24186753	4.27581313	3.30975873	2.34370433	1.37764993	.41159552
.90	3.51076178	11.41070230	9.31370571	7.21670913	5.11971255	3.02271596	.92571938
.91	5.15145827	16.64239220	13.59188733	10.54138246	7.49087759	4.44037273	1.38986786
.92	7.47883378	23.94089980	19.57004819	15.19919658	10.82834496	6.45749335	2.08664173
.93	10.67162145	33.68618367	27.57413829	21.46209291	15.35004753	9.23800215	3.12595677
.94	14.79223282	45.68179330	37.47523970	29.26868609	21.06213248	12.85557888	4.64902527
.95	19.47341229	58.01265161	47.76700252	37.52135343	27.27570433	17.03005524	6.78440615
.96	23.13934536	64.48280475	53.47668684	42.47056893	31.46445102	20.45833311	9.45221520
.97	21.18134698	49.34714597	41.81302367	34.27890137	26.74477908	19.21065678	11.67653448
.98	2.06849051	-21.49262058	-15.32190098	-9.15118139	-2.98046180	3.19025779	9.36097738
.99	-56.33255229	-192.21483366	-156.17259550	-120.13035734	-84.08811918	-48.04588102	-12.00364285
1.00	-101.55665215	-68.23277131	-76.30397933	-84.37518734	-92.44639536	-100.51760338	-108.58881140

THESE ARE THE OUT-OF-PLANE INTERLAMINAR SHEAR STRESSES -- SIGMA YZ
THEY ARE FOUND AT VARIOUS MOISTURE CONTENTS

Y LOCATION	MECH ONLY	H=0.0	H=0.2	H=0.4	H=0.6	H=0.8	H=1.0
.80	1.32976655	4.37292262	3.56528382	2.75764502	1.95000623	1.14236743	.33472863
.82	2.97130973	9.77117861	7.96652670	6.16187479	4.35722288	2.55257097	.74791906
.84	6.63941979	21.83410057	17.80150758	13.76891460	9.73632161	5.70372862	1.67113564
.86	14.83663802	48.79268635	39.78092397	30.76916159	21.75739921	12.74563683	3.73387445
.88	33.15858378	109.05518007	88.91263246	68.77008485	48.62753723	28.48498962	8.34244201
.90	74.12869062	243.83823352	198.79834182	153.75845013	108.71855844	63.67866674	18.63877505
.91	110.86070837	364.70855904	297.33899561	229.96943219	162.59986876	95.23030534	27.86074191
.92	165.83595666	545.65327849	444.85249399	344.05170949	243.25092499	142.45014049	41.64935600
.93	248.16757475	816.71124591	665.82431294	514.93737997	364.05044699	213.16351402	62.27658105
.94	371.58510425	1223.12780736	997.13593640	771.14406544	545.15219448	319.16032352	93.16845256
.95	556.84776170	1833.20386401	1494.47103417	1155.73820433	817.00537449	478.27254465	139.53971481
.96	835.49958063	2750.22755443	2242.07591738	1733.92428033	1225.77264328	717.62100623	209.46936917
.97	1255.78433442	4130.35826748	3367.46245574	2604.56664400	1841.67083225	1078.77502051	315.87920877
.98	1892.06540014	6208.29180153	5062.74636672	3917.20093190	2771.65549709	1626.11006228	480.56462747
.99	2859.77789575	9329.28302912	7612.08957918	5894.89612924	4177.70267929	2460.50922935	743.31577941
1.00	4336.01416454	13960.55352851	11405.37993197	8850.20633544	6295.03273890	3739.85914236	1184.68554582

```
 THE LAMINA PLY CHARACTERISTICS INITIALLY ARE

 THE WIDTH OF THE LAMINATE IS  1.51200
THE NUMBER OF LAMINATES ABOVE AND BELOW THE CRACK IS  3       1

 THE PLYS ARE INPUTTED FROM BOTTOM TO TOP
BUT THE PLY CHARACTERISTICS FROM TOP TO BOTTOM ARE


FOR PLY     1 THE SUBLAMINATE HAS THESE PROPERTIES
THE THICKNESS AND THETA VALUES ARE    .005400       35.000
E1 AND E2 ARE (MSI)                  18.7000          1.2300
THE POISSON RATIO (1,2) IS          .29200
G OF (1-2),  AND (3-1) ARE -MSI       .8320       .8320


FOR PLY     2 THE SUBLAMINATE HAS THESE PROPERTIES
THE THICKNESS AND THETA VALUES ARE    .005400         .000
E1 AND E2 ARE (MSI)                  18.7000          1.2300
THE POISSON RATIO (1,2) IS          .29200
G OF (1-2),  AND (3-1) ARE -MSI       .8320       .8320


FOR PLY     3 THE SUBLAMINATE HAS THESE PROPERTIES
THE THICKNESS AND THETA VALUES ARE    .005400      -35.000
E1 AND E2 ARE (MSI)                  18.7000          1.2300
THE POISSON RATIO (1,2) IS          .29200
G OF (1-2),  AND (3-1) ARE -MSI       .8320       .8320


FOR PLY     4 THE SUBLAMINATE HAS THESE PROPERTIES
THE THICKNESS AND THETA VALUES ARE    .005400       90.000
E1 AND E2 ARE (MSI)                  18.7000          1.2300
THE POISSON RATIO (1,2) IS          .29200
G OF (1-2),  AND (3-1) ARE -MSI       .8320       .8320


 THE STRAIN IS EQUAL TO     .00254000
 THE CHANGE IN TEMPERATURE IS   -280.00000
 THE COEFFICIENTS SWELLING DUE TO MOISTURE ARE       .00000000     .00556000
 THE COEFFICIENTS OF THERMAL EXPANSION ARE        -.000000230       .000014900

 THE MOISTURE COEFFICIENT VARIES FROM 0 TO 1.2


 WITH THIS LAYUP, THE PLYS ARE COUPLED




       THE FOUR CHARACTERISTIC VALUES ASSOCIATED
        WITH THE 8 DEGREE POLYNOMIAL FOR THE COUPLED CASE ARE

 S OF  1 IS EQUAL TO        360.7162423543

 S OF  2 IS EQUAL TO        136.3961604492

 S OF  3 IS EQUAL TO        113.9856584772

 S OF  4 IS EQUAL TO         55.0801738692
```

THE UNCOUPLED SX (1,2) VALUES ARE 352.62874 86.89277

THE UNCOUPLED SY (1,2) VALUES ARE 126.45615 59.53405

THE S VALUES OF THE MEMBRANE ARE 193.07807 70.65819

S1NM AND S2NM ARE EQUAL TO -.0000157292 .0000000000
S1 AND S2 = 134.93247116395780394312025 7 641.50029909958418278794308 9
SX AND SY = 7.00358208142090671392409983 33.29665543989595725571430 52

THETA V IS .9784024562 THETA U IS .0000000000000009718

NY IS -38.32041690358 NXY IS -61.959633961712929972

THE STRAIN IS EQUAL TO .0025400
THE VALUES OF GT, GI, GII, AND GIII ARE IN IN-LB/IN/IN

% CMOIST	GGG (WHITNEY)	GI	GII	GIII	GI/G (W-T)
MECH. ONLY	.094207177	.0078275	.0863797	.0000000	.0830882
.000	.510289070	.2262277	.2840614	.0000000	.4433324
.050	.476405835	.2055316	.2708742	.0000000	.4314212
.100	.443446720	.1857497	.2576970	.0000000	.4188771
.150	.411411727	.1668819	.2445298	.0000000	.4056324
.200	.380300856	.1489284	.2313725	.0000000	.3916067
.250	.350114106	.1318890	.2182251	.0000000	.3767028
.300	.320851477	.1157637	.2050878	.0000000	.3608016
.350	.292512969	.1005526	.1919603	.0000000	.3437545
.400	.265098582	.0862557	.1788428	.0000000	.3253723
.450	.238608317	.0728730	.1657353	.0000000	.3054085
.500	.213042173	.0604044	.1526377	.0000000	.2835328
.550	.188400151	.0488500	.1395501	.0000000	.2592888
.600	.164682250	.0382098	.1264724	.0000000	.2320215
.650	.141888470	.0284838	.1134047	.0000000	.2007475
.700	.120018811	.0196719	.1003469	.0000000	.1639065
.750	.099073274	.0117741	.0872991	.0000000	.1188427
.800	.079051858	.0047906	.0742613	.0000000	.0606005
.850	.059954563	-.0012788	.0612334	.0000000	-.0213295
.900	.041781389	-.0064340	.0482154	.0000000	-.1539925
.950	.024532337	-.0106751	.0352074	.0000000	-.4351429
1.000	.008207406	-.0140020	.0222094	.0000000	-1.7060144
1.050	-.007193403	-.0164147	.0092213	.0000000	2.2819054
1.100	-.021670092	-.0179132	-.0037569	.0000000	.8266329
1.150	-.035222659	-.0184976	-.0167251	.0000000	.5251615
1.200	-.047851104	-.0181678	-.0296833	.0000000	.3796734

THESE ARE THE IN-PLANE INTERLAMINAR SHEAR STRESSES -- SIGMA XZ
THEY ARE FOUND AT VARIOUS MOISTURE CONTENTS

Y LOCATION	MECH ONLY	H=0.0	H=0.2	H=0.4	H=0.6	H=0.8	H=1.0
.80	.07771543	.25410395	.20728704	.16047014	.11365323	.06683632	.02001942
.82	.17995738	.58840154	.47999260	.37158366	.26317472	.15476578	.04635684
.84	.41625242	1.36100874	1.11025224	.85949573	.60873922	.35798272	.10722621
.86	.96042737	3.14028217	2.56170677	1.98313136	1.40455595	.82598055	.24740514
.88	2.20343709	7.20451590	5.87713337	4.54975083	3.22236829	1.89498576	.56760322
.90	4.98862540	16.31116726	13.30594680	10.30072635	7.29550589	4.29028544	1.28506498
.91	7.43148427	24.29851376	19.82167961	15.34484547	10.86801132	6.39117717	1.91434302
.92	10.93853873	35.76543047	29.17589574	22.58636100	15.99682627	9.40729153	2.81775680
.93	15.78922990	51.62559809	42.11393649	32.60227488	23.09061327	13.57895167	4.06729006
.94	22.04642211	72.08456237	58.80347722	45.52239206	32.24130691	18.96022176	5.67913661
.95	28.96545539	94.70752965	77.25831827	59.80910689	42.35989552	24.91068414	7.46147276
.96	33.46881767	109.43204584	89.26994356	69.10784128	48.94573900	28.78363672	8.62153445
.97	26.48582400	86.59994907	70.64450369	54.68905831	38.73361292	22.77816754	6.82272216
.98	-14.02438527	-45.85513558	-37.40664203	-28.95814848	-20.50965493	-12.06116138	-3.61266782
.99	-113.31362224	-370.49834340	-302.23657021	-233.97479701	-165.71302381	-97.45125061	-29.18947741
1.00	85.42214908	279.30238304	227.84283872	176.38329439	124.92375006	73.46420574	22.00466141

THESE ARE THE OUT-OF-PLANE INTERLAMINAR SHEAR STRESSES -- SIGMA YZ
THEY ARE FOUND AT VARIOUS MOISTURE CONTENTS

Y LOCATION	MECH ONLY	H=0.0	H=0.2	H=0.4	H=0.6	H=0.8	H=1.0
.80	.94069588	3.07576670	2.50907783	1.94238895	1.37570008	.80901121	.24232233
.82	2.18029521	7.12884953	5.81540800	4.50196647	3.18852495	1.87508342	.56164190
.84	5.05374241	16.52407852	13.47963063	10.43518274	7.39073485	4.34628695	1.30183906
.86	11.71605439	38.30765144	31.24972996	24.19180849	17.13388701	10.07596554	3.01804406
.88	27.17098279	88.84019338	72.47199838	56.10380339	39.73560839	23.36741339	6.99921839
.90	63.06243899	206.19347184	168.20374189	130.21401195	92.22428201	54.23455207	16.24482213
.91	96.12643272	314.30187627	256.39391588	198.48595549	140.57799510	82.67003472	24.76207433
.92	146.61442086	479.38102208	391.05836372	302.73570537	214.41304702	126.09038866	37.76773031
.93	223.81654951	731.80663700	596.97629411	462.14595122	327.31560833	192.48526545	57.65492256
.94	342.10566992	1118.57322594	912.48379743	706.39436892	500.30494041	294.21551190	88.12608339
.95	523.86709173	1712.87340224	1397.28825109	1081.70309995	766.11794880	450.53279765	134.94764651
.96	804.27369732	2629.71094384	2145.20477742	1660.69861100	1176.19244458	691.68627816	207.18011174
.97	1239.16420856	4051.66013925	3305.16960716	2558.67907507	1812.18854298	1065.69801089	319.20747880
.98	1917.53432739	6269.70771612	5114.55716346	3959.40661080	2804.25605814	1649.10550548	493.95495282
.99	2971.17774803	9714.77578612	7924.89512080	6135.01445547	4345.13379015	2555.25312483	765.37245950
1.00	4429.35526207	14482.53753133	11814.22953505	9145.92153878	6477.61354250	3809.30554622	1140.99754994

THE LAMINA PLY CHARACTERISTICS INITIALLY ARE

THE WIDTH OF THE LAMINATE IS 1.51200
THE NUMBER OF LAMINATES ABOVE AND BELOW THE CRACK IS 2 2

FOR PLY 1 THE SUBLAMINATE HAS THESE PROPERTIES
THE THICKNESS AND THETA VALUES ARE .005400 30.000
E1 AND E2 ARE (MSI) 18.7000 1.2300
THE POISSON RATIO (1,2) IS .29200
G OF (1-2), AND (3-1) ARE -MSI .8320 .8320

FOR PLY 2 THE SUBLAMINATE HAS THESE PROPERTIES
THE THICKNESS AND THETA VALUES ARE .005400 -60.000
E1 AND E2 ARE (MSI) 18.7000 1.2300
THE POISSON RATIO (1,2) IS .29200
G OF (1-2), AND (3-1) ARE -MSI .8320 .8320

FOR PLY 3 THE SUBLAMINATE HAS THESE PROPERTIES
THE THICKNESS AND THETA VALUES ARE .005400 75.000
E1 AND E2 ARE (MSI) 18.7000 1.2300
THE POISSON RATIO (1,2) IS .29200
G OF (1-2), AND (3-1) ARE -MSI .8320 .8320

FOR PLY 4 THE SUBLAMINATE HAS THESE PROPERTIES
THE THICKNESS AND THETA VALUES ARE .005400 -15.000
E1 AND E2 ARE (MSI) 18.7000 1.2300
THE POISSON RATIO (1,2) IS .29200
G OF (1-2), AND (3-1) ARE -MSI .8320 .8320

THE STRAIN IS EQUAL TO .00254000
THE CHANGE IN TEMPERATURE IS -280.00000
THE COEFFICIENTS SWELLING DUE TO MOISTURE ARE .00000000 .00556000
THE COEFFICIENTS OF THERMAL EXPANSION ARE -.000000230 .000014900

THE MOISTURE COEFFICIENT VARIES FROM 0 TO 1.2

WITH THIS LAYUP, THE PLYS ARE COUPLED

THE FOUR CHARACTERISTIC VALUES ASSOCIATED
WITH THE 8 DEGREE POLYNOMIAL FOR THE COUPLED CASE ARE

S OF 1 IS EQUAL TO 202.3666962066

S OF 2 IS EQUAL TO 150.2447234209

S OF 3 IS EQUAL TO 96.3990023366

S OF 4 IS EQUAL TO 72.1855545293

THE UNCOUPLED SX (1,2) VALUES ARE 178.08581 90.73315

THE UNCOUPLED SY (1,2) VALUES ARE 137.79324 77.57481

THE S VALUES OF THE MEMBRANE ARE 107.30164 75.55664

S1NM AND S2NM ARE EQUAL TO -.0013126127 .0012407192
S1 AND S2 = 145.71273839436314520123430 4 261.71259626539561223754217 5
SX AND SY = 35.57568511674391151901478 79 60.95855496773143123195533 12

THETA V IS .2402517909 THETA U IS 2.0734384470218017861

NY IS -35.48501616832 NXY IS -61.461850910940726086

THE STRAIN IS EQUAL TO .0025400
THE VALUES OF GT, GI, GII, AND GIII ARE IN IN-LB/IN/IN

% CMOIST	GGG (WHITNEY)	GI	GII	GIII	GI/G (W-T)
MECH. ONLY	.174065036	.0136734	.0093651	.1510265	.0785535
.000	.288599244	.0062276	.0365562	.2458155	.0215787
.050	.277169512	.0030909	.0347433	.2393353	.0111516
.100	.266289514	.0005010	.0329323	.2328563	.0018813
.150	.255959252	-.0015422	.0311230	.2263784	-.0060250
.200	.246178724	-.0030385	.0293156	.2199016	-.0123427
.250	.236947932	-.0039880	.0275100	.2134260	-.0168309
.300	.228266874	-.0043908	.0257062	.2069515	-.0192354
.350	.220135552	-.0042468	.0239042	.2004781	-.0192916
.400	.212553964	-.0035559	.0221040	.1940059	-.0167296
.450	.205522112	-.0023183	.0203057	.1875347	-.0112801
.500	.199039994	-.0005339	.0185092	.1810647	-.0026824
.550	.193107612	.0017973	.0167144	.1745959	.0093072
.600	.187724965	.0046753	.0149215	.1681281	.0249050
.650	.182892052	.0081001	.0131304	.1616615	.0442888
.700	.178608875	.0120716	.0113412	.1551961	.0675870
.750	.174875432	.0165900	.0095537	.1487317	.0948676
.800	.171691725	.0216552	.0077681	.1422685	.1261282
.850	.169057753	.0272671	.0059842	.1358064	.1612888
.900	.166973515	.0334259	.0042022	.1293454	.2001866
.950	.165439013	.0401314	.0024220	.1228856	.2425751
1.000	.164454245	.0473837	.0006436	.1164269	.2881270
1.050	.164019213	.0551828	-.0011329	.1099693	.3364412
1.100	.164133916	.0635287	-.0029077	.1035129	.3870542
1.150	.164798353	.0724214	-.0046806	.0970576	.4394548
1.200	.166012526	.0818609	-.0064517	.0906034	.4931008

THESE ARE THE IN-PLANE INTERLAMINAR SHEAR STRESSES -- SIGMA XZ
THEY ARE FOUND AT VARIOUS MOISTURE CONTENTS

Y LOCATION	MECH ONLY	H=0.0	H=0.2	H=0.4	H=0.6	H=0.8	H=1.0
.80	.05676172	.13383978	.11323003	.09262028	.07201053	.05140078	.03079103
.82	.16404039	.38262997	.32416132	.26569268	.20722403	.14875538	.09028674
.84	.47716558	1.09647535	.93073896	.76500256	.59926616	.43352976	.26779336
.86	1.40027761	3.15249905	2.68324457	2.21399008	1.74473560	1.27548112	.80622663
.88	4.15778238	9.10572208	7.77928135	6.45284061	5.12639987	3.79995914	2.47351840
.90	12.53662711	26.47078249	22.72981406	18.98884564	15.24787721	11.50690879	7.76594036
.91	21.92391761	45.27705638	39.00125296	32.72544955	26.44964613	20.17384271	13.89803930
.92	38.55372890	77.65399817	67.13410301	56.61420784	46.09431268	35.57441752	25.05452235
.93	68.22669529	133.62809212	116.00701342	98.38593472	80.76485602	63.14377733	45.52269863
.94	121.62386648	230.94006045	201.43654971	171.93303897	142.42952823	112.92601749	83.42250675
.95	218.74381651	401.50598451	352.07750811	302.64903171	253.22055531	203.79207891	154.36360251
.96	398.03248718	704.47704597	621.39034887	538.30365177	455.21695468	372.13025758	289.04356048
.97	736.82244009	1255.70230253	1114.59938720	973.49647187	832.39355653	691.29064120	550.18772587
.98	1403.24313766	2305.35974007	2059.22700449	1813.09426892	1566.96153334	1320.82879776	1074.69606219
.99	2809.86570653	4480.13776195	4023.01286260	3565.88796325	3108.76306390	2651.63816455	2194.51326520
1.00	6138.30786283	9650.30926292	8687.60293079	7724.89659866	6762.19026652	5799.48393439	4836.77760226

THESE ARE THE OUT-OF-PLANE INTERLAMINAR SHEAR STRESSES -- SIGMA YZ
THEY ARE FOUND AT VARIOUS MOISTURE CONTENTS

Y LOCATION	MECH ONLY	H=0.0	H=0.2	H=0.4	H=0.6	H=0.8	H=1.0
.80	.16585980	.40442354	.34069983	.27697611	.21325240	.14952869	.08580498
.82	.46943498	1.14791593	.96669931	.78548269	.60426608	.42304946	.24183285
.84	1.32621331	3.25626779	2.74082736	2.22538692	1.70994649	1.19450605	.67906562
.86	3.73681543	9.22891300	7.76243950	6.29596600	4.82949250	3.36301900	1.89654550
.88	10.48846496	26.12319742	21.94948048	17.77576354	13.60204660	9.42832966	5.25461272
.90	29.26971559	73.80117525	61.91744992	50.03372460	38.14999927	26.26627395	14.38254862
.91	48.74474315	123.91308072	103.85796283	83.80284494	63.74772705	43.69260916	23.63749127
.92	80.94539936	207.83462309	173.98914281	140.14366253	106.29818225	72.45270198	38.60722170
.93	133.89723658	348.06735925	290.95937200	233.85138474	176.74339749	119.63541023	62.52742298
.94	220.24445378	581.52733260	485.22950028	388.93166795	292.63383563	196.33600331	100.03817099
.95	359.01194536	967.47546061	805.37239730	643.26933399	481.16627068	319.06320737	156.96014406
.96	575.60439987	1596.12349454	1324.41972889	1052.71596324	781.01219759	509.30843195	237.60466630
.97	890.96357501	2584.87680021	2134.31704487	1683.75728954	1233.19753421	782.63777888	332.07802355
.98	1261.01507117	3998.83788332	3271.80265391	2544.76742450	1817.73219508	1090.69696567	363.66173626
.99	1302.72815835	5415.47562712	4327.26291739	3239.05020766	2150.83749794	1062.62478821	-25.58792151
1.00	-883.85251960	3927.98882475	2670.82514260	1413.66146045	156.49777830	-1100.66590385	-2357.82958600

THE LAMINA PLY CHARACTERISTICS INITIALLY ARE

THE WIDTH OF THE LAMINATE IS 1.51200
THE NUMBER OF LAMINATES ABOVE AND BELOW THE CRACK IS 2 2

FOR PLY 1 THE SUBLAMINATE HAS THESE PROPERTIES
THE THICKNESS AND THETA VALUES ARE .005400 -35.000
E1 AND E2 ARE (MSI) 18.7000 1.2300
THE POISSON RATIO (1,2) IS .29200
G OF (1-2), AND (3-1) ARE -MSI .8320 .8320

FOR PLY 2 THE SUBLAMINATE HAS THESE PROPERTIES
THE THICKNESS AND THETA VALUES ARE .005400 55.000
E1 AND E2 ARE (MSI) 18.7000 1.2300
THE POISSON RATIO (1,2) IS .29200
G OF (1-2), AND (3-1) ARE -MSI .8320 .8320

FOR PLY 3 THE SUBLAMINATE HAS THESE PROPERTIES
THE THICKNESS AND THETA VALUES ARE .005400 10.000
E1 AND E2 ARE (MSI) 18.7000 1.2300
THE POISSON RATIO (1,2) IS .29200
G OF (1-2), AND (3-1) ARE -MSI .8320 .8320

FOR PLY 4 THE SUBLAMINATE HAS THESE PROPERTIES
THE THICKNESS AND THETA VALUES ARE .005400 -80.000
E1 AND E2 ARE (MSI) 18.7000 1.2300
THE POISSON RATIO (1,2) IS .29200
G OF (1-2), AND (3-1) ARE -MSI .8320 .8320

THE STRAIN IS EQUAL TO .00254000
THE CHANGE IN TEMPERATURE IS -280.00000
THE COEFFICIENTS SWELLING DUE TO MOISTURE ARE .00000000 .00556000
THE COEFFICIENTS OF THERMAL EXPANSION ARE -.000000230 .000014900

THE MOISTURE COEFFICIENT VARIES FROM 0 TO 1.2

WITH THIS LAYUP, THE PLYS ARE COUPLED

THE FOUR CHARACTERISTIC VALUES ASSOCIATED
WITH THE 8 DEGREE POLYNOMIAL FOR THE COUPLED CASE ARE

S OF 1 IS EQUAL TO 233.9388572236

S OF 2 IS EQUAL TO 156.9014619788

S OF 3 IS EQUAL TO 115.2992565645

S OF 4 IS EQUAL TO 48.0575100718

THE UNCOUPLED SX (1,2) VALUES ARE 186.41344 96.42124

THE UNCOUPLED SY (1,2) VALUES ARE 128.78572 49.37034

THE S VALUES OF THE MEMBRANE ARE 119.36060 57.91987

S1NM AND S2NM ARE EQUAL TO -.0007221149 -.0007139234
S1 AND S2 = 143.691863396728751259452089 285.264127104852281159045526
SX AND SY = 32.143697954679144782027210 62.204997893976699205071133 9

THETA V IS .4347536621 THETA U IS -1.7344415408201789576

NY IS -54.36619889946 NXY IS 45.618657445050692111

THE STRAIN IS EQUAL TO .0025400
THE VALUES OF GT, GI, GII, AND GIII ARE IN IN-LB/IN/IN

% CMOIST	GGG (WHITNEY)	GI	GII	GIII	GI/G (W-T)
MECH. ONLY	.131525889	.0207693	.0219689	.0887877	.1579102
.000	.394637005	.1683076	.0866210	.1397084	.4264871
.050	.369347077	.1508205	.0823114	.1362152	.4083435
.100	.345184223	.1344556	.0780061	.1327225	.3895185
.150	.322148443	.1192131	.0737050	.1292304	.3700564
.200	.300239735	.1050929	.0694082	.1257387	.3500298
.250	.279458102	.0920949	.0651156	.1222475	.3295483
.300	.259803542	.0802193	.0608274	.1187569	.3087691
.350	.241276055	.0694660	.0565434	.1152667	.2879108
.400	.223875642	.0598350	.0522636	.1117771	.2672688
.450	.207602302	.0513262	.0479882	.1082879	.2472335
.500	.192456036	.0439398	.0437170	.1047992	.2283110
.550	.178436843	.0376757	.0394500	.1013111	.2111431
.600	.165544724	.0325339	.0351874	.0978235	.1965264
.650	.153779678	.0285144	.0309290	.0943363	.1854237
.700	.143141706	.0256172	.0266748	.0908497	.1789638
.750	.133630807	.0238423	.0224250	.0873635	.1784190
.800	.125246982	.0231897	.0181794	.0838779	.1851516
.850	.117990230	.0236594	.0139381	.0803928	.2005198
.900	.111860552	.0252514	.0097010	.0769081	.2257398
.950	.106857947	.0279657	.0054683	.0734240	.2617089
1.000	.102982416	.0318023	.0012397	.0699404	.3088128
1.050	.100233958	.0367612	-.0029845	.0664573	.3667539
1.100	.098612573	.0428424	-.0072045	.0629747	.4344517
1.150	.098118262	.0500459	-.0114202	.0594925	.5100571
1.200	.098751025	.0583717	-.0156316	.0560109	.5910999

THESE ARE THE IN-PLANE INTERLAMINAR SHEAR STRESSES -- SIGMA XZ
THEY ARE FOUND AT VARIOUS MOISTURE CONTENTS

Y LOCATION	MECH ONLY	H=0.0	H=0.2	H=0.4	H=0.6	H=0.8	H=1.0
.80	-.57590259	-1.81324378	-1.48462505	-1.15600631	-.82738757	-.49876884	-.17015010
.82	-1.15500766	-3.63542168	-2.97665842	-2.31789515	-1.65913188	-1.00036862	-.34160535
.84	-2.31809701	-7.29018842	-5.96965162	-4.64911482	-3.32857801	-2.00804121	-.68750441
.86	-4.66121070	-14.62677009	-11.97991892	-9.33306775	-6.68621658	-4.03936541	-1.39251424
.88	-9.41933953	-29.38693329	-24.08301174	-18.77909019	-13.47516863	-8.17124708	-2.86732552
.90	-19.28114635	-59.25567119	-48.63455785	-38.01344451	-27.39233116	-16.77121782	-6.15010448
.91	-27.86803356	-84.38953087	-69.36790478	-54.34627868	-39.32465259	-24.30302649	-9.28140039
.92	-40.76807828	-120.61801802	-99.38712650	-78.15623498	-56.92534347	-35.69445195	-14.46356043
.93	-60.74791755	-173.40082769	-143.42661283	-113.45239797	-83.47818312	-53.50396826	-23.52975340
.94	-93.01797598	-251.60892083	-209.36180513	-167.11468943	-124.86757373	-82.62045803	-40.37334233
.95	-148.04567478	-370.59922298	-311.19653492	-251.79384686	-192.39115881	-132.98847075	-73.58578269
.96	-248.37373255	-559.47456937	-476.16166609	-392.84876280	-309.53585952	-226.22295624	-142.91005296
.97	-446.98922674	-881.36980878	-764.37575049	-647.38169221	-530.38763392	-413.39357564	-296.39951735
.98	-885.27484698	-1503.21141125	-1335.11941983	-1167.02742841	-998.93543699	-830.84344557	-662.75145415
.99	-2013.12212234	-2986.72662307	-2717.77038626	-2448.81414945	-2179.85791263	-1910.90167582	-1641.94543901
1.00	-5568.98832566	-7674.18805110	-7084.53781995	-6494.88758880	-5905.23735765	-5315.58712650	-4725.93689534

THESE ARE THE OUT-OF-PLANE INTERLAMINAR SHEAR STRESSES -- SIGMA YZ
THEY ARE FOUND AT VARIOUS MOISTURE CONTENTS

Y LOCATION	MECH ONLY	H=0.0	H=0.2	H=0.4	H=0.6	H=0.8	H=1.0
.80	3.27617888	10.31723571	8.44724614	6.57725656	4.70726699	2.83727741	.96728784
.82	6.56753777	20.68268192	16.93393167	13.18518142	9.43643117	5.68768092	1.93893067
.84	13.16491904	41.46150260	33.94640184	26.43130108	18.91620032	11.40109956	3.88599881
.86	26.38654493	83.11303161	68.04745804	52.98188448	37.91631091	22.85073735	7.78516379
.88	52.87019183	166.59261716	136.39009616	106.18757515	75.98505414	45.78253314	15.58001213
.90	105.84680471	333.84310700	273.29260785	212.74210869	152.19160953	91.64111038	31.09061122
.91	149.66289213	472.50148909	386.76451483	301.02754057	215.29056630	129.55359204	43.81661778
.92	211.43474532	668.58894580	547.18476643	425.78058706	304.37640769	182.97222833	61.56804896
.93	298.27565716	945.66979161	773.75215728	601.83452295	429.91688862	257.99925428	86.08161995
.94	419.76910709	1336.64857623	1093.18597910	849.72338197	606.26078483	362.79818770	119.33559056
.95	588.25330316	1886.88626457	1542.09703881	1197.30781306	852.51858731	507.72936156	162.94013580
.96	817.80756656	2656.91555150	2168.73092336	1680.54629522	1192.36166707	704.17703893	215.99241079
.97	1117.61798402	3719.40898556	3029.03467417	2338.66036279	1648.28605140	957.91174002	267.53742864
.98	1460.19459243	5123.16377041	4151.96405479	3180.76433917	2209.56462355	1238.36490793	267.16519231
.99	1628.54905698	6683.48801754	5345.79387584	4008.09973414	2670.40559244	1332.71145074	-4.98269096
1.00	446.83474448	6857.50214542	5171.81141375	3486.12068207	1800.42995039	114.73921872	-1570.95151296

APPENDIX II

FRACTURE ANALYSIS OF LOCAL DELAMINATIONS IN LAMINATED COMPOSITES

P. Sriram and E. A. Armanios
School of Aerospace Engineering
Georgia Institute of Technology
Atlanta, Georgia 30332

Abstract

Delamination is a predominant failure mode in continuous fiber reinforced laminated composite structures. One type of delamination is the transverse crack tip delamination which originates at the tip of transverse matrix cracks. An analytical model based on the sublaminate approach and fracture mechanics is developed in this paper to study the growth of such delaminations. Plane strain conditions are assumed and estimates are provided for the total strain energy release rate as well as the mode I and mode II contributions. The energy release rate estimates are used to predict critical delamination growth strains and stresses by assuming a critical energy release rate. These predictions are compared with experimental data on T300/934 Graphite Epoxy $[\pm 25/90_n]_s$ laminates in the range n=.5 to 8. A good agreement is demonstrated for the range of n where the experimental observations indicate transverse crack tip delamination to be the predominant failure mode.

Introduction

Fiber reinforced composites are now being used in a wide variety of engineering structures. The concept of directional strength and stiffness has been, for the most part, understood sufficiently to enable efficient load bearing designs. One of the current major issues in composite structures is the understanding and prediction of damage modes and failure mechanisms. A thorough knowledge of the failure mechanisms is bound to lead to the design of efficient and durable structures. Failures in these materials often initiate in the form of matrix cracks or delaminations.

Matrix cracks refer to intralaminar failures whereas delaminations refer to interlaminar failures.

Matrix cracks usually occur within laminates where the fibers run at an angle to the primary load direction. Hence, such matrix cracks are also called transverse cracks. Based on the location and direction of growth, two distinct types of delamination can be discerned. These two types are called edge delamination and local or transverse crack tip delamination. Edge delaminations initiate at the load free edges of the structure whereas local delaminations start from a transverse matrix crack. In many cases, both types occur concurrently with varying levels of interaction. It has been observed in simple tension tests of uniform rectangular cross section specimen (Edge Delamination test) that delaminations initiate along the load free edges and propagate normal to the load direction. Transverse matrix cracks running parallel to the fibers have also been observed in off axis plies such as 90° plies. Such transverse cracks terminate where the ply orientation changes. Delaminations can originate at the interface where transverse cracks terminate. These delaminations, called transverse crack delaminations or local delaminations, grow normal to the transverse crack from which they originate. In the case of 90° plies, the growth direction is parallel to the load.

The growth process of edge delaminations and local delaminations is often modelled using a fracture mechanics approach leading to the calculation of a strain energy release rate. This is because the strain energy release rate can correlate delamination behavior from different loading conditions and can account for geometric dependencies. The strain energy release rate associated with a particular growth configuration is a measure of the driving force behind that failure mode. In combination with

appropriate failure criteria, the strain energy release rate provides a means of predicting the failure loads of the structure.

Several methods are available in the literature for analyzing edge delaminations. These include finite element modelling[1-3], complex variable stress potential approach[4], simple classical laminate theory based technique[5] and higher order laminate theory including shear deformations[6]. Finite element models provide accurate solutions but involve intensive computational effort. Classical laminate theory (CLT) based techniques provide simple closed form solutions and are thus well suited for preliminary design evaluation. Classical laminate theory based techniques provide only the total energy release rate, and thus in a mixed mode situation, there is insufficient information to completely assess the delamination growth tendency. A higher order laminate theory including shear deformations has the ability to provide the individual contributions of the three fracture modes while retaining the simplicity of a closed form solution. A shear deformation model is available for edge delamination and has been shown to agree well with finite element predictions[6].

Crossman and Wang[7] have tested T300/934 Graphite epoxy $[\pm 25/90_n]_s$ specimens in simple tension and reported a range of behavior including transverse cracking, edge delamination and local delamination. O'Brien[8] has presented classical laminate theory solutions for these specimen, demonstrating reasonable agreement in the case of edge delamination but with some discrepancies in the local delamination predictions. An empirical finite element based combined edge and local delamination formulation has also been proposed[9]. Its predictions, however, do not fully explain the dependency of the critical strain on the number of 90° plies.

In this paper, a shear deformation model is developed for the analysis of local delaminations originating from transverse cracks in 90° plies

located in and around the specimen midplane. Plane strain conditions are assumed and thickness strain is neglected. Delaminations are assumed to grow from both ends of the transverse crack tip. The transverse crack is treated as a free boundary and the delamination is considered to be the crack whose growth behavior is to be modelled. The sublaminate approach[10,11] is used to model different regions of the specimen. The resulting boundary value problem is solved to obtain the interlaminar stresses, total strain energy release rate and energy release rate components. Critical local delamination growth loads are predicted for the $[\pm 25/90_n]_s$ specimen.

Analytical Model

The formulation is based on the sublaminate approach detailed in ref. 10. A longitudinal section illustrating the geometry of a generic configuration is shown in fig. 1. The central region is assumed to be made of 90° plies with an isolated transverse crack in the middle. Delaminations are assumed to grow from both ends of the transverse crack, and towards both ends as shown. From symmetry considerations, only one quarter of the configuration is modelled. The modelled portion is divided into four sublaminates as shown in fig. 2. The top surface (sublaminates 1 and 4) is stress free. In order to simplify the analysis, plane strain conditions are assumed and the thickness strain (ε_z) is set to zero. The consequence of this combined with the fact that the w displacement is zero along the center line is that w is zero in sublaminates 1,2 and 3. Further, this approximation does not allow for the enforcement of boundary conditions on the shear stress resultants, leading to incorrect estimates of the interlaminar normal stresses. The interlaminar shear stresses, however, are not affected by this assumption[6,10]. The assumptions lead to considerable simplifications in the analysis. In spite of the simplifications, reliable

energy release rate components can be estimated based on the interlaminar shear stress distributions[6,10].

A generic sublaminate is shown in fig. 3 along with the notations and sign conventions. The peel and interlaminar shear stresses are denoted by P and T respectively with t and b subscripts for the top and bottom surface respectively. The axial stress resultant, shear stress resultant and bending moment resultant are denoted by N, Q and M respectively. A summary of the governing equations is presented here for convenience. These are derived for a generic sublaminate using the principle of virtual work in Reference 12.

The x and z displacements within the sublaminate are assumed to be of the form

$$u(x,z)=U(x)+z\beta(z) \tag{1}$$

$$w(x,z)=W(x). \tag{2}$$

Here U represents the axial midplane stretching and W is the transverse displacement. The shear deformation is recognized through the rotation β. The origin of the coordinate axes for the sublaminates is taken at the delamination tip as shown in fig. 4. The equilibrium equations take the form

$$N_{,x}+T_t-T_b=0 \tag{3}$$

$$Q_{,x}+P_t-P_b=0 \tag{4}$$

$$M_{,x}-Q+(h/2)(T_t+T_b)=0. \tag{5}$$

where h is the thickness of the sublaminate. The constitutive relations in terms of the force and moment resultants are

$$N=A_{11}U_{,x}+B_{11}\beta_{,x} \tag{6}$$

$$Q=A_{55}(\beta+W_{,x}) \tag{7}$$

$$M=B_{11}U_{,x}+D_{11}\beta_{,x} \tag{8}$$

where the A_{ij}, B_{ij} and D_{ij} are the classical laminate theory axial, coupling and bending stiffnesses. The boundary variables to be prescribed at the sublaminate edges are

N or U

M or β

Q or W.

Additionally, at the interfaces between sublaminates, reciprocal traction and displacement matching boundary conditions have to specified.

Solution Procedure

A detailed solution is provided in the Appendix. A brief summary is provided here for convenience. The variables in sublaminates 1 and 2 are coupled by their reciprocal interlaminar stresses denoted T_1 and P_1 and by displacement continuity at their common interface. Assuming exponential solutions for the axial force and bending moment resultants ($N_1=Ae^{sx}$, $M_1=Be^{sx}$ etc.) leads to an eigen value problem involving the parameter s. The eigen values turn out to be 0 and two nonzero values (say s_1 and s_2) occurring in positive and negative pairs. Since the resultants maintain finite values as x tends to large negative values (left end of sublaminates 1 and 2), the negative roots are dropped out of the solution.

The following boundary conditions from the ends of the modelled region are enforced.

$$N_2(0)=0 \tag{9}$$

$$Q_4(a)=0 \tag{10}$$

$$\beta_4(a)=0 \tag{11}$$

$$N_1+N_2=\text{Applied Load} \tag{12}$$

Further, the following displacement matching conditions are applied.

$$u_1(x,-.5h_1)=u_2(x,.5h_2) \tag{13}$$

$$U_1(0)=U_4(0) \tag{14}$$

$$U_2(0)=U_3(0) \tag{15}$$

$$\beta_1(0)=\beta_4(0) \tag{16}$$

It should be noted that a β_2 and β_3 matching condition cannot be applied at this level of modeling since it would amount to specifying both W and Q[6,12]. Consequently, there is a displacement discontinuity at the delamination tip. The effect of this will be discussed subsequently. To eliminate rigid body displacements, U_1 is set to zero at the left end. The following solutions can then be obtained for the resultants in sublaminates 1 and 2.

$$N_1=a_1e^{s_1x}+a_2e^{s_2x}+\varepsilon A_{11(1)} \tag{17}$$

$$N_2=-a_1e^{s_1x}-a_2e^{s_2x}+\varepsilon A_{11(2)} \tag{18}$$

$$M_1=a_1k_1e^{s_1x}+a_2k_2e^{s_2x} \tag{19}$$

$$M_2=a_1k_3e^{s_1x}+a_2k_4e^{s_2x} \tag{20}$$

The interlaminar shear and peel stresses between sublaminates 1 and 2 can be obtained as

$$T_1=a_1s_1e^{s_1x}+a_2s_2e^{s_2x} \tag{21}$$

$$P_1=(k_1+.5h_1)(a_1s_1^2e^{s_1x})+(k_2+.5h_1)(a_2s_2^2e^{s_2x}) \tag{22}$$

In the above solutions, the k parameters are dependent on the eigen values and the stiffness of sublaminates 1 and 2, the a parameters depend on the k parameters and the initial crack length a, and ε is defined as

$$\varepsilon=\sigma(h_1+h_2)/(A_{11(1)}+A_{11(2)}) \tag{23}$$

where σ is the applied uniform axial stress. Complete expressions for the eigen values and the a and k parameters can be found in the Appendix.

Proceeding on to sublaminates 3 and 4, the following solutions can be written.

$$N_3=0 \tag{24}$$

$$M_3=\phi_1\sinh\ \omega_3x+\phi_2\cosh\ \omega_3x \tag{25}$$

where

$$\phi_2=a_1k_3+a_2k_4, \tag{26}$$

$$\phi_1=-\phi_2 \coth \omega_3 a \tag{27}$$

and

$$\omega_3=(A_{55(2)}/D_{11(2)})^{0.5} \tag{28}$$

$$N_4=\varepsilon(A_{11(1)}+A_{11(2)}) \tag{29}$$

$$M_4=a_1k_1+a_2k_2 \tag{30}$$

The corresponding displacement solutions are provided in the Appendix. The compliance of the specimen can be evaluated as

$$C=2U_4(a)/P \tag{31}$$

where P/2 is the load applied to the modelled section. The total energy release rate for the modelled section i.e. the total energy release rate G_T per crack is then given by

$$G_T=P^2/2\ w\ (dC/da) \tag{32}$$

where w is the specimen width. Use of the previously described solutions leads to the following expression.

$$G_T = \frac{P^2}{2w^2}\left(\frac{1}{A_{11(1)}} - \frac{1}{A_{11(1)}+A_{11(2)}} + I_1 - I_2\right) \tag{33}$$

where the quantities I_1 and I_2 contain exponential terms dependent on the initial delamination length. Using the virtual crack closure technique, from the relative displacements in the cracked portion and the interlaminar stresses ahead of the crack tip, the mode I and mode II energy release rate contributions can be obtained. The mode III energy release rate is zero from the assumption of plane strain. The mode II energy release rate is given by

$$G_{II} = \lim_{\delta\to 0}\frac{1}{2\delta}\int_0^{\delta} T_1(x-\delta)\Delta u(x)\,dx \tag{34}$$

where δ is the virtual crack step size. The result of the limiting process is zero if there is no singularity in the stress field[10]. So, the limit is usually taken as the crack step size δ tends to a small value, say Δ, based on the decay length or the length required to capture the essential features of the stress and displacement fields near the crack tip. The decay

length is dependent on the eigen values s_1 and s_2. In this study, the value of Δ has been set to

$$\Delta_0=.25(1/s_1 + 1/s_2) \tag{35}$$

since it reasonably fulfills the criterion given above. In a similar fashion, the mode I energy release rate can be obtained based on the normal stress (P) and the w displacements near the crack front. The normal (peel) stress estimate is inaccurate due to the absence of thickness strain. Hence, an alternate approach was used to estimate G_I, the mode I energy release rate. The total energy release rate for this problem is made up entirely of G_I and G_{II} (G_{III}=0). From an estimate of G_T and G_{II}, an estimate for G_I can be obtained simply as

$$G_I=G_T-G_{II} \tag{36}$$

The critical load for a given specimen can then be evaluated based on an appropriate fracture law. This is illustrated in the following section.

Results and Discussion

The solutions derived in the previous section have been used to model the behavior of $[\pm 25/90_n]_s$ T300/934 Graphite Epoxy specimen for n values of .5,1,2,3,4,6,and 8. These correspond to the specimen tested by Crossman and Wang[7]. The specimen width and length were fixed at .0381 m and .015m respectively, as in the tests. The solutions were generated using a simple computer program based on the closed form expressions for the interlaminar stress and energy release rates. The applied load was set to 100 MPa, of the same order as in the tests.

An example of the total energy release rate variation with the crack length is presented in fig. 5. The asymptotic value of G_T is denoted by G_{T0} in the figure. It can be observed that after a certain crack length, the G_T is independent of the crack length. On the basis of curves like the one shown in fig. 5, the crack length was fixed at 10 ply thicknesses for

the remainder of the study. The dependence of the mode II contribution of the energy release rate on initial crack length (a) is depicted in fig. 6. Typical interlaminar shear and normal stress profiles are presented in figs. 7 and 8 respectively. The corresponding energy release rates have also been calculated and are presented in Table 1 and fig. 9.

In order to evaluate the critical loads, an appropriate mixed mode fracture law has to be applied, based on the calculated energy release components. Since the calculated mode split shows only a small variation with n, the simple Griffith criterion $G_T=G_{Tc}$ has been used to scale the stresses to obtain the critical delamination growth stress (σ_c) and strain (ε_c) values. The critical energy release rate G_{Tc} was chosen as 415 J/m^2 to obtain the critical stresses and strains listed in Table 1. This value of G_{Tc} is larger than G_{Ic} to account for the presence of mode II and the fact that G_{IIc} is about four times G_{Ic} for the material system under consideration. The critical strains are plotted against n, the number of 90° plies in fig. 10. The experimental results of ref. 7 and the predictions of refs. 8 and 9 are also presented in the figure for comparison. The predictions of the model developed in this paper are represented by the solid line while the experimental results are shown as filled squares. The classical laminate theory and finite element critical strain predictions of refs. 8 and 9 are represented by triangles with a connecting line and a dotted line respectively.

In the experiments, the local delamination phenomenon was observed as the predominant failure mode only for the n=4,6 and 8 specimens. The shear deformation model presented in this paper provides good agreement with the experimental data in this range. For n<4, edge delamination either in the mid plane or in the 25/90 interface was observed in the tests. Hence, the predictions of the local delamination models in this region are not of

consequence as long as they do not predict critical loads lower than those predicted by edge delamination models. Thus, it can be seen that the shear deformation model predicts the observed behavior with reasonable accuracy and can be used in conjunction with an appropriate edge delamination model to predict critical loads accurately for the complete range of n values. The edge delamination model presented in References 6 and 12 can be used for this purpose. However, a separate model is required to account for the mid-plane (Mode I) edge delamination behavior.

Conclusions

A shear deformation model has been developed to analyze local delaminations growing from transverse cracks in 90° plies located around the mid plane of symmetric laminates. The predictions of the model agree reasonably with experimental data from $[\pm 25/90_n]_s$ T300/934 Graphite Epoxy laminates. The predicted behavior is such that, in combination with an edge delamination model, the critical loads can be predicted accurately in the range of n from .5 to 8.

Acknowledgements

The authors gratefully acknowledge the financial support provided by NASA under grant NAG-1-637 for performing the research reported in this paper. The authors also wish to thank Mr. A. Badir for help in verifying the analytical model.

References

[1] Wilkins, D.J., Eisemann, J.R., Camin, R.A., Margolis, W.S. and Benson, R.A., "Characterizing Delamination Growth in Graphite-Epoxy," in Damage in Composite Materials, ASTM STP 775, K.L. Reifsnider, Ed., pp. 168-183 (1982).

[2] O'Brien, T.K., "Mixed-Mode Strain Energy Release Rate Effects on Edge Delamination of Composites," in Effects of Defects in Composite Materials, ASTM STP 836, pp. 125-142 (1984).

[3] Wang, S.S. and Choi, I., "The Mechanics of Delamination in Fiber Reinforced Composite Materials. Part II - Delamination Behavior and Fracture Mechanics Parameters," NASA CR-172270 (1983).

[4] Wang, S.S., "Edge Delamination in Angle Ply Composite Laminates," Proceedings of the 22nd AIAA/ASME/ASCE/AHS Structures, Structural Dynamics and Materials (SDM) Conference, Atlanta, Georgia, 6-8 April, 1981, pp. 473-484.

[5] O'Brien, T.K., "Characterization of Delamination Onset and Growth in a Composite Laminate," in Damage in Composite Materials, ASTM STP 775, K.L. Reifsnider, Ed., pp. 140-167 (1982).

[6] Armanios, E.A., and Rehfield, L.W., "Interlaminar Analysis of Laminated Composites using a Sublaminate Approach," Proceedings of the 27th AIAA/ASME/ASCE/AHS Structures, Structural Dynamics and Materials (SDM) Conference, San Antonio, Texas, 19-21 May, 1986, Part 1, pp. 442-452. AIAA Paper 86-0969CP.

[7] Crossman, F.W., and Wang, A.S.D.,"The Dependence of Transverse Cracking and Delamination on Ply Thickness in Graphite/Epoxy Laminates," in Damage in Composite Materials, ASTM STP 775, K.L. Reifsnider, Ed., pp. 118-139 (1982).

[8] O'Brien, T.K., "Analysis of Local Delaminations and Their Influence on Composite Laminate Behavior," in Delamination and Debonding of Materials, ASTM STP 876, Johnson, W.S., Ed., pp. 282-297 (1985).

[9] Law, G.E., "A Mixed Mode Fracture Analysis of $(\pm 25/90_n)_s$ Graphite/Epoxy Composite Laminates," in Effects of Defects in Composite Materials, ASTM STP 836, pp. 143-160 (1984).

[10] Armanios, E.A., "New Methods of Sublaminate Analysis for Composite Structures and Applications to Fracture Processes," Ph.D. Thesis, Georgia Institute of Technology (1984).

[11] Armanios, E.A., Rehfield, L.W., and Reddy, A.D., "Design Analysis and Testing for Mixed-Mode and Mode II Interlaminar Fracture of Composites," in Composite Materials: Testing and Design (Seventh Conference), ASTM STP 893, J.M.Whitney, Ed., pp. 232-255 (1986).

[12] Armanios, E.A., and Rehfield, L.W., "Sublaminate Analysis of Interlaminar Fracture in Composites: Part I - Analytical Model", submitted for publication in the Journal of Composites Technology and Research (July, 1988).

Appendix A

Sublaminate Analysis for Local Delaminations

Interlaminar Stresses and Energy Release Rates

A generic sublaminate is shown in figure 3 along with the notations and sign conventions. The interlaminar normal (peel) and shear stresses are denoted by P and T respectively with the t and b subscripts for the top and bottom surfaces respectively. The axial force resultant, shear force resultant and bending moment resultant are denoted by N, Q and M respectively. Plane strain conditions are assumed to prevail in the $x-z$ plane and the thickness strain ϵ_{zz} is neglected. These assumptions lead to considerable simplification in the analysis. The displacements in the x and z directions are assumed to be of the form

$$u = U(x) + z\beta(x) \tag{A.1}$$

$$w = W(x) \tag{A.2}$$

Here U represents the axial stretching and W is the transverse (thickness direction) displacement. This formulation recognizes shear deformation through the rotation β. The equilibrium equations take the form

$$N_{,x} + T_t - T_b = 0 \tag{A.3}$$

$$Q_{,x} + P_t - P_b = 0 \tag{A.4}$$

$$M_{,x} - Q + \frac{h}{2}(T_t + T_b) = 0 \tag{A.5}$$

where h is the thickness of the sublaminate. The constitutive equations in terms of the force and moment resultants are

$$N = A_{11}U_{,x} + B_{11}\beta_{,x} \tag{A.6}$$

$$Q = A_{55}(\beta + W_{,x}) \tag{A.7}$$

$$M = B_{11}U_{,x} + D_{11}\beta_{,x} \tag{A.8}$$

where A, B and D are the classical laminate theory axial, coupling and bending stiffnesses defined in the customary manner as

$$A_{11} = \int_{-\frac{h}{2}}^{\frac{h}{2}} C_{11}\, dz$$

$$B_{11} = \int_{-\frac{h}{2}}^{\frac{h}{2}} C_{11}\, z\, dz$$

$$D_{11} = \int_{-\frac{h}{2}}^{\frac{h}{2}} C_{11}\, z^2\, dz$$

$$A_{55} = \int_{-\frac{h}{2}}^{\frac{h}{2}} C_{55}\, dz$$

Here, the Cs are the material moduli. For the case of plane strain in the $x - z$ plane, the Cs are defined as follows.

$$\begin{Bmatrix} \sigma_{xx} \\ \sigma_{zz} \\ \tau_{xz} \end{Bmatrix} = \begin{bmatrix} C_{11} & C_{13} & 0 \\ C_{13} & C_{22} & 0 \\ 0 & 0 & C_{55} \end{bmatrix} \begin{Bmatrix} \epsilon_{xx} \\ \epsilon_{zz} \\ \gamma_{xz} \end{Bmatrix} \tag{A.9}$$

The boundary quantities to be prescribed at the sublaminate edges are

$$N \text{ or } U$$

$$M \text{ or } \beta$$

$$Q \text{ or } W$$

Further, at the interfaces between sublaminates, appropriate reciprocal traction and displacement matching boundary conditions have to be used.

The four sublaminates along with the loads acting on each are shown in figure 4. Setting P_1 and T_1 as shown automatically satisfies the traction matching boundary condition at the 1-2 interface. From symmetry, we get $w = 0$ and zero shear stress along the bottom faces of sublaminates 2 and 3. This leads to $w = 0$ in sublaminates 1,2 and 3. Thus, W has been prescribed in these sublaminates and the vertical shear force resultant Q cannot be prescribed at both ends of the sublaminates. Consequently, the calculated peel stress distribution will not be correct. In addition, at the 2-3 interface, the βs cannot be matched, since in these sublaminates, specifying β is equivalent to specifying Q (through eq. A.7). Inspite of these simplifications, reliable energy release rate components can be estimated based on the interlaminar shear stress distributions. The mode I contribution can then be evaluated using the total energy release rate, which is not affected significantly by these simplifications.

For the $(\pm 25/90_n)_s$ laminates under consideration, B_{11} is zero in all the four sublaminates. For sublaminates 1 and 2, the equilibrium equations and constitutive relationships can be written as

$$N_{1,x} - T_1 = 0 \tag{A.10}$$

$$N_{2,x} + T_1 = 0 \tag{A.11}$$

$$Q_{1,x} - P_1 = 0 \tag{A.12}$$

$$Q_{2,x} + P_1 - P_2 = 0 \tag{A.13}$$

$$M_{1,x} + \frac{h_1}{2} T_1 - Q_1 = 0 \tag{A.14}$$

$$M_{2,x} + \frac{h_2}{2} T_1 - Q_2 = 0 \tag{A.15}$$

$$N_1 = A_{11(1)} U_{1,x} \tag{A.16}$$

$$N_2 = A_{11(2)}U_{2,x} \tag{A.17}$$

$$Q_1 = A_{55(1)}\beta_1 \tag{A.18}$$

$$Q_2 = A_{55(2)}\beta_2 \tag{A.19}$$

$$M_1 = D_{11(1)}\beta_{1,x} \tag{A.20}$$

$$M_2 = D_{11(2)}\beta_{2,x} \tag{A.21}$$

The subscripts in brackets refer to the sublaminates to which the stiffness coefficients correspond. Equations A.14, A.15 and A.12 can be rewritten in a modified form as

$$M_{1,x} + \frac{h_1}{2}N_{1,x} = A_{55(1)}\beta_1 \tag{A.22}$$

$$M_{2,x} - \frac{h_2}{2}N_{2,x} = A_{55(2)}\beta_2 \tag{A.23}$$

$$\begin{aligned} P_1 &= Q_{1,x} \\ &= M_{1,xx} + \frac{h_1}{2}T_{1,x} \end{aligned} \tag{A.24}$$

Matching the u displacement along the 1-2 interface implies

$$\begin{aligned} u_1\left(-\tfrac{h_1}{2}, x\right) &= u_2\left(\tfrac{h_2}{2}, x\right) \\ \text{or} \quad U_1 - \tfrac{h_1}{2}\beta_1 &= U_2 + \tfrac{h_2}{2}\beta_2 \end{aligned} \tag{A.25}$$

Combining the equations to eliminate the displacement and interlaminar stress terms leads to the following homogeneous coupled system of ordinary differential equations.

$$N_{1,x} + N_{2,x} = 0 \tag{A.26}$$

$$M_{1,xx} + \frac{h_1}{2}N_{1,xx} - \frac{A_{55(1)}}{D_{11(1)}}M_1 = 0 \tag{A.27}$$

$$M_{2,xx} - \frac{h_2}{2}N_{2,xx} - \frac{A_{55(2)}}{D_{11(2)}}M_2 = 0 \tag{A.28}$$

$$\frac{N_1}{A_{11(1)}} - \frac{h_1}{2}\frac{M_1}{D_{11(1)}} - \frac{N_2}{A_{11(2)}} - \frac{h_2}{2}\frac{M_2}{D_{11(2)}} = 0 \tag{A.29}$$

The solution is assumed of the form

$$\begin{Bmatrix} N_1 \\ N_2 \\ M_1 \\ M_2 \end{Bmatrix} = \begin{Bmatrix} A_1 \\ A_2 \\ A_3 \\ A_4 \end{Bmatrix} e^{sx} \tag{A.30}$$

Substitution of this solution into the governing equations results in the following system of algebraic equations.

$$\begin{bmatrix} s & s & 0 & 0 \\ s^2\frac{h_1}{2} & 0 & s^2 - \frac{A_{55(1)}}{D_{11(1)}} & 0 \\ 0 & -s^2\frac{h_2}{2} & 0 & s^2 - \frac{A_{55(2)}}{D_{11(2)}} \\ \frac{1}{A_{11(1)}} & -\frac{1}{A_{11(2)}} & -\frac{h_1}{2}\frac{1}{D_{11(1)}} & -\frac{h_2}{2}\frac{1}{D_{11(2)}} \end{bmatrix} \begin{Bmatrix} A_1 \\ A_2 \\ A_3 \\ A_4 \end{Bmatrix} e^{sx} = \begin{Bmatrix} 0 \\ 0 \\ 0 \\ 0 \end{Bmatrix} \tag{A.31}$$

The corresponding eigenvalue problem has to be solved in order to obtain non trivial solutions. The eigenvalues turn out to be the roots of the following characteristic equation.

$$s\left[B_1 s^4 + B_2 s^2 + B_3\right] = 0 \tag{A.32}$$

where

$$\begin{aligned} B_1 &= -\frac{1}{A_{11(2)}} - \frac{1}{A_{11(1)}} - \frac{1}{D_{11(2)}}\left(\frac{h_2}{2}\right)^2 - \frac{1}{D_{11(1)}}\left(\frac{h_1}{2}\right)^2 \\ B_2 &= \frac{1}{A_{11(2)}}\frac{A_{55(2)}}{D_{11(2)}} + \frac{1}{A_{11(2)}}\frac{A_{55(1)}}{D_{11(1)}} + \frac{A_{55(1)}}{D_{11(1)}}\frac{1}{D_{11(2)}}\left(\frac{h_2}{2}\right)^2 \\ &\quad + \frac{1}{A_{11(1)}}\frac{A_{55(1)}}{D_{11(1)}} + \frac{1}{A_{11(1)}}\frac{A_{55(2)}}{D_{11(2)}} + \frac{A_{55(2)}}{D_{11(2)}}\frac{1}{D_{11(1)}}\left(\frac{h_1}{2}\right)^2 \\ B_3 &= -\frac{1}{A_{11(2)}}\frac{A_{55(1)}}{D_{11(1)}}\frac{A_{55(2)}}{D_{11(2)}} - \frac{1}{A_{11(1)}}\frac{A_{55(1)}}{D_{11(1)}}\frac{A_{55(2)}}{D_{11(2)}} \end{aligned}$$

For the material system and ply stacking sequence considered, $B_2^2 > 4B_1B_3$. Hence, the roots can be written as

$$s = 0, \pm\sqrt{\frac{-B_2 \pm \sqrt{B_2^2 - 4B_1B_3}}{2B_1}} \tag{A.33}$$

Only the zero and positive roots of eq. A.33 are considered as they give exponentially decaying solutions, leading to finite values for the resultants at the sublaminate ends. Hence, the solution for N_1 can be written as

$$N_1 = a_1 e^{s_1 x} + a_2 e^{s_2 x} + \alpha_1 \tag{A.34}$$

Using this in eq. A.26 yields

$$N_2 = -a_1 e^{s_1 x} - a_2 e^{s_2 x} + \alpha_2 \tag{A.35}$$

Substituting N_1 and N_2 in eqs. A.27 and A.28 provides the solutions for the bending moments as

$$M_1 = a_1 k_1 e^{s_1 x} + a_2 k_2 e^{s_2 x} \tag{A.36}$$

$$M_2 = a_1 k_3 e^{s_1 x} + a_2 k_4 e^{s_2 x} \tag{A.37}$$

The k parameters in the above solutions are defined as follows.

$$k_1 = \frac{\frac{h_1}{2} s_1^2}{\frac{A_{55(1)}}{D_{11(1)}} - s_1^2} \tag{A.38}$$

$$k_2 = \frac{\frac{h_1}{2} s_2^2}{\frac{A_{55(1)}}{D_{11(1)}} - s_2^2} \tag{A.39}$$

$$k_3 = \frac{\frac{h_2}{2} s_1^2}{\frac{A_{55(2)}}{D_{11(2)}} - s_1^2} \tag{A.40}$$

$$k_4 = \frac{\frac{h_2}{2} s_2^2}{\frac{A_{55(2)}}{D_{11(2)}} - s_2^2} \tag{A.41}$$

If P is the applied force and w represents the specimen width,

$$N_1 + N_2 = \frac{P}{2w} \tag{A.42}$$

Using this in conjunction with eq. A.29 allows determination of the constants α_1 and α_2. The following solutions for the stresses and the resultants can then be obtained.

$$N_1 = a_1 e^{s_1 x} + a_2 e^{s_2 x} + \frac{P}{2w}\frac{A_{11(1)}}{A_{11(1)} + A_{11(2)}} \quad (A.43)$$

$$N_2 = -a_1 e^{s_1 x} - a_2 e^{s_2 x} + \frac{P}{2w}\frac{A_{11(2)}}{A_{11(1)} + A_{11(2)}} \quad (A.44)$$

$$T_1 = N_{1,x}$$

$$= a_1 s_1 e^{s_1 x} + a_2 s_2 e^{s_2 x} \quad (A.45)$$

$$P_1 = M_{1,xx} + \frac{h_1}{2} T_{1,x}$$

$$= (k_1 + \frac{h_1}{2}) a_1 s_1^2 e^{s_1 x} + (k_2 + \frac{h_1}{2}) a_2 s_2^2 e^{s_2 x} \quad (A.46)$$

The constitutive equations are used to write down the displacement solutions. The rigid body displacements of sublaminates 1 and 2 are matched (in order to satisfy the displacement continuity condition) to obtain

$$U_1 = \frac{a_1}{A_{11(1)} s_1} e^{s_1 x} + \frac{a_2}{A_{11(1)} s_2} e^{s_2 x} + \frac{P}{2w}\frac{1}{A_{11(1)} + A_{11(2)}} x + a_3 \quad (A.47)$$

$$U_2 = -\frac{a_1}{A_{11(1)} s_1} e^{s_1 x} - \frac{a_2}{A_{11(1)} s_2} e^{s_2 x} + \frac{P}{2w}\frac{1}{A_{11(1)} + A_{11(2)}} x + a_3 \quad (A.48)$$

$$\beta_1 = \frac{1}{A_{55(1)}}[a_1 k_1 s_1 e^{s_1 x} + a_2 k_2 s_2 e^{s_2 x} + \frac{h_1}{2}(a_1 s_1 e^{s_1 x} + a_2 s_2 e^{s_2 x})] \quad (A.49)$$

$$\beta_2 = \frac{1}{A_{55(2)}}[a_1 k_3 s_1 e^{s_1 x} + a_2 k_4 s_2 e^{s_2 x} + \frac{h_2}{2}(a_1 s_1 e^{s_1 x} + a_2 s_2 e^{s_2 x})] \quad (A.50)$$

The constants a_1, a_2 and a_3 occurring in the solutions are determined using the boundary condtions. For sublaminate 3 the governing equations are

$$N_{3,x} = 0 \quad (A.51)$$

$$Q_{3,x} + P_3 = 0 \quad (A.52)$$

$$M_{3,x} - Q_3 = 0 \quad (A.53)$$

$$N_3 = A_{11(2)} U_{3,x} \tag{A.54}$$

$$Q_3 = A_{55(2)} \beta_3 \tag{A.55}$$

$$M_3 = D_{11(2)} \beta_{3,x} \tag{A.56}$$

Matching U at the 2-3 interface and applying $N_3(a) = 0$ gives

$$N_3 = 0 \tag{A.57}$$

$$U_3 = U_2(0) \tag{A.58}$$

$$= -\frac{a_1}{s_1 A_{11(2)}} - \frac{a_2}{s_2 A_{11(2)}} + a_3 \tag{A.59}$$

In order to solve for the bending moment, eqs. A.53, A.55 and A.56 are combined to obtain

$$M_{3,xx} - \frac{A_{55(2)}}{D_{11(2)}} M_3 = 0 \tag{A.60}$$

The solution of eq. A.60 can be written as

$$M_3 = \phi_1 \sinh \omega_3 x + \phi_2 \cosh \omega_3 x \tag{A.61}$$

where the quantity ω_3 is defined by

$$\omega_3^2 = \frac{A_{55(2)}}{D_{11(2)}} \tag{A.62}$$

Since the β matching conditon cannot be used at the 2-3 interface, the (remaining) boundary conditions are

$$\left.\begin{aligned} M_3(a) &= 0 \\ M_3(0) &= M_2(0) \end{aligned}\right\} \tag{A.63}$$

The ϕs can be solved using the boundary conditions A.63 as

$$\phi_2 = a_1 k_3 + a_2 k_4 \tag{A.64}$$

$$\phi_1 = -\phi_2 \coth \omega_3 a \tag{A.65}$$

The solution for sublaminate 3 can be completed by writing the following expressions.

$$Q_3 = \phi_1\omega_3\cosh\omega_3 x + \phi_2\omega_3\sinh\omega_3 x \tag{A.66}$$

$$\beta_3 = \frac{1}{A_{55(2)}}[\phi_1\omega_3\cosh\omega_3 x + \phi_2\omega_3\sinh\omega_3 x] \tag{A.67}$$

$$P_3 = \frac{A_{55(2)}}{D_{11(2)}}[\phi_1\sinh\omega_3 x + \phi_2\cosh\omega_3 x] \tag{A.68}$$

The equilibrium equations for sublaminate 4 are

$$N_{4,x} = 0 \tag{A.69}$$

$$Q_{4,x} = 0 \tag{A.70}$$

$$M_{4,x} - Q_4 = 0 \tag{A.71}$$

The constitutive relations take the form

$$N_4 = A_{11(1)}U_{4,x} \tag{A.72}$$

$$Q_4 = A_{55(1)}(\beta_4 + W_{4,x}) \tag{A.73}$$

$$M_4 = D_{11(1)}\beta_{4,x} \tag{A.74}$$

Using eq. A.69 with the boundary condition $N_4(a) = \frac{P}{2w}$ yields

$$N_4 = \frac{P}{2w} \tag{A.75}$$

Similarly, using eq. A.70 with $Q_4(a) = 0$ results in

$$Q_4 = 0 \tag{A.76}$$

Matching M_1 and M_4 at the 1-4 interface and using eq. A.71 gives

$$M_4 = a_1k_1 + a_2k_2 \tag{A.77}$$

The U_4 displacement is obtained by integrating eq. A.72 and using the displacement matching boundary condition $U_4(0) = U_1(0)$.

$$U_4 = \frac{P}{2w}\frac{1}{A_{11(1)}}x + \frac{a_1}{s_1 A_{11(1)}} + \frac{a_2}{s_2 A_{11(1)}} + a_3 \tag{A.78}$$

Similarly, integrating eq. A.74 and setting $\beta_4(a) = 0$ gives

$$\beta_4 = \frac{1}{D_{11(1)}}[a_1 k_1 + a_2 k_2](x - a) \tag{A.79}$$

Using the solutions for Q_4 and β_4 and the boundary condition $W_4(0) = 0$ in eq. A.73 yields the following solution for W_4.

$$W_4 = \frac{A_{55(1)}}{D_{11(1)}}[a_1 k_1 + a_2 k_2](\frac{x^2}{2} - ax) \tag{A.80}$$

In order to determine a_1, a_2 and a_3, the following boundary conditions are used.

$$\begin{aligned} N_1(0) &= \frac{P}{2w} \\ \beta_1(0) &= \beta_4(0) \\ U_1(-l + a) &= 0 \end{aligned}$$

It is convenient to define the following parameters.

$$\theta_1 = \frac{s_1}{A_{55(1)}}(k_1 + \frac{h_1}{2}) \tag{A.81}$$

$$\theta_2 = \frac{k_1}{D_{11(1)}} \tag{A.82}$$

$$\theta_3 = \frac{s_2}{A_{55(1)}}(k_2 + \frac{h_1}{2}) \tag{A.83}$$

$$\theta_4 = \frac{k_2}{D_{11(1)}} \tag{A.84}$$

$$\theta_d = \theta_3 - \theta_1 + (\theta_4 - \theta_2)a \tag{A.85}$$

The nominal (far field) strain is given by

$$\epsilon = \frac{P}{2w}\frac{1}{A_{11(1)} + A_{11(2)}} \tag{A.86}$$

The a parameters are obtained as

$$a_1 = A_{11(2)}\,\epsilon\,\frac{\theta_3 + \theta_4 a}{\theta_d} \tag{A.87}$$

$$a_2 = -A_{11(2)}\,\epsilon\,\frac{\theta_1 + \theta_2 a}{\theta_d} \tag{A.88}$$

$$a_3 = \epsilon(l-a) - \frac{a_1}{s_1 A_{11(1)}} e^{-s_1(l-a)} - \frac{a_2}{s_2 A_{11(1)}} e^{-s_2(l-1)} \tag{A.89}$$

The specimen compliance C is defined as the ratio of specimen extension to applied load. This is obtained as

$$\begin{aligned} C &= \frac{2U_4(a)}{P} \\ &= \frac{2}{P}\left\{\frac{Pa}{2wA_{11(1)}} + \frac{a_1}{s_1 A_{11(1)}} + \frac{a_2}{s_2 A_{11(1)}} + a_3\right\} \end{aligned} \tag{A.90}$$

The total energy release rate associated with the crack (delamination) growth under a constant load P is given by

$$G_T = \frac{P^2}{2w}\frac{dC}{da} \tag{A.91}$$

Using the compliance expression from eq. A.90 in eq. A.91 yields the following expression for G_T.

$$G_T = \frac{P^2}{2w^2}\left(\frac{1}{A_{11(1)}} - \frac{1}{A_{11(1)} + A_{11(2)}} + I_1 - I_2\right) \tag{A.92}$$

where

$$I_1 = \frac{1}{A_{11(1)} + A_{11(2)}}\frac{A_{11(2)}}{A_{11(1)}}\frac{\theta_2\theta_3 - \theta_1\theta_4}{\theta_d^2}\left(\frac{1 - e^{-s_1(l-a)}}{s_1} - \frac{1 - e^{-s_2(l-a)}}{s_2}\right) \tag{A.93}$$

$$I_2 = \frac{1}{A_{11(1)} + A_{11(2)}}\frac{A_{11(2)}}{A_{11(1)}}\frac{(\theta_3 + \theta_4 a)e^{-s_1(l-a)} - (\theta_1 + \theta_2 a)e^{-s_2(l-a)}}{\theta_d} \tag{A.94}$$

The individual fracture mode contributions to the energy release rate can be calculated using the virtual crack closure method, based on the interlaminar stresses and displacements in the vicinity of the crack tip. From the assumed plane strain

condition, the mode III contribution is zero ($G_{III} = 0$). The mode II energy release rate, G_{II}, is calculated using the virtual crack closure technique while G_I is evaluated using

$$G_I = G_T - G_{II} \tag{A.95}$$

G_{II} is calculated from the interlaminar shear stress and relative sliding displacement as

$$G_{II} = \lim_{\delta \to 0} \frac{1}{2\delta} \int_0^{\delta} T_1(x - \delta) \Delta u(x)\, dx \tag{A.96}$$

In the absence of a singularity in the stress field, the result of the limiting process leads to the trivial result $G_{II} = 0$. Hence, the limit is calculated as δ tends to some finite value, say Δ. The value of Δ is chosen depending on the decay length associated with the problem i.e. the length within which the presence of the crack significantly alters the specimen response in comparison with the corresponding far field values. Evidently, the decay length in this problem is dependent on the eigenvalues s_1 and s_2. The following value of Δ has been chosen in order to reasonably fulfil the decay length criterion.

$$\Delta = \frac{1}{4}\left(\frac{1}{s_1} + \frac{1}{s_2}\right) \tag{A.97}$$

The relative sliding displacement Δu is based only on the difference $U_4 - U_3$ so that the kinematic condition of zero relative displacement at the crack tip is fulfilled. This also simplifies the calculations. The mode II energy release rate component is obtained as

$$G_{II} = \frac{I_3 + I_4}{2\Delta} \tag{A.98}$$

where I_3 and I_4 are defined as

$$I_3 = \left(\frac{1}{A_{11(1)}} + \frac{1}{A_{11(2)}}\right)\left(\frac{a_1}{s_1} + \frac{a_2}{s_2}\right)\left[a_1(1 - e^{-s_1\Delta}) + a_2(1 - e^{-s_2\Delta})\right] \tag{A.99}$$

$$I_4 = \left(\frac{s_1\Delta - 1 + e^{-s_1\Delta}}{s_1} a_1 + \frac{s_2\Delta - 1 + e^{-s_2\Delta}}{s_2} a_2 \right) \epsilon \frac{A_{11(1)} + A_{11(2)}}{A_{11(1)}} \qquad \text{(A.100)}$$

Transverse Crack Spacing

Shear Deformation Model

The model presented so far has dealt with delaminations growing from a transverse crack. The same model can be modified to predict the spacing of these transverse cracks. In order to accomplish this, the delamination effect has to be isolated from the model. This can be achieved approximately by letting the crack length a tend to zero. This yields an approximation since the boundary conditions are not accounted for properly by this limiting process. To get an accurate shear deformation model, we consider only sublaminates 1 and 2 and apply the following boundary conditions for sublaminate 2.

$$N_2(0) = 0 \qquad \text{(A.101)}$$

$$M_2(0) = 0 \qquad \text{(A.102)}$$

Using these boundary conditions in eqs. A.37 and A.44 yields two equations in a_1 and a_2 which can be solved to obtain

$$a_1 = \frac{k_4}{k_4 - k_3} \frac{P}{2w} \frac{A_{11(2)}}{A_{11(1)} + A_{11(2)}} \qquad \text{(A.103)}$$

$$a_2 = \frac{k_3}{k_3 - k_4} \frac{P}{2w} \frac{A_{11(2)}}{A_{11(1)} + A_{11(2)}} \qquad \text{(A.104)}$$

The interlaminar shear stress can now be obtained using eq. A.45. The saturation crack spacing corresponds to the distance from the crack where the broken plies regain their uniform stress/strain state i.e. where the interlaminar shear stress has decayed down to its far field (uniform) value. Practically, this distance is calculated by looking for the x where the interlaminar shear stress is some small fraction (say

.001) of its maximum value. The maximum shear stress evidently occurs at $x = 0$ and is given by

$$T_1^{(max)} = a_1 s_1 + a_2 s_2 \tag{A.105}$$

The crack spacing λ can then be determined by solving the following transcendental equation.

$$\frac{a_1 s_1 e^{s_1 \lambda} + a_2 s_2 e^{s_2 \lambda}}{a_1 s_1 + a_2 s_2} = 0.001 \tag{A.106}$$

Membrane Model

A simpler model can be used to estimate the saturation spacing of the transverse cracks. This model treats the sublaminates as membranes i.e. the bending effects are ignored. The equilibrium equations for a generic membrane sublaminate are

$$N_{,x} + T_t - T_b = 0 \tag{A.107}$$

$$\frac{h}{2}(T_t - T_b) - Q = 0 \tag{A.108}$$

The constitutive equations take the form

$$N = \left(A_{11} - \frac{B_{11}^2}{D_{11}}\right) U_{,x} \tag{A.109}$$

$$Q = A_{55}\beta \tag{A.110}$$

The displacements are assumed to be of the following form.

$$u = U(x) + z\beta(x) \tag{A.111}$$

$$w = 0 \tag{A.112}$$

The following governing equations can now be written

$$N_{1,x} - T_1 = 0 \tag{A.113}$$

$$N_{2,x} + T_1 = 0 \tag{A.114}$$

$$\frac{h_1}{2}T_1 - Q_1 = 0 \tag{A.115}$$

$$\frac{h_2}{2}T_1 - Q_2 = 0 \tag{A.116}$$

$$N_1 = \gamma_1 U_{1,x} \tag{A.117}$$

$$N_2 = \gamma_2 U_{2,x} \tag{A.118}$$

$$Q_1 = A_{55(1)}\beta_1 \tag{A.119}$$

$$Q_2 = A_{55(2)}\beta_2 \tag{A.120}$$

$$U_1 - \frac{h_1}{2}\beta_1 = U_2 + \frac{h_2}{2}\beta_2 \tag{A.121}$$

where the γs are defined as

$$\gamma_1 = A_{11(1)} - \frac{B_{11(1)}^2}{D_{11(1)}} \tag{A.122}$$

$$\gamma_2 = A_{11(2)} - \frac{B_{11(2)}^2}{D_{11(2)}} \tag{A.123}$$

Eqs. A.113 and A.115 can be combined as

$$Q_1 = \frac{h_1}{2}N_{1,x} \tag{A.124}$$

Using eqs. A.119 and A.117 in this leads to

$$\beta_1 = \frac{h_1}{2}\frac{1}{A_{55(1)}}\gamma_1 U_{1,xx} \tag{A.125}$$

Following a similar procedure for β_2 yields

$$\beta_2 = \frac{h_2}{2}\frac{1}{A_{55(2)}}\gamma_1 U_{1,xx} \tag{A.126}$$

Using these two relations in eq. A.121 leads to

$$U_1 - \left(\frac{h_1}{2}\right)^2 \frac{\gamma_1}{A_{55(1)}}U_{1,xx} = U_2 - \left(\frac{h_2}{2}\right)^2 \frac{\gamma_1}{A_{55(2)}}U_{1,xx} \tag{A.127}$$

Combining eqs. A.113, A.114, A.117 and A.118 gives

$$\gamma_1 U_{1,xx} + \gamma_2 U_{2,xx} = 0 \tag{A.128}$$

Substituting this into eq. A.127 results in

$$U_{1,xx} - \left[\left(\frac{h_1}{2}\right)^2 \frac{\gamma_1}{A_{55(1)}} + \left(\frac{h_2}{2}\right)^2 \frac{\gamma_1}{A_{55(2)}}\right] U_{1,xxxx} + \frac{\gamma_1}{\gamma_2} U_{1,xx} = 0 \tag{A.129}$$

The characteristic roots of this differential equation are

$$s = 0, 0, \pm \sqrt{\frac{\gamma_1 + \gamma_2}{\gamma_1 \gamma_2 \left[\left(\frac{h_1}{2}\right)^2 \frac{1}{A_{55(1)}} + \left(\frac{h_2}{2}\right)^2 \frac{1}{A_{55(2)}}\right]}} \tag{A.130}$$

The solution for U_1 can then be written as

$$U_1 = A_1 e^{s_1 x} + A_2 x + A_3 \tag{A.131}$$

where the As are arbitrary constants to be determined from the boundary conditions. The root s_1 is the positive root such that a decaying solution is obtained in the negative x region. For the special case of $B_{11(1)} = B_{11(2)} = 0$, the nonzero roots can be written in a simpler form as

$$s^2 = \frac{4(A_{11(1)} + A_{11(2)})}{A_{11(1)} A_{11(2)}} \frac{1}{\frac{h_1^2}{A_{55(1)}} + \frac{h_2^2}{A_{55(2)}}} \tag{A.132}$$

The interlaminar shear stress can be obtained as follows.

$$\begin{aligned} T_1 &= N_{1,x} \\ &= \gamma_1 U_{1,xx} \\ &= \gamma_1 A_1 s_1^2 e^{s_1 x} \end{aligned} \tag{A.133}$$

The maximum shear stress is

$$T_1^{(max)} = \gamma_1 A_1 s_1^2 \tag{A.134}$$

Then, the saturation crack spacing λ corresponds to

$$e^{s_1 \lambda} = 0.001 \tag{A.135}$$

Shear Lag Model

This model allows for a nonlinear displacement field through the thickness of the sublaminate. Its fundamental assumption is that the shear deformation neglected in the classical theory of bending can be estimated using the shear stress. The sublaminate axial force equilibrium condition can be written as

$$N_{,x} + (T_t - T_b) = 0 \tag{A.136}$$

The axial stress is assumed to be uniform and is given by

$$\sigma_{xx} = \frac{N}{h} \tag{A.137}$$

The shear stress is estimated as follows

$$\begin{aligned} \sigma_{xz,z} &= -\sigma_{xx,x} \\ &= \frac{-N_{,x}}{h} \\ &= \frac{T_t - T_b}{h} \end{aligned} \tag{A.138}$$

This can be integrated to obtain

$$\sigma_{xz} = \frac{T_t - T_b}{h} z + \frac{T_t + T_b}{2} \tag{A.139}$$

Neglecting transverse displacement, the axial displacement can be obtained by integrating the shear strain, which in turn is obtained from the shear stress.

$$\begin{aligned} u_{,z} &= \frac{\sigma_{xz}}{C'_{55}} \\ &= \frac{1}{C'_{55}} \left[(T_t - T_b)\frac{z}{h} + \frac{T_t + T_b}{2} \right] \end{aligned} \tag{A.140}$$

$$u = U(x) + \frac{1}{2C'_{55}} \left[(T_t - T_b)\frac{z^2}{h} + (T_t + T_b)z \right] \tag{A.141}$$

where $U(x)$ is the mid-plane axial displacement. This displacement expression can be used to obtain an improved axial stress estimate as follows.

$$\sigma_{xx} = C_{11} u_{,x}$$

$$= C_{11}\left[U_{,x} + \frac{1}{2C_{55}}(T_t - T_b)_{,x}\frac{z^2}{h} + (T_t + T_b)_{,x}z\right] \quad \text{(A.142)}$$

The corresponding axial stress resultant can be written as

$$\begin{aligned} N &= \int_{-\frac{h}{2}}^{\frac{h}{2}} \sigma_{zz}\, dz \\ &= C_{11}\left[hU_{,x} + \frac{h^2}{24C_{55}}(T_t - T_b)_{,x}\right] \end{aligned} \quad \text{(A.143)}$$

The governing equations for the sublaminate are thus eqs. A.136 (equilibrium), A.141 (displacement field) and A.143 (constitutive relationship). Using these to model sublaminates 1 and 2 results in the following governing equations.

$$N_{1,x} - T_1 = 0 \quad \text{(A.144)}$$

$$N_{2,x} + T_2 = 0 \quad \text{(A.145)}$$

$$N_1 = C_{11(1)}\left[h_1 U_{1,x} - \frac{h_1^2}{24C_{55(1)}}T_{1,x}\right] \quad \text{(A.146)}$$

$$N_2 = C_{11(2)}\left[h_2 U_{2,x} + \frac{h_2^2}{24C_{55(2)}}T_{1,x}\right] \quad \text{(A.147)}$$

$$u_1 = U_1 + \frac{1}{2C_{55(1)}}\left[-T_1\frac{z^2}{h_1} + T_1 z\right] \quad \text{(A.148)}$$

$$u_2 = U_2 + \frac{1}{2C_{55(2)}}\left[T_1\frac{z^2}{h_2} + T_1 z\right] \quad \text{(A.149)}$$

Displacement continuity at the 1-2 interface implies

$$u_1(x, -\frac{h_1}{2}) = u_2(x, \frac{h_2}{2}) \quad \text{(A.150)}$$

or

$$U_2 = U_1 - \frac{3T_1}{8}\left[\frac{h_1}{C_{55(1)}} + \frac{h_2}{C_{55(2)}}\right] \quad \text{(A.151)}$$

Equation A.146 can be rewritten as

$$U_{1,x} = \frac{N_1}{C_{11(1)}h_1} + \frac{h_1}{24C_{55(1)}}T_{1,x} \quad \text{(A.152)}$$

Combining eqs. A.147, A.151 and A.152 results in

$$N_2 = C_{11(2)}\left\{\frac{h_2 N_1}{h_1 C_{11(1)}} - \frac{h_2 T_{1,x}}{3}\left[\frac{h_1}{C_{55(1)}} + \frac{h_2}{C_{55(2)}}\right]\right\} \quad \text{(A.153)}$$

But from eqs. A.144 and A.145, we have

$$N_{2,x} = -T_1 = -N_{1,x} \tag{A.154}$$

Using this in the differentiated form of eq. A.153 leads to

$$\left[\frac{1}{h_2 C_{11(2)}} + \frac{1}{h_1 C_{11(1)}}\right] N_{1,x} = \frac{1}{3}\left[\frac{h_1}{C_{55(1)}} + \frac{h_2}{C_{55(2)}}\right] N_{1,xxx} \tag{A.155}$$

The nonzero characteristic roots of this equation are given by

$$s^2 = 3\left(\frac{C_{55(1)}}{h_1 C_{11(1)}}\right)\left(\frac{C_{55(2)}}{h_2 C_{11(2)}}\right)\left(\frac{h_1 C_{11(1)} + h_2 C_{11(2)}}{h_2 C_{55(1)} + h_1 C_{55(2)}}\right) \tag{A.156}$$

This is the same as in the membrane model except for the factor 3 which is 4 in the membrane model. This difference is related to the fact that the axial displacement distribution through the thickness is parabolic in the shear lag model and linear in the membrane model. The crack spacing λ for the shear lag model is determined as in the case of the membrane model but using the modified characteristic root.

Table 1 Summary of Results

number of 90° plies	G_T J/m^2	G_{II}/G_T	σ_c MPa	ϵ_c %
1/2	2.404	0.276	1313.9	1.6747
1	6.752	0.275	784.0	1.1685
2	22.849	0.267	426.2	0.8058
3	51.049	0.261	285.1	0.6427
4	93.603	0.256	210.6	0.5444
6	228.871	0.250	134.7	0.4264
8	440.065	0.247	97.1	0.3555

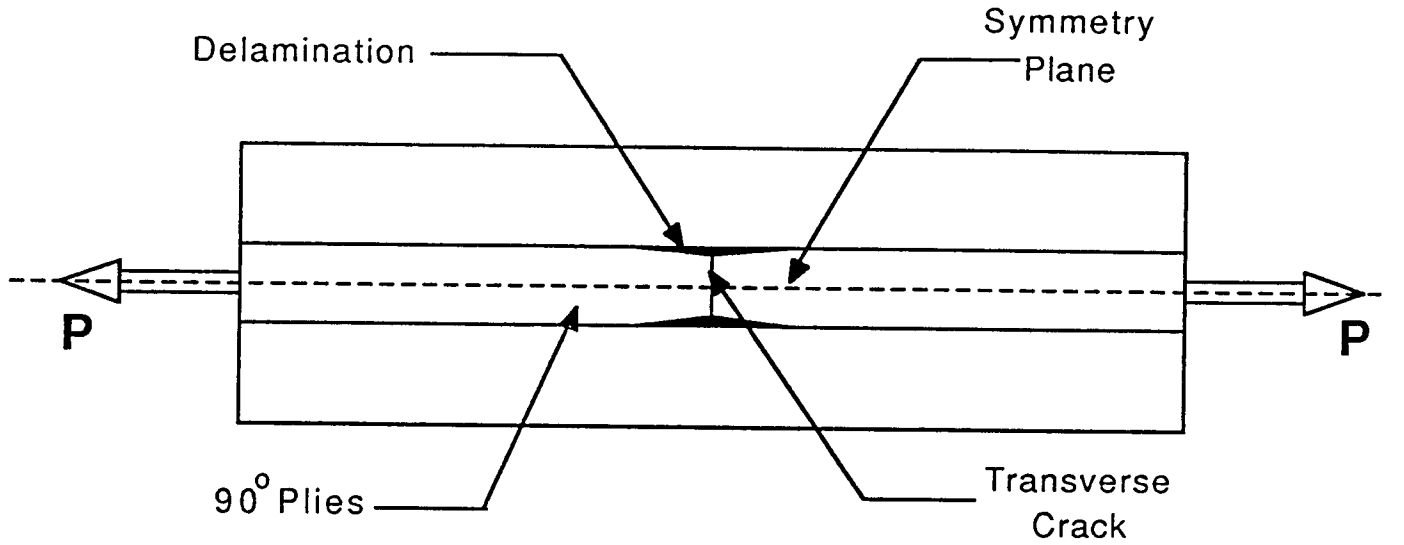

Fig. 1 Specimen Cross Section

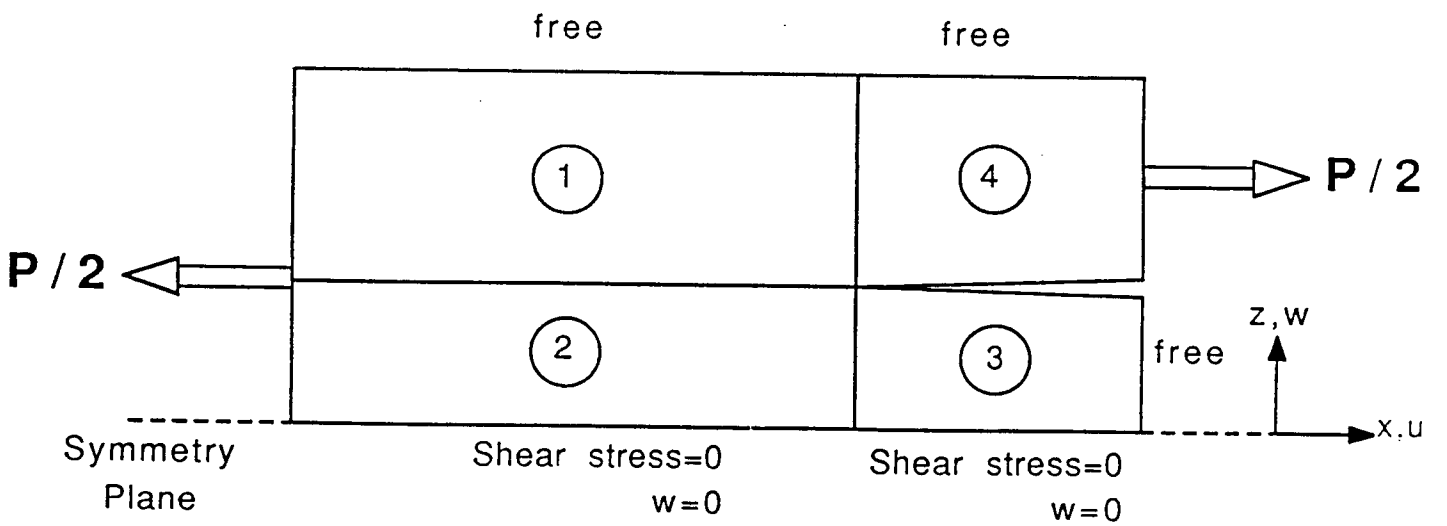

Fig. 2 Modelled Region and Sublaminate Scheme

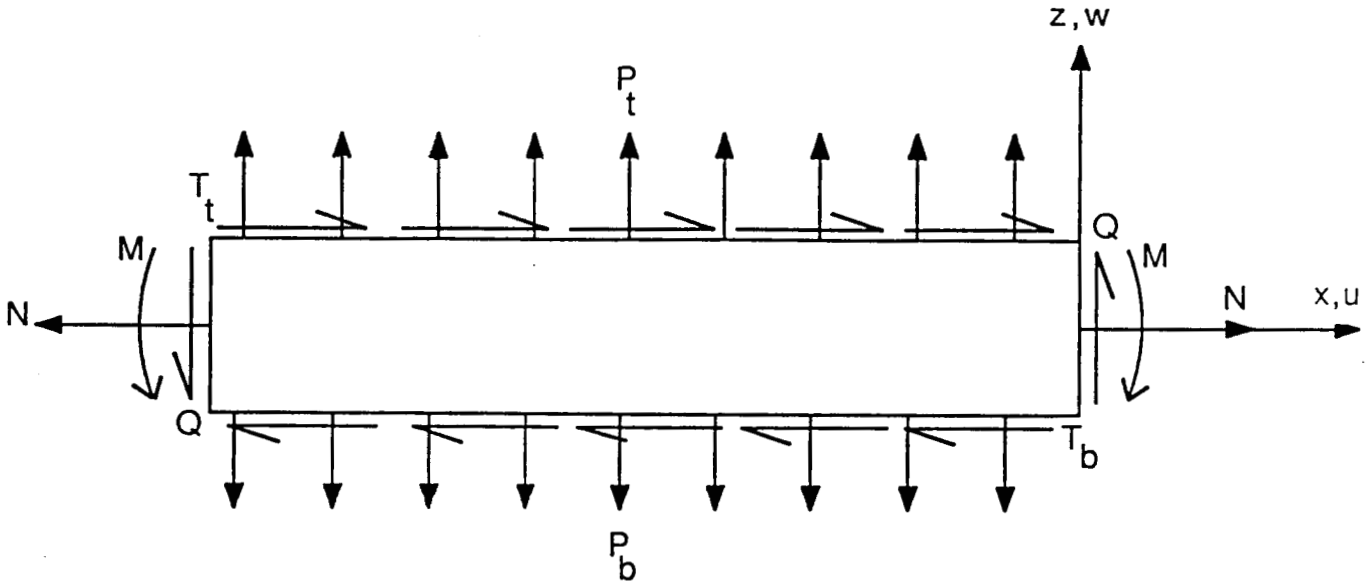

Fig. 3 Generic Sublaminate

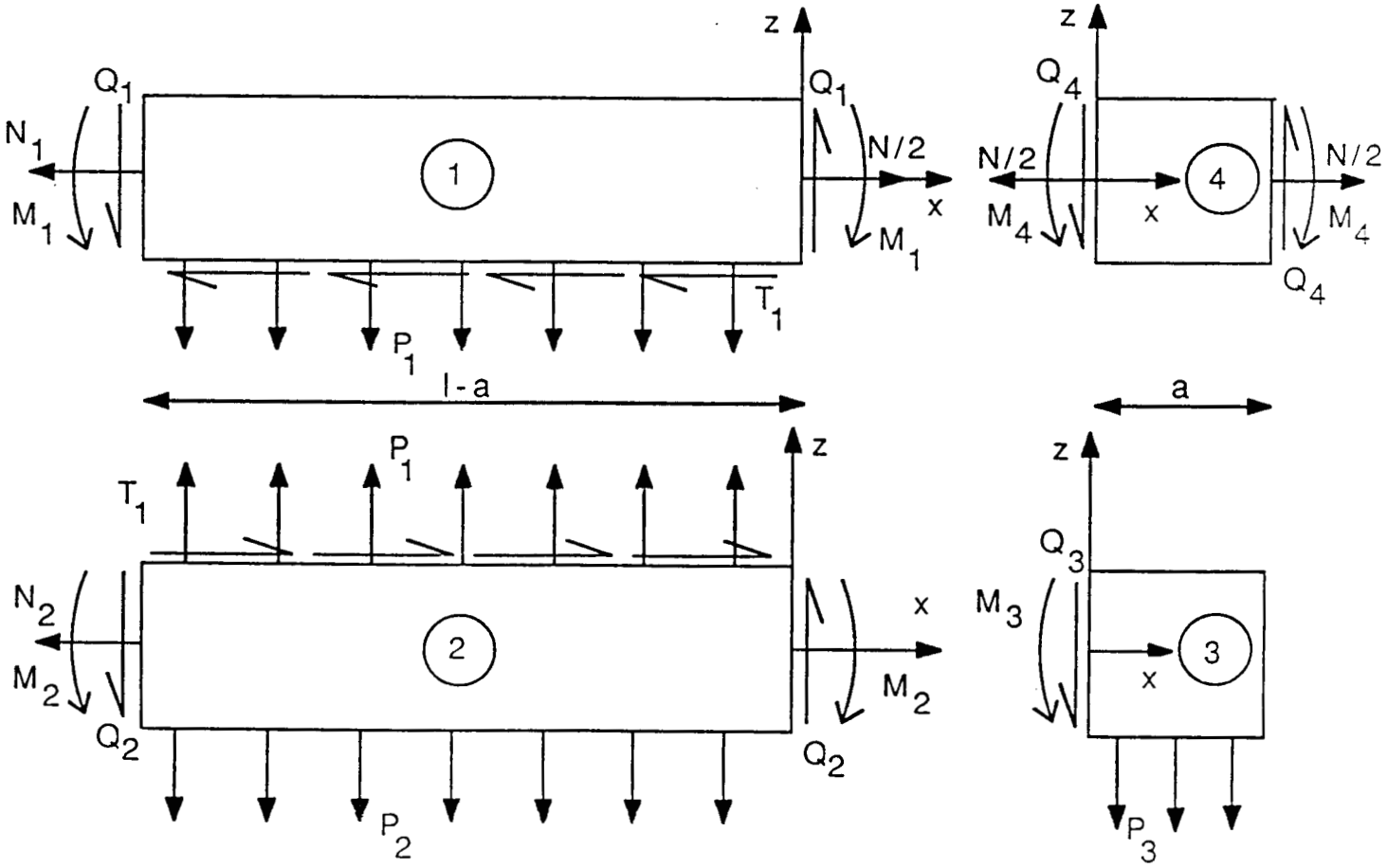

Fig. 4 Sublaminate Forces and Coordinate Systems

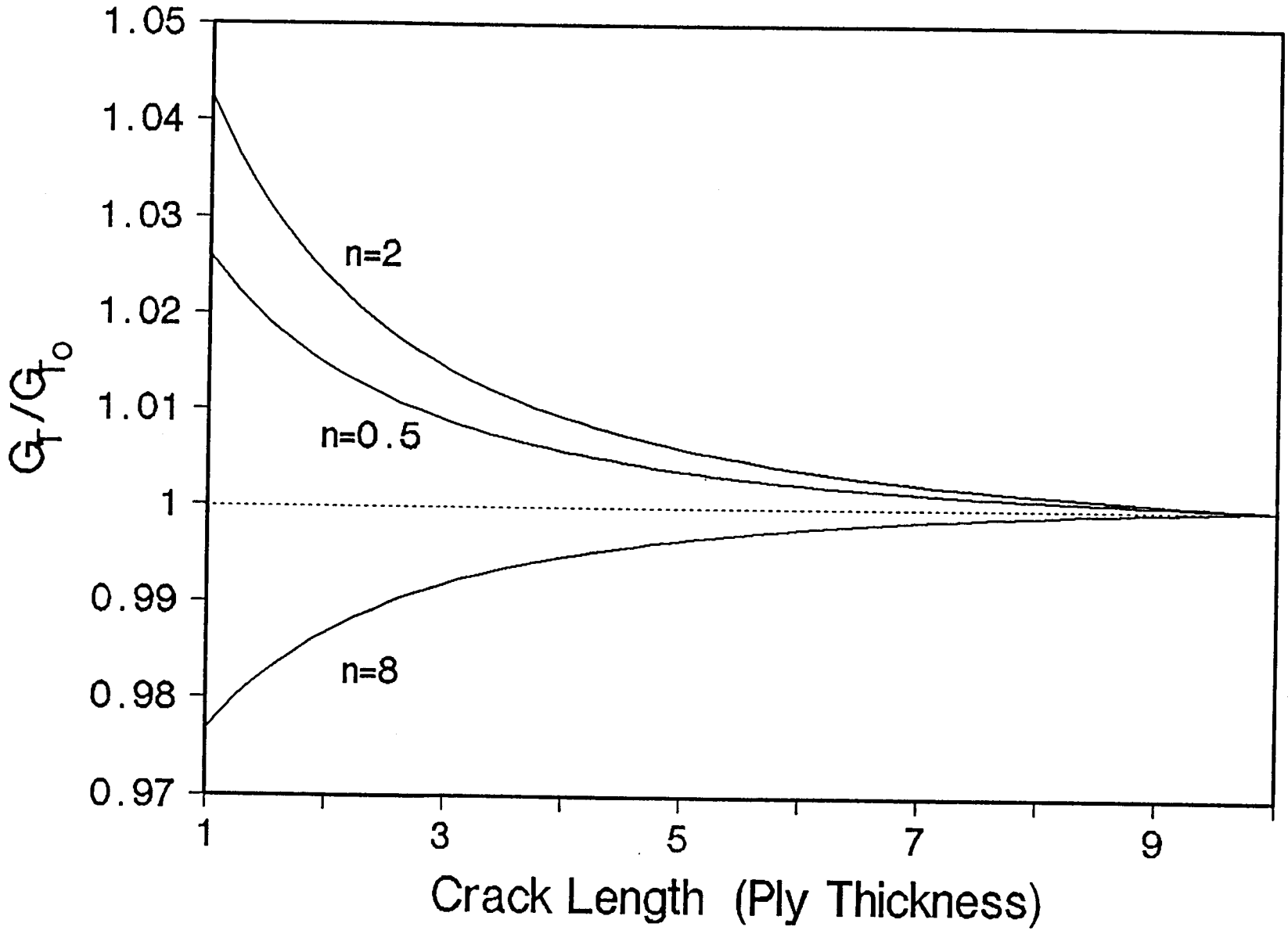

Fig. 5 Total Energy Release Rate Variation with Initial Crack Size

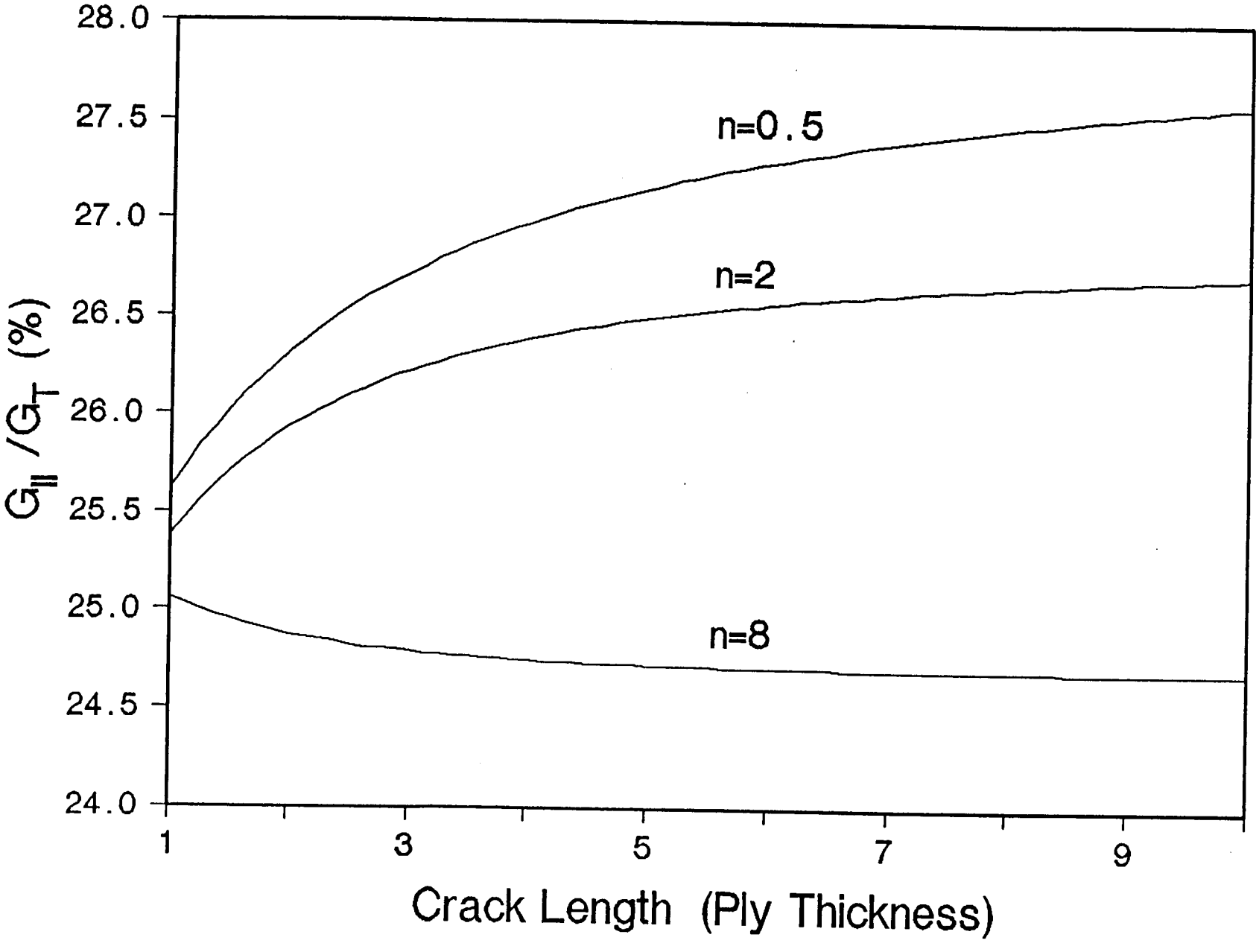

Fig. 6 Mode II Energy Release Rate Dependence on Crack Size

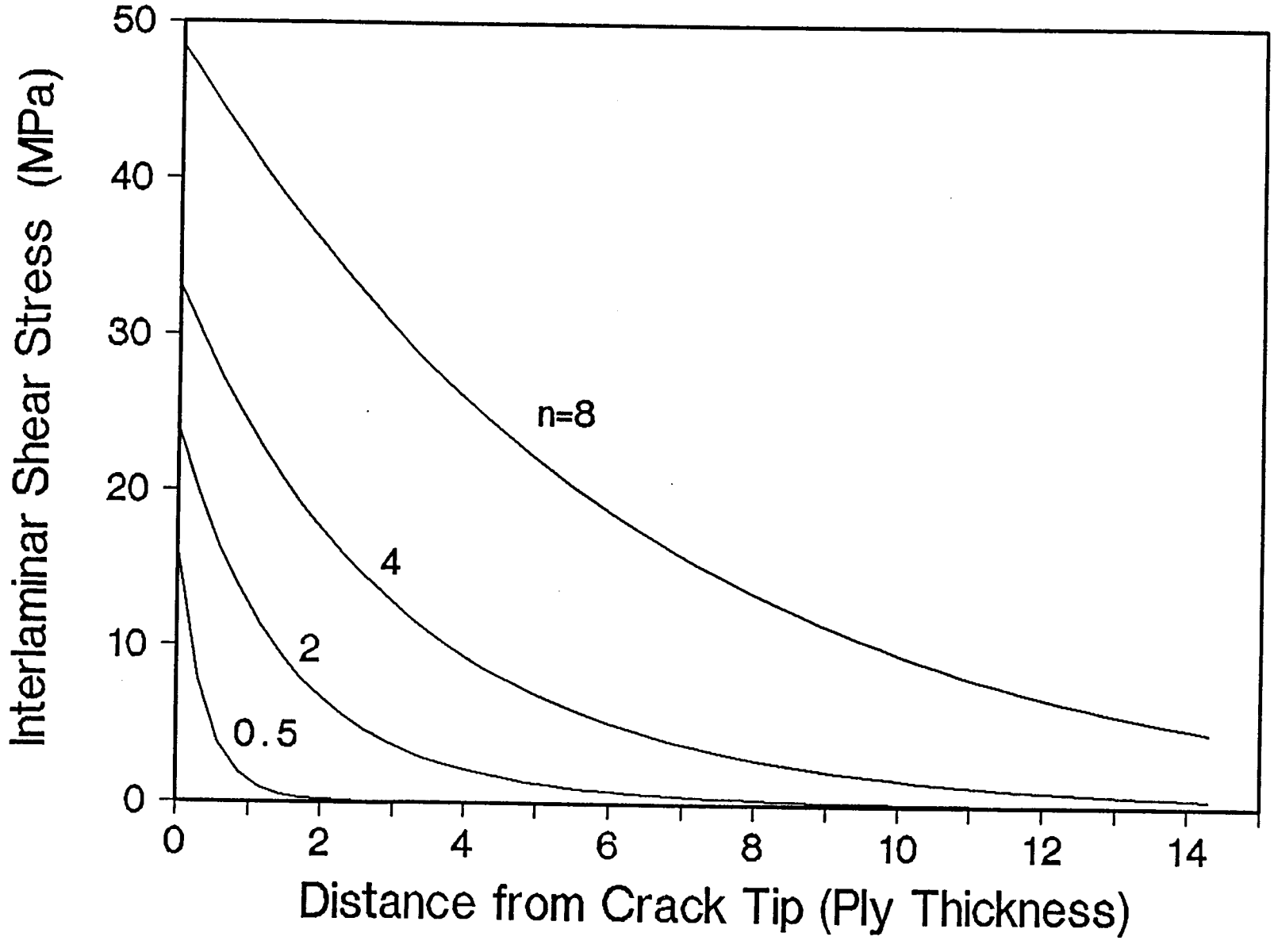

Fig. 7 Interlaminar Shear Stress Distribution

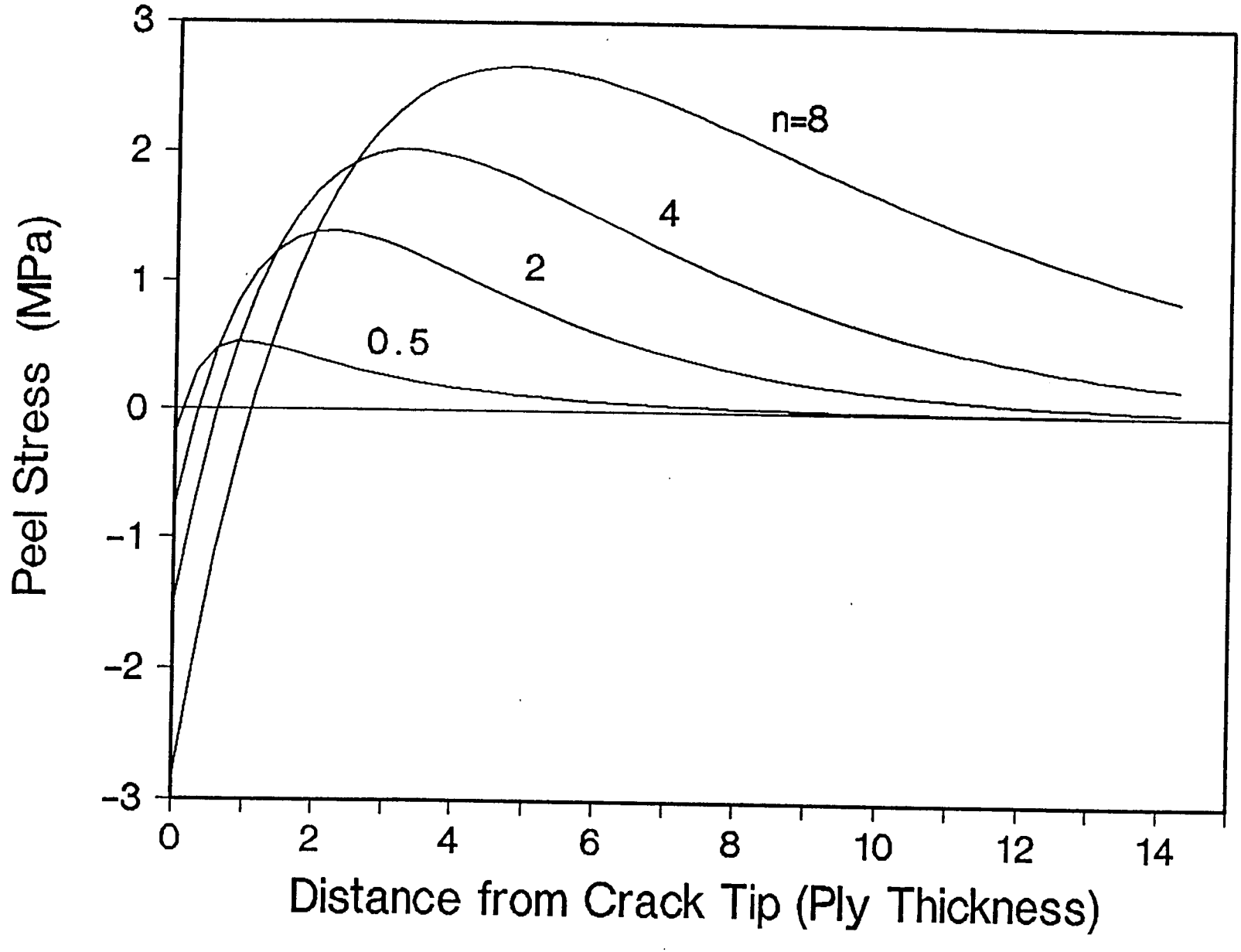

Fig. 8 Interlaminar Normal Stress (Peel Stress) Distribution

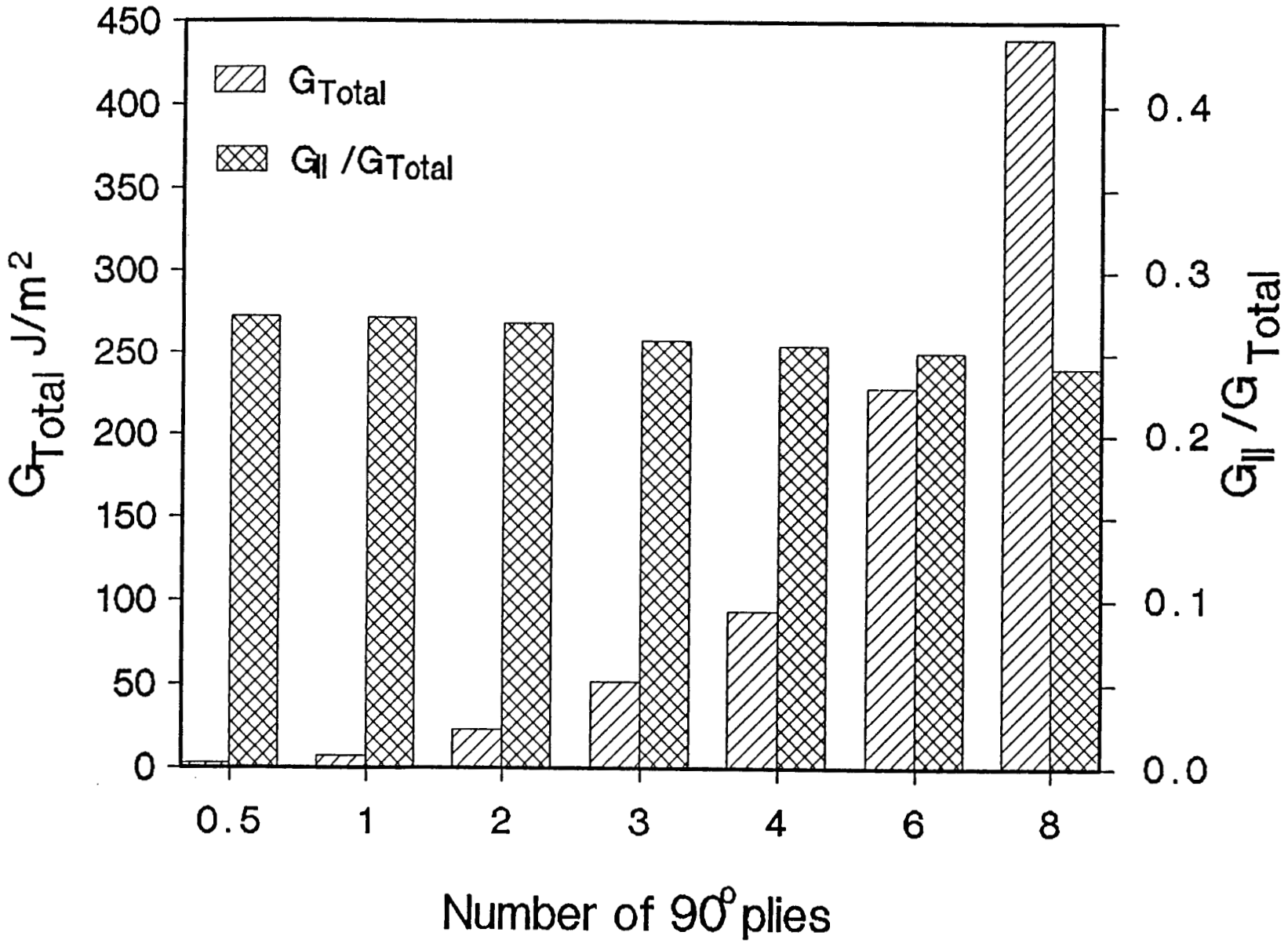

Fig. 9 Energy Release Rate Comparison

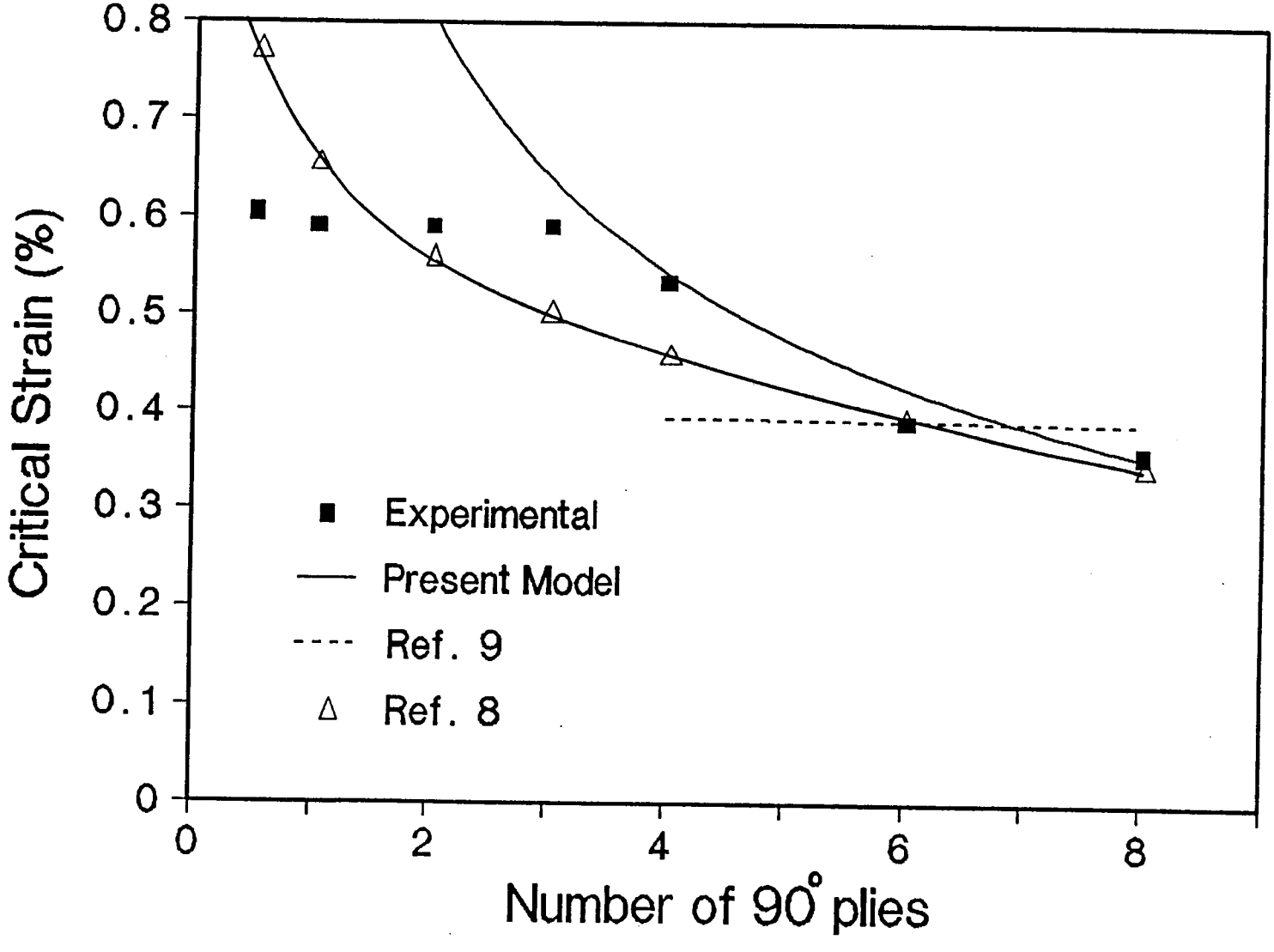

Fig. 10 Critical Delamination Growth Strain Variation

APPENDIX III

Appendix III

III.1 Strain Energy Release Rate

In this analysis, a delamination between belt and core sections is assumed to grow parallel to the belt direction in the tapered and uniform sections. These delaminations in each section are denoted by a and b respectively. The core section in the taper portion is modelled by two equivalent sublaminates. The stiffness properties are smeared to obtain the effective cracked and uncracked stiffnesses which are designated by A_u and A_c as shown in Figure III.1. These stiffnesses change from one ply drop group to another with crack growth a by experiencing a sudden change at discrete locations. Therefore A_u and A_c can be represented in three consecutive regions as follows,

- Region 1: $0 < a < l$

$$A_u = \frac{d + 3l - a}{\frac{d}{A_{BD}} + \frac{l}{A_1} + \frac{l}{A_2} + \frac{l-a}{A_3}} \tag{III.1}$$

$$A_c = A_3 \tag{III.2}$$

- Region 2: $l < a < 2l$

$$A_u = \frac{d + 3l - a}{\frac{d}{A_{BD}} + \frac{l}{A_1} + \frac{2l-a}{A_2}} \tag{III.3}$$

$$A_c = \frac{a + b}{\frac{a-l}{A_2} + \frac{l+b}{A_3}} \tag{III.4}$$

- Region 3: $2l < a < 3l$

$$A_u = \frac{d + 3l - a}{\frac{d}{A_{BD}} + \frac{l}{A_1}} \tag{III.5}$$

$$A_c = \frac{a + b}{\frac{a-2l}{A_1} + \frac{l}{A_2} + \frac{l+b}{A_3}} \tag{III.6}$$

where

h = ply thickness

d = length of uniform thick portion

l = distance between two consecutive ply drop locations

$A_1 = 6hQ^{45} + 2hQ^0$

$A_2 = 4hQ^{45} + 2hQ^0$

$A_3 = 2hQ^{45} + 2hQ^0$

$A_{BD} = 7hQ^0 + 2hQ^{45}$

$Q^0 = Q_{11}$ of a 0 degree ply

$Q^{45} = Q_{11}$ of a ± 45 degree ply

Geometry of the sublaminate model is shown in Figure (III.1)
Also axial stiffnesses A_B, A_s and A_F are given by

$$A_B = \frac{d + 3l - a}{\frac{d}{A_{BD}} + \frac{3l-a}{A_{BT}}} \tag{III.7}$$

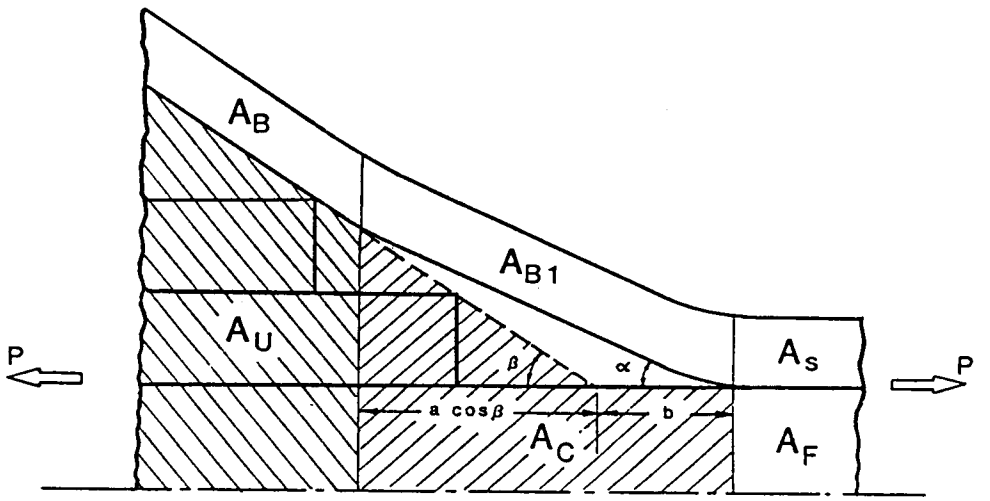

Figure III.1: Geometry of the Sublaminate Model

$$A_F = A_3 \tag{III.8}$$

$$A_s = A_{BD} \tag{III.9}$$

where

A_{BT} =Taper belt stiffness

For a membrane behavior, equilibrium equations are reduced to

$$N_{,x} = 0 \tag{III.10}$$

and the displacement field is assumed to be

$$u(x,z) = U(x) \tag{III.11}$$

and

$$w = 0 \tag{III.12}$$

The constitutive relations are represented by

$$N = A_{11} U_{,x} \tag{III.13}$$

The stress and displacement fields, are determined based on the stiffnesses derived in Equations(III.1-III.9). In this model, load is shared by the core and the belt portions according to their respective stiffness ratios

$$P_1 = \frac{P A_B}{A_B + A_u} \tag{III.14}$$

$$P_2 = \frac{P A_u}{A_B + A_u} \tag{III.15}$$

where P is half of the total axial load applied at the ends.

Using the Equations (III.10), (III.13), and the expressions for P_1 and P_2 from Equations (III.14), (III.15) the axial displacement at $x = c$ can be written as

$$\begin{aligned} U_5 &= \frac{P A_B c}{A_s(A_B + A_u)} + \frac{P(d + 3l + b)}{(A_B + Au)} \left(\frac{A_B}{A_{B1}} - \frac{A_B}{A_s} \right) \\ &\quad + \frac{P(d + 3l - a)}{(A_B + Au)} \left(1 - \frac{A_B}{A_{B1}} \right) \end{aligned} \tag{III.16}$$

$$\begin{aligned} U_6 &= \frac{P A_u c}{A_3(A_B + A_u)} + \frac{P(d + 3l + b)}{(A_B + Au)} \left(\frac{A_u}{A_c} - \frac{A_u}{A_F} \right) \\ &\quad + \frac{P(d + 3l - a)}{(A_B + Au)} \left(1 - \frac{A_u}{A_c} \right) \end{aligned} \tag{III.17}$$

where A_{B1} is the belt stiffness in the pop-off region as shown in Figure III.1.

A three-dimensional transformation is required in order to estimate the effective axial stiffness of the belt region A_B and A_{B1}. This is due to the belt layup and

the orientation of the different belt portions to the loading axis as shown in Figure III.1. The three-dimensional transformation is presented in section III.3.

The tapered laminate is assumed to be fixed at $x = 0$. Therefore the external work done is given by

$$W = P_1 U_5 + P_2 U_6 \tag{III.18}$$

Substitute from Equations (III.14) through (III.17) into Equation (III.18) to get

$$\frac{W}{P^2} = \frac{1}{(A_B + A_u)^2} \left[(c - d - 3l - b) \left(\frac{A_B^2}{A_s} + \frac{A_u^2}{A_F} \right) + (d + 3l - a)(A_B + A_u) + (a + b) \left(\frac{A_B^2}{A_{B1}} + \frac{A_u^2}{A_c} \right) \right] \tag{III.19}$$

The strain energy release rate G due to the external work done is determined by

$$G = \frac{1}{2P^2} \frac{dW}{dA} \tag{III.20}$$

where A is the delamination surface area. G is calculated for delamination lengths ranging from 0 to $60h$. In the analysis, S2/SP250 Glass-Epoxy is used. Its properties are given in Table III.1.

Table III.1: Material Properties of S2/SP250 Glass-Epoxy

E_{11} (MSI)	E_{22} (MSI)	G_{12} (MSI)	G_{13} (MSI)	G_{23} (MSI)	ν_{12}
7.3	2.1	0.87	0.5	0.5	0.275

III.2 Interlaminar Stresses

In this part, an analysis for the interlaminar stresses in the belt-core interface in the tapered section will is developed.

The simple analytical model assumes a beam model for the belt in the tapered section which is shown in Figure III.2 . Material and geometric discontinuities are modelled as extensional k_i and concentrated shear springs g_i (i=1-4) as shown in Figure III.3. The resin pockets are assumed to be subjected primarily to shear stress and they are represented by a distributed shear spring with a constant stiffness G. The effect of the core is incorporated as elastic supports on the beam-belt model.

A minimum complementary potential energy formulation is used to estimate the interlaminar stresses. The total complementary potential energy consists of bending, shear and extensional energy contributions,

$$\Pi^c = \Pi_b + \Pi_s + \Pi_e + \Pi_k \tag{III.21}$$

where Π_b, Π_s, Π_e, Π_k represent bending, shear and extensional energy components and energy stored in elastic springs, respectively. These are given as,

$$\Pi_b = \frac{1}{2}\int_0^{3l} \frac{M^2(s)}{D_{11}} ds \tag{III.22}$$

$$\Pi_s = \frac{1}{2}\int_0^{3l} \frac{\alpha V^2(s)}{G_1} ds \tag{III.23}$$

$$\Pi_e = \frac{1}{2}\int_0^{3l} \frac{N^2(s)}{A_{11}} ds \tag{III.24}$$

$$\Pi_k = \frac{1}{2}\int_0^{3l} \frac{\tau^2(s)}{G_2} ds + \frac{R_1^2}{2k_1} + \frac{R_2^2}{2k_2} + \frac{R_3^2}{2k_3} + \frac{R_4^2}{2k_4} + \frac{T_1^2}{2g_1} + \frac{T_2^2}{2g_2} + \frac{T_3^2}{2g_3} + \frac{T_4^2}{2g_4} \tag{III.25}$$

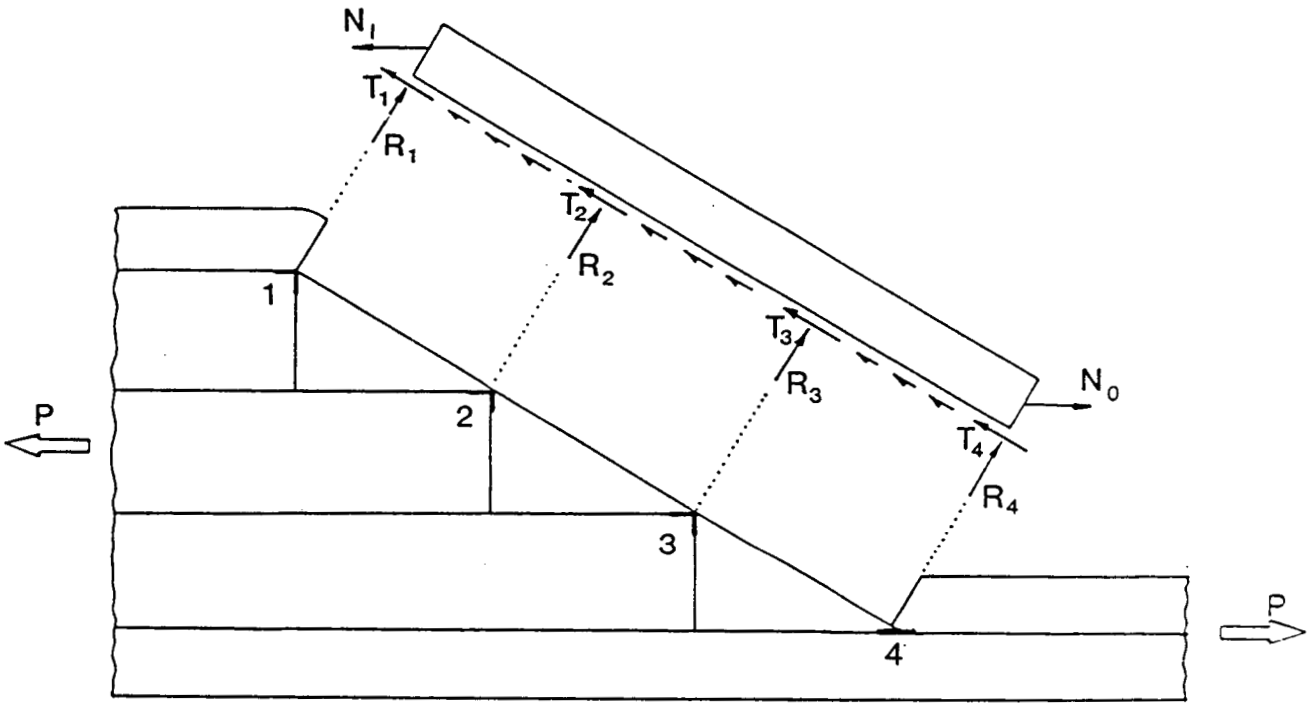

Figure III.2: Geometry of the Model

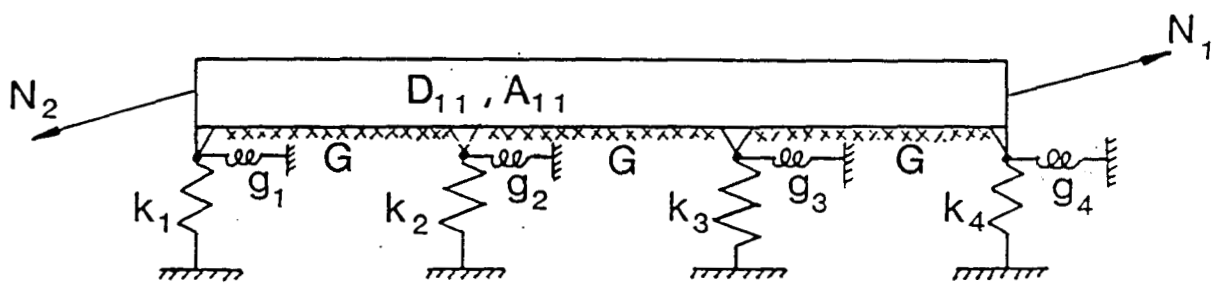

Figure III.3: Modelling of the Beam-Belt

where R_i, T_i (i=1,2,3,4) are unknowns. The constant shear stress,c, due to resin filler is an additional unknown. The total number of unknowns in this formulation is nine. These unknowns are constrained by following equilibrium equations.

$$R_1 = -R_3 - 2R_4 + 2N_{12} + N_{22} - \frac{t}{2l}(N_{11} - N_{21}) \tag{III.26}$$

$$R_2 = 2R_3 + 3R_4 - 3N_{12} + \frac{t}{2l}(N_{11} - N_{21}) \tag{III.27}$$

$$T_1 = -T_2 - T_3 - T_4 - 3cl - N_{12} + N_{11} \tag{III.28}$$

where N_{11}, N_{12}, N_{21} and N_{22} denote the components of the extensional load at two ends of the belt section.

The bending moment, shear force and axial force in each of the three ply drop regions are written as

- Region 1: $0 < s < l$

$$M(s) = -N_{12}s + \frac{ct}{2}s + R_4 s + T_4\frac{t}{2} \tag{III.29}$$

$$V(s) = N_{12} - R_4 \tag{III.30}$$

$$N(s) = N_{11} - cs - T_4 \tag{III.31}$$

• Region 2: $l < s < 2l$

$$M(s) = -N_{12}s + \frac{ct}{2}s + (R_3 + R_4)s - R_3 l + (T_3 + T_4)\frac{t}{2} \tag{III.32}$$

$$V(s) = N_{12} - R_3 - R_4 \tag{III.33}$$

$$N(s) = N_{11} - cs - T_3 - T_4 \tag{III.34}$$

• Region 3: $2l < s < 3l$

$$M(s) = -N_{12}s + \frac{ct}{2}s + (-R_2 + R_3 + R_4)s + (2R_2 - R_3)l + (T_2 + T_3 + T_4)\frac{t}{2} \tag{III.35}$$

$$V(s) = N_{12} - R_2 - R_3 - R_4 \tag{III.36}$$

$$N(s) = N_{11} - cs - T_2 - T_3 - T_4 \tag{III.37}$$

Therefore the bending energy in Equation (III.22) can be written as

$$\begin{aligned}
\Pi_b &= \frac{1}{2D_{11}} \int_0^l \left[-N_{12}s + \frac{ct}{2}s + R_4 s + T_4 \frac{t}{2} \right]^2 ds \\
&\quad + \frac{1}{2D_{11}} \int_l^{2l} \left[-N_{12}s + \frac{ct}{2}s + (R_3 + R_4)s - R_3 l + (T_3 + T_4)\frac{t}{2} \right]^2 ds \\
&\quad + \frac{1}{2D_{11}} \int_{2l}^{3l} \left\{ -N_{12}s + \frac{ct}{2}s + \left[-R_3 - 2R_4 + N_{12} - \frac{t}{2l}(N_{11} - N_{21}) \right] s \right.
\end{aligned}$$

$$+\left[3R_3+6R_4-6N_{12}+\frac{t}{2l}(N_{11}-N_{21})\right]l$$

$$+(T_2+T_3+T_4)\frac{t}{2}\Big\}^2 ds \qquad \text{(III.38)}$$

Similarly for the shear energy

$$\Pi_s = r\int_0^l (N_{12}-R_4)^2\,ds + r\int_l^{2l}(N_{12}-R_3-R_4)^2\,ds$$

$$+ r\int_{2l}^{3l}\left[-2N_{12}+R_3+2R_4+\frac{t}{2l}(N_{11}-N_{21})\right]^2 ds \qquad \text{(III.39)}$$

where

$$r=\tfrac{3}{5G_2A}\ .$$

The energy of extensional loads can be expressed by

$$\Pi_e = \frac{1}{2A_{11}}\int_0^l (N_{11}-cs-T_4)^2\,ds + \frac{1}{2A_{11}}\int_l^{2l}(N_{11}-cs-T_3-T_4)^2\,ds$$

$$+\frac{1}{2A_{11}}\int_{2l}^{3l}(N_{11}-cs-T_2-T_3-T_4)^2\,ds \qquad \text{(III.40)}$$

The energy stored in the elastic springs is written as

$$\Pi_k = \frac{3}{2}\frac{c^2}{G_2}l+\frac{1}{2k_1}\left[-R_3-2R_4+2N_{12}+N_{22}-\frac{t}{2l}(N_{11}-N_{21})\right]^2$$

$$+\frac{1}{2k_2}\left[2R_3+3R_4-\frac{1}{l}M_1+\frac{1}{l}M_2-3N_{12}+\frac{t}{2l}(N_{11}-N_{21})\right]^2$$

$$+\frac{R_3^2}{2k_3}+\frac{R_4^2}{2k_4}+\frac{T_1^2}{2g_1}+\frac{T_2^2}{2g_2}+\frac{1}{2g_1}\left[-T_2-T_3-T_4-3cl-N_{12}+N_{11}\right]^2$$

$$+\frac{T_2^2}{2g_2}+\frac{T_3^2}{2g_3}+\frac{T_4^2}{2g_4} \qquad \text{(III.41)}$$

The complementary potential energy in Equations (III.38) through (III.41) is expressed in terms of 6 unknowns, namely R_3, R_4, T_i (i=2,3,4) and c. By minimizing these expressions the following system of linear equations is obtained

$$\left(\frac{27t^2l^3}{12D}+\frac{3l}{G_2}+\frac{9l^2}{g_1}\right)c+\frac{tl^3}{D}R_3+\frac{5tl^3}{2D}R_4+\left(\frac{5t^2l^2}{8D}+\frac{3l}{g_1}\right)T_2+\left(\frac{t^2l^2}{D}+\frac{3l}{g_1}\right)T_3$$

$$+\left(\frac{9t^2l^2}{8D}+\frac{3l}{g_1}\right)T_4=\frac{5tl^3}{2D}N_{12}+\frac{3l}{g_1}(N_{11}-N_{21})+\frac{t^2l^2}{3D}(N_{11}-N_{21}) \qquad \text{(III.42)}$$

$$\frac{tl^3}{D}c+\left(\frac{2l^3}{3D}+\frac{1}{k_1}+\frac{4}{k_2}+\frac{1}{k_3}\right)R_3+\left(\frac{3l^3}{2D}+\frac{2}{k_1}+\frac{6}{k_2}\right)R_4+\frac{tl^2}{4D}T_2$$

$$+\frac{tl^2}{2D}T_3+\frac{tl^2}{2D}T_4=\left(\frac{3l^3}{2D}+\frac{2}{k_1}+\frac{6}{k_2}\right)N_{12}+\frac{2N_{22}}{k_1}$$

$$+\left(\frac{tl^3}{12D}-\frac{t}{2k_1l}-\frac{t}{k_2l}\right)(N_{11}-N_{21}) \qquad \text{(III.43)}$$

$$\frac{5tl^3}{2D}c+\left(\frac{3l^3}{2D}+\frac{2}{k_1}+\frac{6}{k_2}\right)R_3+\left(\frac{4l^3}{D}+\frac{4}{k_1}+\frac{9}{k_2}+\frac{1}{k_4}\right)R_4+\frac{tl^2}{2D}T_2+\frac{5tl^2}{4D}T_3$$

$$+\frac{3tl^2}{2D}T_4=\left(\frac{4l^3}{D}+\frac{4}{k_1}+\frac{9}{k_2}\right)N_{12}+\frac{2N_{22}}{k_1}+\frac{tl^2}{6D}(N_{11}-N_{21}) \qquad \text{(III.44)}$$

$$\left(\frac{5t^2l^2}{8D}+\frac{3l}{g_1}\right)c+\frac{tl^2}{4D}R_3+\frac{tl^2}{2D}R_4+\left(\frac{t^2l}{4D}+\frac{1}{g_1}+\frac{1}{g_2}\right)T_2+\left(\frac{t^2l}{4D}+\frac{1}{g_1}\right)T_3$$

$$+\left(\frac{t^2l}{4D}+\frac{1}{g_1}\right)T_4=\frac{tl^2}{2D}N_{12}+\frac{1}{g_1}(N_{11}-N_{21})+\frac{t^2l}{8D}(N_{11}-N_{21}) \qquad \text{(III.45)}$$

$$\left(\frac{t^2l^2}{D}+\frac{3l}{g_1}\right)c+\frac{tl^2}{2D}R_3+\frac{5tl^2}{4D}R_4+\left(\frac{t^2l}{4D}+\frac{1}{g_1}\right)T_2+\left(\frac{t^2l}{2D}+\frac{1}{g_1}+\frac{1}{g_3}\right)T_3$$

$$+\left(\frac{t^2l}{2D}+\frac{1}{g_1}\right)T_4=\frac{5tl^2}{4D}N_{12}+\frac{1}{g_1}(N_{11}-N_{21})+\frac{t^2l}{8D}(N_{11}-N_{21}) \qquad \text{(III.46)}$$

$$\left(\frac{9t^2l^2}{8D}+\frac{3l}{g_1}\right)c+\frac{tl^2}{2D}R_3+\frac{3tl^2}{2D}R_4+\left(\frac{t^2l}{4D}+\frac{1}{g_1}\right)T_2+\left(\frac{t^2l}{2D}+\frac{1}{g_1}\right)T_3$$

$$+\left(\frac{3t^2l}{4D}+\frac{1}{g_1}+\frac{1}{g_4}\right)T_4=\frac{3tl^2}{2D}N_{12}+\frac{1}{g_1}(N_{11}-N_{21})$$

$$+\frac{t^2l}{16D}(N_{11}-N_{21}) \qquad \text{(III.47)}$$

The concentrated normal and shear forces at the ply drop regions and the interlaminar shear in the resin filler are estimated by solving the simultaneous system of equations in (III.42) through (III.47) and using Equation (III.26) through (III.28).

III.3 3-D Transformation of Stiffnesses

It has been determined that a three dimensional transformation of stiffnesses is required in order to estimate the effective axial stiffness of the belt regions, A_B and A_{B1}. This is due to the belt layup and the orientation of the different belt portions to the loading axis as shown in Figure III.4.

The loading axis corresponds to axis 1 in the 123 coordinate system which is the transformed system. The principal material coordinates are denoted by $1'$,$2'$ and $3'$.

The stress-strain relationships in the principal material coordinates for an orthotropic laminate are given by

$$\{\bar{\sigma}\}_{6\times1} = [Q]_{6\times6}\{\bar{\epsilon}\}_{6\times1} \tag{III.48}$$

where

$$Q_{11} = (1-\nu_{23}\nu_{32})VE_{11} \tag{III.49}$$

$$Q_{22} = (1-\nu_{31}\nu_{13})VE_{22} \tag{III.50}$$

$$Q_{33} = (1-\nu_{12}\nu_{21})VE_{33} \tag{III.51}$$

$$Q_{12} = (\nu_{21}+\nu_{23}\nu_{31})VE_{11} = (\nu_{12}+\nu_{13}\nu_{32})VE_{22} \tag{III.52}$$

$$Q_{13} = (\nu_{31}+\nu_{21}\nu_{32})VE_{11} = (\nu_{13}+\nu_{23}\nu_{12})VE_{33} \tag{III.53}$$

$$Q_{23} = (\nu_{32}+\nu_{12}\nu_{31})VE_{22} = (\nu_{23}+\nu_{21}\nu_{13})VE_{33} \tag{III.54}$$

$$Q_{44} = G_{23} \tag{III.55}$$

$$Q_{55} = G_{31} \tag{III.56}$$

$$Q_{66} = G_{12} \tag{III.57}$$

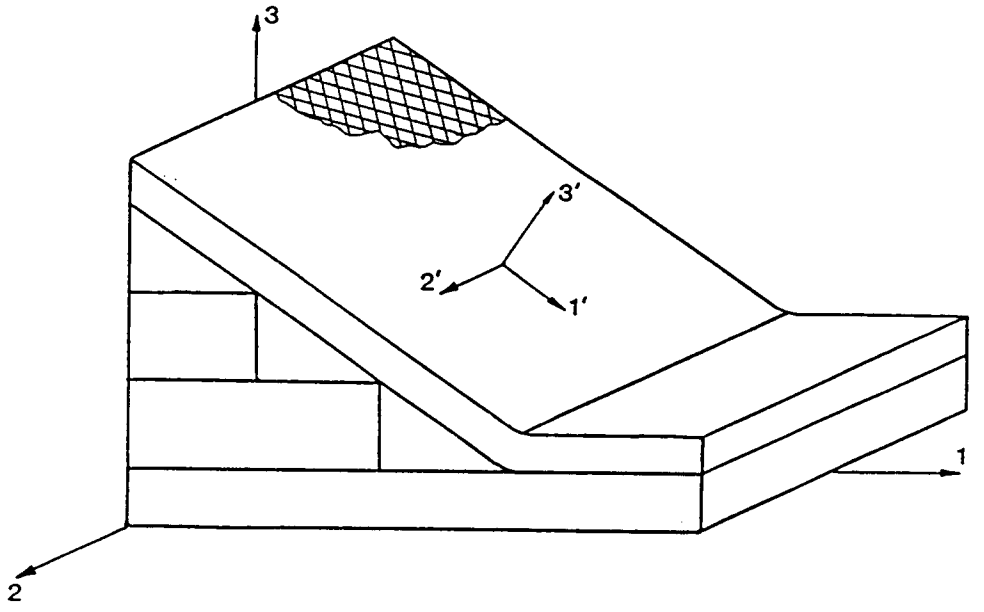

Figure III.4:

$$V = (1 - \nu_{12}\nu_{21} - \nu_{23}\nu_{32} - \nu_{31}\nu_{13} - 2\nu_{12}\nu_{23}\nu_{31})^{-1} \qquad \text{(III.58)}$$

The presence of angle plies in the belt region making an angle θ in the $1'2'$-plane results in the following constitutive relationship

$$\{\sigma'\} = [\overline{Q}]\ \{\epsilon'\} \qquad \text{(III.59)}$$

where the transformed reduced stiffnesses $\overline{Q}_{ij}$ are given in terms of reduced stiffnesses Q_{ij} as

$$\overline{Q}_{11} = c^4 Q_{11} + 2c^2 s^2 Q_{12} + s^4 Q_{22} + 4c^2 s^2 Q_{66} \qquad \text{(III.60)}$$

$$\overline{Q}_{22} = s^4 Q_{11} + 2c^2 s^2 Q_{12} + c^4 Q_{22} + 4c^2 s^2 Q_{66} \qquad \text{(III.61)}$$

$$\overline{Q}_{12} = c^2 s^2 Q_{11} + (c^4 + s^4) Q_{12} + c^2 s^2 Q_{22} - 4c^2 s^2 Q_{66} \qquad \text{(III.62)}$$

$$\overline{Q}_{66} = 4c^2 s^2 Q_{11} - 8c^2 s^2 Q_{12} + 4c^2 s^2 Q_{22} + 4(c^2 - s^2)^2 Q_{66} \qquad \text{(III.63)}$$

$$\overline{Q}_{33} = Q_{33} \tag{III.64}$$

$$\overline{Q}_{13} = c^2 Q_{13} + s^2 Q_{23} \tag{III.65}$$

$$\overline{Q}_{23} = s^2 Q_{13} + c^2 Q_{23} \tag{III.66}$$

$$c = cos\theta$$

$$s = sin\theta$$

Any ply in the belt portion of the taper makes an angle β with the loading axis if it is in the uncracked belt portion and an angle α if it is in the cracked belt portion. By performing a rotation about the 2-axis, the stiffness along the loading axis , takes the form

$$\{\sigma\} = [C]\{\epsilon\} \tag{III.67}$$

where σ_{ij} and ϵ_{ij} are in 123-axis system and C_{ij} represent the elements of transformed stiffness matrix in this coordinate system.

Since we have assumed

$$u(x, z) = U(x) \tag{III.68}$$

and

$$w = 0 \tag{III.69}$$

For plane stress condition in 1-3 plane (i.e. $\sigma_{i2} = 0$; i =1,2,3) stress strain relations reduce to

$$\sigma_{11} = \left(C_{11} - C_{12}^2/C_{22}\right) \epsilon_{11} \tag{III.70}$$

where

$$C_{11} = \overline{c}^4\overline{Q}_{11} + 2\overline{c}^2\overline{s}^2\overline{Q}_{13} + \overline{s}^4\overline{Q}_{33} + \overline{c}^2\overline{s}^2\overline{Q}_{55} \quad \text{(III.71)}$$

$$C_{12} = \overline{c}^2\overline{Q}_{12} + \overline{s}^2\overline{Q}_{23} \quad \text{(III.72)}$$

$$C_{22} = \overline{Q}_{22} \quad \text{(III.73)}$$

where $\overline{c}$ and $\overline{s}$ are cosine and sine of the angle which the cracked and uncracked belt portions makes with the loading axis.

The coefficient of ϵ_{11} in Equation (III.70) represents the transformed axial stiffness. This value is used in the derivation of A_B and A_{B1}.